BACHELOR´S THESIS

NUMERICAL SIMULATION OF IMPACT BIRD AGAINST RIGID FLAT PLATE AND RIGID EDGE FOR BIRD SPLITTING ANALYSIS

BSc AEROSPACE ENGINEERING-VEHICLES

AUTHOR: LAURA RAMOS VALLE

SUPERVISOR: HÉCTOR CLIMENT

DATE: 24/09/2015

Author: Laura Ramos Valle

Supervisors: Héctor Climent and Juan Tomás Viana

Title: Numerical simulation of impact bird against rigid flat plate and rigid edge for bird splitting analysis

TRIBUNAL

President: Merino Martinez, Mario

Secretary: Gonzalo Grande, Alejandro

Vocal: Melendez Sanchez, Juan

The defence of this Bachelor Thesis took place on October 16th 2015 in Leganes, at the EPS (Escuela Politécnica Superior, School of Engineering) of the Universidad Carlos III de Madrid (UC3M).

ACKNOWLEDGEMENTS

The effort reported in this thesis was supervised and managed by the Structural Dynamics and Aeroelasticity Department at the company *Airbus Defence and Space*, division from *Airbus Group* together with Aeroelasticity Department at *Universidad Carlos III de Madrid*, Spain. The main supervisor of the work was Héctor Climent, manager of the Airbus Department mentioned above, together with Juan Tomás Viana.

The research of this thesis started on March 2014 and lasted 7 months till September 2014. The principal investigator was Laura Ramos Valle, Aerospace engineering bachelor student at *Universidad Carlos III de Madrid*.

The author of this thesis wish to acknowledge for all the effort provided to Héctor Climent as well as Juan Tomás Viana, who contributed in a highly significant way to the flourish of this thesis, as well as to family and friends who supported when necessary.

ABSTRACT

Nowadays, bird impact against an aircraft implies high risk for human life safety. Aerospace field covers not only the assembly of aircraft but also the safety these aircraft must gain. To guarantee human life´s safety, a parallel study regarding the impact of birds against plates and edges is developed. Since the aircraft preservation is tested under specific conditions by numerical simulations, the same will be done for the testing of the impacts. Numerical simulations consists on the exact reproduction of the bird impact regarding different scenarios as for the flat plate and the rigid edge recreating the same initial and boundary conditions. Both original tests and numerical simulations are compared for the correct analysis of the materials and characteristics to be applied on the aircraft for its safety.

TABLE OF CONTENTS

LIST OF TABLES

LIST OF FIGURES

LIST OF UNITS

Mass	g (gram)	=0.0022046 lb (pounds-mass)
	Kg (kilogram)	$=10^3$ g
Length	m (meter)	=3.2808 ft. (feet)
		=39.37 in (inches)
	cm (centimetre)	=0.01 m
		=2.54 in
Time	s (second)	
Force	N (Newton)	=0.2248 lb. (pounds-force)
	MN (Mega Newton)	$=10^6$ N
Density	kg/m^3	$=0.0624$ lb/ft^3
		$=3.613 \times 10^{-5}$ lb/in^3
Pressure	MN/m^2	=10 Bars
		=145.04 lbf/in^2

CHAPTER 1

PRELIMINARY REMARKS

1.1. INTRODUCTION

Calbraith Perry Rodgers, the American aviation pioneer that made the first US coast to coast flight in November 1911 was killed in a fatal crash when his aircraft met a flock of birds on 3^{rd} April 1912. This is the first fatality reported of an accident due to bird strike.

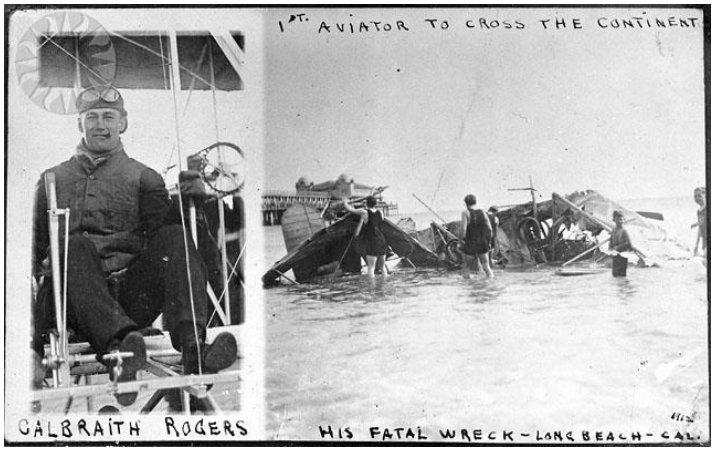

Figure 1.1: Calbraith Rodgers and his fatal aircraft accident [7]

Bird strike consists on the collision of a flying bird such as geese, gulls, pigeons, ducks, etc. and a human-made vehicle, especially aircrafts. The collision can be into the surface of an aircraft or either the absorption of the bird by the jet engine and crash into de compressor blades. The term is also used for bird deaths resulting from collisions with human-made structures such as power lines, towers and wind turbines.

Bird strikes are a significant threat to flight safety, and have caused a number of accidents with human casualties. The number of major accidents involving civil aircraft is quite low and has been estimated that there is only about 1 accident resulting in human death in one billion flying hours. The majority of bird strikes (65%) cause little damage to the aircraft; however the collision is usually fatal to the bird(s) involved. [6]

If a flying bird impacts an aircraft, not only would be a bloody scenario for the bird, but also it will be a high risk for the passengers and crew inside the aircraft. Even though, several small birds can cause failure in an engine.

These impacts or ingestions normally occur at landing/landing roll and approaching configurations, as well as take-off and climbing. At these configurations, the aircraft flies at low altitudes below 100 feet

above sea level, routine heights for birds to travel. When the aircraft climbs to higher altitudes, the probability of the aircraft to be hit by some bird reduces significantly as birds cannot stand high flight altitudes. Somehow, birds have been seen in some occasions at altitudes higher than 30,000 feet above sea level, which is considerable unusual. The highest revealed strike was reported at 37,000 feet [6]. Most of the bird strikes occur during daylight, which is when they use to migrate.

Noticeable differences appear when talking about the strike into small or large aircrafts. Structural failures, such as damage to control surfaces, are more prominent at small aircrafts rather than large commercial. These last ones are more likely to ingest the birds by the engines.

Here can be shown some statistics about different locations where bird strike takes place:

Table 1.1: Statistical comparison between impact birds locations in the aircraft [4]

Aircraft Locations	Percentage
Nose radome and Windshield	41%
Engine	41%
Wings	7%
Fuselage	7%
Gear	3%
Tail	1%

Airplanes departing from airports located near wetlands, coastal regions or next to high wildlife areas will have higher feasibility to be targeted by a bird or a flock of birds. Bird flocks are notably dangerous, involving 100 birds at a time. The damage of the aircraft will depend not only on the weight of the bird and the speed but the number of birds hitting the structure and the impact location.

Despite the robustness of the engines, it is known that the fact that a bird hits one of the engines is the most frequent damaging accident because their exposed prolonged areas. The vast problem comes at the point when the pilot losses total control of the aircraft in case a flock of birds is ingested by all or most of the engines and, without relief, it leads to crash. Moreover, birds can also penetrate into the windscreen and cause serious injuries to the pilots or passengers. CAA and ICAO institutions report that 7% of the bird strikes cause aircraft structural damage [4].

The Federal Aviation Administration (FAA) reports that bird strikes have caused over $600 million of monetary loses per year (200 aircrafts damaged) and 200 deaths since 1988, included direct repair cost and revenues and assessing the out of service aircraft [4].

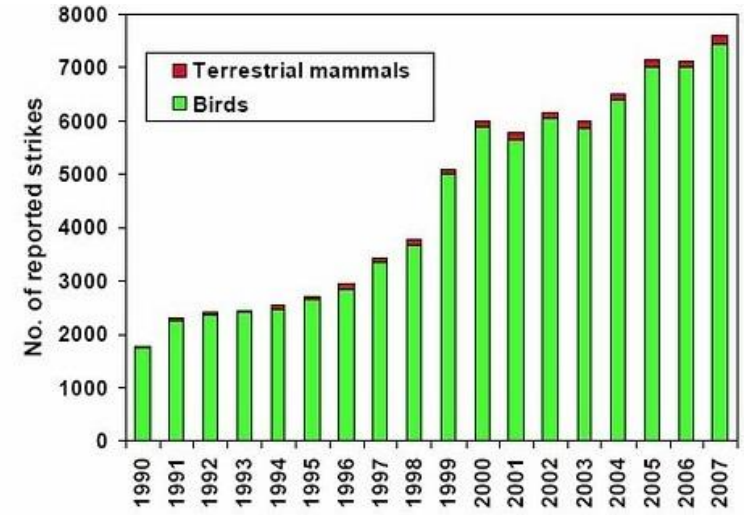

Figure 1.2: Number of reported birds strike compared to terrestrial mammals strike between 1990 and 2007 [4]

In this graph it can be seen that the number of bird strikes since 1990 have been increased till 2007 because the population of some certain types of birds increases from year to year. For example, Canada goose population in the US and Canada has been quadrupled till 2012 and the snow American goose population has triplicated till nowadays since 1990. As well as air traffic movements have increased at a rate of 1.4 percent per year.

1.2. HISTORY ACCIDENTS

The regular crashes caused by bird strikes are: ingestion of birds by the engines and thrust reduction; and penetration into the windscreen and structural damage causing loss of control. Some examples have been reported:

- **7 September 1905, Dayton, Ohio, US, Wright III**

As written by Orville Wright in his diary, this was the first bird strike reported by an aircraft. Orville was able to fly 4,751 meters in 45 seconds. When the Wright III was flying, a red-winged blackbird stroke and fortunately Orville, who was the only passenger, didn´t suffered from injuries.

- **1912, Long Beach California, US**

Cal Rodgers, the American aviation pioneer that made the first transcontinental airplane flight across the US in November 1911, was killed in April 1912 by the impact of a flock of birds at the moment of flying his aircraft. The aircraft hit a goose, which tangled with the control wiring. The aircraft crashed and Cal drowned in the ocean. This is the first reported death in a bird strike accident.

- **12 November 1975, NY, US, DC-10**

During take-off at the John Federal Kennedy airport, the pilot of the DC-10 aborted after ingesting a few seagulls by the rotors. Few moments later, the aircraft couldn´t make it inside the limits of the runway and caught into fire. 138 members were able to evacuate the aircraft and none of them were killed. This accident spotted a before and after in aviation history and consequently, FAA reconsidered to evaluate ingestion of birds effects in engines.

- **7 April 1981, Cincinnati, Ohio, US, Lear 23**

While climbing configuration at 4000 feet, the Lear 23 suffered a penetration in the right windshield by an 8 pounds bird which killed the co-pilot and caused injuries to the pilot, causing damage in the brake and hydraulic systems and in the engine number 2, shuttled down by security. The pilot had to return to the airport and arranged a forced landing.

- **25 July 1990, Addis Ababa, Ethiopia, Ethiopian Airlines, Boing 707-300**

The aircraft was taking off and the pilots reported some ingestion of pigeons in at least two of the engines, they tried to abort the take-off but it was too late, the engines lost thrust and the aircraft fired. Just one member of the crew was seriously injured.

- **25 January 1992, Maasi-Mara, Kenya, Cessna 401**

For the time being in cruise, the aircraft stroke a 13 pounds bird, which caused separation of a wing tip fuel tank and aileron. All passengers and crew in the aircraft were killed.

- **8 July 2003, Cessna 172S, Texas, US**

During an instructional flight, the Cessna impacted with a bird causing structural failure in the left wing. It resulted in loss of control of the whole aircraft, which crashed into terrain surface.

- **April 2012, Embraer 190, Canada**
  During take-off at 100 feet above sea level two geese stroke the windshield of the Embraer, declaring emergency landing.

Figure 1.3: Impact of a goose into the windshield of an Embraer 190 [4]

It can be concluded with the data of the reported accidents that the highest number of events leading to fatal errors was due to ingestion of the bird by engines and the second, impact at windshield injuring crew.

1.3. AIRWORTHINESS REGULATIONS

Federal Aviation Administration´s (FAA) main goal is to provide a safe and secure aviation system in the US. On the other hand the European Aviation Safety Security (EASA) controls Europe continent. Its main goal consists on security management, aviation products certifications, etc.

The study of the FAA and EASA regulations on bird strike is listed for each of the six categories (CS European regulation and FAR American regulation):

1) **CS-23/FAR Part 23-Normal, Utility, Acrobatic and Commuter Category Aeroplanes**

- This type of airplanes must resist the windshield impacts of birds weighting 2 LB (1 kg) without penetrating the glass panel. If the pilot or the co-pilot cannot see through the glass, the other member must be able to view the horizon through it.
- If a single bird strikes the bottom side of the aircraft where pitot tubes are located, these should be such distant apart not to be damaged at the same impact.
- CS-23: Stabilizers must be able to resist the impact of a 4 LB (1.8 kg) Bird.
- FAR Part 23: Stabilizers must be able to resist the impact of an 8 LB (3.6 kg) bird.

2) **CS-25/FAR Part 25-Large Turbine Powered/Transport Airplanes**

- They must be able to remain at safe flight when a bird of 4 LB (1.8 kg) impacts the aircraft at a cruise velocity at sea level or, 85 percent of the cruise velocity at 8000 feet above sea level.

- This type of aircrafts must resist the windshield impacts without fragmentation or penetration of the bird inside the cabin.
- CS-25: If the pilot or co-pilot cannot see through the windshield due to an impact of a 4 LB (1.8 kg) at cruise velocity, an openable window must be available.
- FAR Part 25: The empennage structure must be able to resist the impact of an 8 LB (3.6 kg) bird at cruise speed.

3) CS-29/FAR Part 29-Large Rotorcraft

- The pilots must be able to remain the aircraft at safe flight and landing or at safe landing for a bird strike of 1 kg at maximum cruise speed at the highest altitude of 8000 feet.

4) Engine Certification Standards

- The engines shall not burn up, must be able to provide at least 50 per cent of the thrust or be able to be shuttled down at least 14 minutes after ingestion of bird weighting as much as 8 LB (3.6 kg) during take-off and initial climb.
- For the ingestion of a bird of 3 LB (1.35 kg) during take-off and initial climb the engine must be able not to suffer a 25 per cent loss of thrust and must not be shuttled down before 5 minutes after ingestion.
- During take-off and initial climb, the engines must be prepared to ingest as much as 7 medium sized birds at the same time weighting a maximum of 2 LB (1.15 kg) and should not arrive into complete failure. They must be operative, although not at maximum thrust, within 20 minutes after ingestion.
- During take-off and initial climb, the engines must be prepared to ingest as much as 7 small sized birds at the same time weighting a maximum of 1.5 LB (0.85 kg) and should not arrive into complete failure. They must be operative, although not at maximum thrust within 20 minutes after ingestion.

5) Airports

- Each certified airport must accomplish a risk assessment for wildlife according to the airport security and rules office by the FAA. Some programs such as USDA/WS can support the airports to help them accomplish the risk assessment.
- Air traffic controllers must undoubtedly update and warn pilots and control tower about the presence of birds and their activity when they represent a risk for the aircrafts, passengers, crew and any other staff member working at the airport.
- Although fauna cannot be controlled by humans, in some occasions birds can be killed in case they suppose a risk for the security of passengers and crew.
- It is possible to reshape the habitat for birds not to approach airport areas. For example, architects can build infrastructures which are not attractive for birds, or apply the

usage of nets, as well as chemical products or other animals to chase them.

6) Pilots

- Any unsafe condition inside or nearby an airport related to birds or other wildlife must be reported by pilots. Furthermore, pilots, crew and other airport staff should inform or notice about every bird strike to an aircraft.
- Lights inside the aircraft must be switched off during take-off till the aircraft reaches 10000 feet, not to attract the birds.[1]

1.4. BIRD STRIKE TESTING/AVAILABLE TESTS

Airworthiness Authority use to request to check how aircraft behave at a bird strike and improve the structure when necessary for the aircraft security and its passengers and crew. A real alive and sedated goose or chicken (smaller) is launched against cabin windshield, leading edge of wing or engines to prove if the structure is safe enough. A dead bird cannot be launched because its organs, skin and bones do not behave as real.

The birds are launched in a gun originally designed in 1950 by Havilland Company, UK [23]. They remain inside a compressed air capsule which stays inside the gun at the moment the bird leaves the end of it. The bird is completely tied so the feathers and the wings remain all together with the bird´s body. Before launching the final bird, calibrated velocities are being tested impacting a rigid concrete surface.

Manufactures also do impact tests against the cabin windshield and windows to ensure they are not damaged and flight route and direction is not being affected in case of bird strike.

According to airworthiness regulations, bird strikes at simulation test must ensure same conditions as regular flight.

Adam Tischler from the Communications Division of flight tests at Boing ensures "we have used poultry to test the structure of the aircraft. This is not a common test but it can be an effective way to evaluate the results of the impact of animals on the aircraft" [1].

Sophisticated experimental test are performed at essential aerospace companies like Bombardier. *Virtual iron bird* consists on a specified internal aircraft system located at *CIASTA (Complete Integrated Aircraft Systems Test Area)* laboratory created by Bombardier Company at Montreal, Canada. It's a testing area used to "reproduce a virtual flight before the aircraft takes-off in real life" claims Sebastien Mullot [3]. *Virtual Iron Bird* can reproduce each of the states of flight such as take-off, cruise and landing. The aircraft is being subjected to virtual testing of real flights. This simulation can be

used to identify and predict each of the problems in the structure and indeed structural damage and damage due to bird strike [3].

"We can predict the structural behaviour according to the weight of the bird and the collision point" declares Jean-Louis Montel, ambassador at design department of Dassault Aviation [3].

According to International Committee of collisions with birds, one aircraft crashes every thousand million flight hours.

1.5. BIRD STRIKE TESTS RELEVANT FOR THIS THESIS

Airbus Company has also performed different experimental test for bird strike against rigid plate and rigid edge. Lasts of these experiments were performed at Lichtenburg, Bavaria, Germany by the research and technology group in May 2013 [18].

For the rigid plate, two cases have been evaluated: frontal/normal impact (90 degrees) and oblique impact (45 degrees), where 34 tests have been performed (13 oblique and 20 frontal). Test number 1 and number 8 were performed with paper birds to compare the results with real ones. The bird weight in the tests remain between 1.0 and 3.635 kilograms representing three main groups: 1 kg (2 LB), 1.8 kg (4 LB) and 3.6 kg (8 LB) and between 85 and 180 m/s (impact velocity). Test number 31 was an additional test performed with a bird weighting 3.643 kilograms, the heaviest one.

On the other hand, for the rigid edge 24 test were performed: 6 at 22.5 degrees and 18 at 90 degrees. These birds oscillated between 0.998 and 3.652 kilograms and between 85 and 180 m/s representing the three same groups as for the rigid flat plate impacts. Tests 16, 17 and 18 were additional tests performed for a bird with 3.449, 3.454 and 3.498 kilograms at 125 m/s of impact velocity.

1.6. BIRD STRIKE NUMERICAL SIMULATION: COMPARATIVE OF MODELLING APPROACHES

Because of bird trike relevance in current aviation it is important to be able to predict how the damage will be created using a numerical simulation. This model must be able to recreate similar or identical conditions (impulses and loads) as the original event.

Numerical simulation will use the explicit Finite Element Method (FEM) because it allows considering its complex geometries, non-linearity of the impactor (bird) material and contacts, interactions between elements and collapse sequence.

Classified according to FEM, three different bird models exist: Lagrangian, Smoothed-Particle Hydrodynamics (SPH) and Arbitrary Lagrangian Eulerian (ALE) method.

- The Lagrangian method contains solid elements where the nodes of the mesh move according with the material. This method can lead

to some numerical stability problems due to the large distortions of the bird sometimes interpreted by the code as negative volumes [15].

- The Smoothed-Particle Hydrodynamics (SPH) method is a computational method used for simulation fluid flows. It was developed by Gingols and Monaghan (1977) and Lucy (1977) initially for astrophysical problems. It is a mesh-free Lagrangian method (where the coordinates move with the fluid), and the resolution of the method can easily be adjusted with respect to variables as the density [27].
  The SPH method works by dividing the fluid into a set of discrete elements, referred to as particles. These particles have a spatial distance known as "smoothing length" over which their properties are "smoothed" by a kernel function. The physical quantity of any particle can be obtained by summing the relevant properties of all the particles which lie within the range of the kernel. The contributions of each particle to a property are weighted according to their distance from the particle of interest, and their density [27].
- IN ALE method Lagrangian or Eulerian particles can be chosen depending on their motion. Nodes are fixed and material moves through the mesh [15].

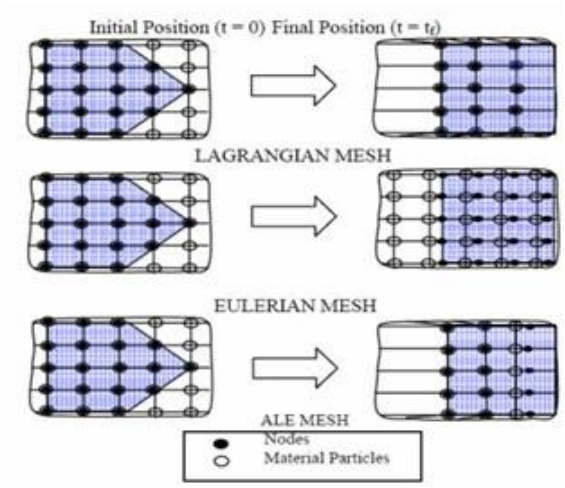

Figure 1.4: Lagrangian, Eulerian, ALE Methods [15]

In the next paragraphs, a comparative/historic description of bird modelling is presented:

The first person who studied an impact of a bird into a flat surface was Barber et al (1975) using Lagrangian modelling [22]. He found out that when impacting a bird into a flat surface, peak pressures appeared dependent on bird weight and on impact velocity. As the impact velocity increased, so does the pressure at each peak.

In the year 1997, Hut et al. [22] explained briefly the SPH method, its applications, computational parameters and improvements in the processing time.

Neiring (1988) [22] discovered that using the Lagrangian method, numerous and large distortions in the bird appeared, causing inaccuracy at results. He suggested some improvements in the theory.

A detailed explanation about ALE method, including basis of continuum mechanics was demonstrated by Stoker in the year 1999 [22]. Compared to Lagrangian method, ALE proved compelling fewer distortions in the mesh of the bird. This improvement generated longer processing time for the simulation.

Some other simulations were reproduced at rigid and flexible targets by Moffat and Cleghorn in 2001 for an ALE method and results were similarly interpreted as those obtained by Barber et al. [22] Likewise, Metrisin and Potter [22] figured out a bird-strike simulation using implicit and explicit models.

Shultz and Peters (2002) [22] used LS-DYNA and ANSYS software simulating a bird with Euler Mesh and blades with Lagrangian mesh, where the bird was colliding the fan blades of a jet engine of an aircraft. At the moment of collision, momentum was transferred from one rigid body to the other and results were outputted. Some recommendations were displayed at the end of the simulation.

Linder (2003) [22] compared the three different methods. For Eulerian method, he stated that the mesh flowed around the stationary model (no need of remesh). Flow and interface definition is not as defined as for the rest of the models, which is the primary disadvantage. In Lagrangian method, the mesh motion is exactly identical to the original motion. In ALE method, the most optimal method is applied depending on the step, which allows the method to be separated into three different phases: Lagrangian, Eulerian and a phase in between these two. Improvements of the model were executed and higher resolutions were obtained.

The same year, PAM CRASH program was used for the first time applied to bird-strike simulation at the edge of an aircraft wing, by Ubels et al. [22] .These simulations were created to estimate the optimal impact velocity at which the bird should strike the surface in the SPH model at the leading edge of the wing. It resulted to be 100 m/s.

In the year 2004 Martin [22] chose to study a simulation of a soft body impact at a deformable disc and tapered plate and discovered that the results were very similar to those projected by SPH model, as well as, for the better understanding of ALE method and the description of the motion, Donea et al. [22] defined spatial and material domains.

According to these investigators, the three methods vary from one to another in such a way that, although Lagrangian method exposes

mismatched results depending on the loading rate due to the mesh degradation of the model, it is the most rapid and gives the most accurate results. On the other hand, ALE method cancels the element distortion founded in the Lagrangian model, but the termination time is highly elevated (high CPU time).

The most impeccable method results to be a combination between Lagrangian approach for the specimen and SPH model with high material distortion for the impactor. This method reveals higher accuracy for the simulation of bird-strikes as well as lower CPU times rather than ALE, SPH or Lagrangian full methods. This arrangement is used in current simulations of impacts, not only for birds but also for trucks, cars, animals, etc.

1.7. REQUIRED RESOURCES

For the correct evaluation of the analysis explained, three main computer programs are used:

- Mat Lab
- Virtual and Visual Performance (Pam Crash)
- Hyper Mesh
- Unix Operating System

Mat Lab is a coding program that can be used for multiple tasks. It helps to compare the test results with the simulations developed at Pam Crash. Pam Crash is an engineering program mainly designed for impact simulation and can perform tasks related to structures. Designed up to 7 interfaces, divided in two big categories: design process and view process. The designing process extends from creating the nodes and the geometry, going through the mesh design and ending up defining materials of the elements and its properties, boundary conditions, contacts between surfaces, initial conditions, transformations, loads, output… The viewing process consists on analysing the results after the launching through Unix Operating System.

For defining the geometry of the modelled birds, Pam Crash could be used at the designing interface. But finally Hyper Mesh program was decided to be used because the meshing is more detailed and so the transformation from elements to SPH (Smoothed-Particle Hydrodynamics) is more precise.

Lastly and the most important, is to learn how Unix Operating System works. The interface at Airbus Group is called Multivac, which retains the information from each of the users at the system. It is a programming system which works by exchanging commands that must be interpreted. It is mainly used to do the launching from the Pam Crash designed interface to the viewer interface. This intermediate process could be done by the own Pam Crash but as the number of nodes in the simulation is quite high, the required time of the CPU would be 10 times slower.

1.8. MOTIVATION AND OBJECTIVES OF THE PRESENTED WORK

As mentioned before, bird strikes against aircrafts can cause the damage of considerable factors, regarding human lives, repair costs, loss of incomes, among others.

The objectives of this Bachelor´s Thesis mainly are summarized as:

- Comparison between numerical simulation and test results of bird strikes on
  - Flat rigid plates
  - Rigid edges
- Optimization of the impactor (bird) model to match test results by deriving a design guidelines to obtain the best impactor (bird) model as a function of the bird weight and in particular for:
  - 2 LB (1 kg)
  - 4 LB (1.8 kg)
  - 8 LB (3.6 kg)
- Elaborate a statistical treatment for the rigid edge test and numerical results of the splitting analysis of the bird.

Numerical analysis is evaluated with PAM CRASH program (Virtual and Visual Performance from ESI Group Solutions mainly used for structures and impact analysis) and experimental results are obtained by the launch of birds against rigid flat and edge surfaces. Experimental data have been post processed in order to extract information to optimize the SPH bird FE model.

The numerical simulation includes obtaining values for impact forces and modifying the bird characteristics in addition to adjust the impact speed and angle for different flying configurations and situations.

The aim of this comparison is to be able to reproduce the experimental tests with the numerical simulations.

1.9. THESIS PLANNING

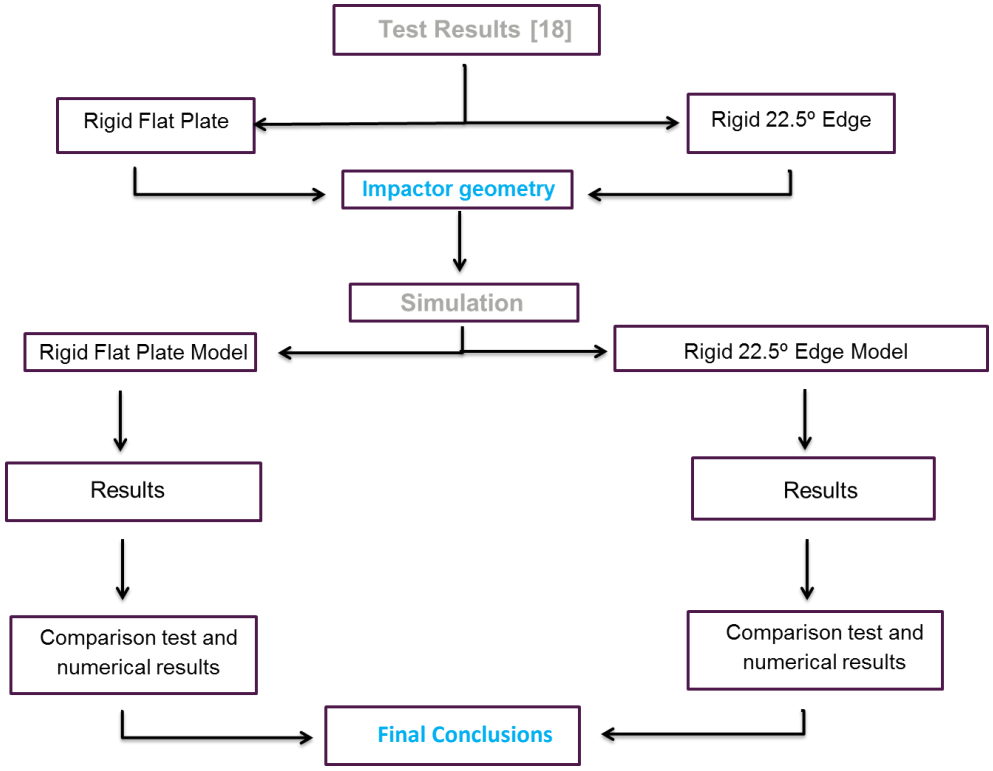

Figure 1.5: Thesis planning flowchart

Firstly, in Chapter 2 some theoretical considerations must be taken into account to understand the main goals of the thesis: how is the projectile reacting at impacts, which variables must be measured for the correct analysis of the impact and diverse characteristics for the selection of the valid tests, among others. In Chapter 3, results on rigid flat surfaces are going to be evaluated. Statistical treatment of available tests will be generated and the results will be digested. To simulate the impact in PAM CRASH, the SPH bird model will need to be designed firstly in Chapter 4. The improvement of the bird modelling is developed with FORTRAN code. An extension of the thesis "*Bird strike on transparencies*" by Tamara Casillas [8], graduated in Aerospace engineering by Universidad Carlos III de Madrid and previous intern in Structural Dynamics and Aeroelasticity department at Airbus Defence and Space, is accomplished by modifying the SPH geometry of the projectile model. Secondly, results of collapse sequence and impact forces are obtained from the numerical simulation of the bird strike against the flat rigid surface in Chapter 5. Undoubtedly, the most decisive section of Chapter 5 is the comparison with available test results taking into account the sensitivity to bird shape, mass, impact speed and impact angle. But, not only is the rigid surface relevant for the projectile simulation, rigid edge takes an essential role too. Chapter 6 deals with the same points as listed in Chapters 3 and 5, but for rigid edge simulations and the evaluation of its

results compared to experimental tests. Additionally, a statistical treatment of the bird splitting meaning is performed in order to evaluate the different phases at impact against rigid edge. To sum up, a complete and summarized digestion of the results regarding final conclusions is reported in Chapter 7 and 8. Economic framework, a designed guidelines, recommendations and proposal of future activities are recorded in Chapter 9 and 10. Finally, references are listed in Chapter 11.

CHAPTER 2

THEORETICAL CONSIDERATIONS

2.1. BEHAVIOR AT IMPACT

To completely understand and analyse the impact of a projectile against rigid surfaces, flat plates or edges, it is necessary to have a fully developed knowledge of how is the performance of the projectile at the moment of impact [23].

The impact against a rigid plate consists on 4 different phases:

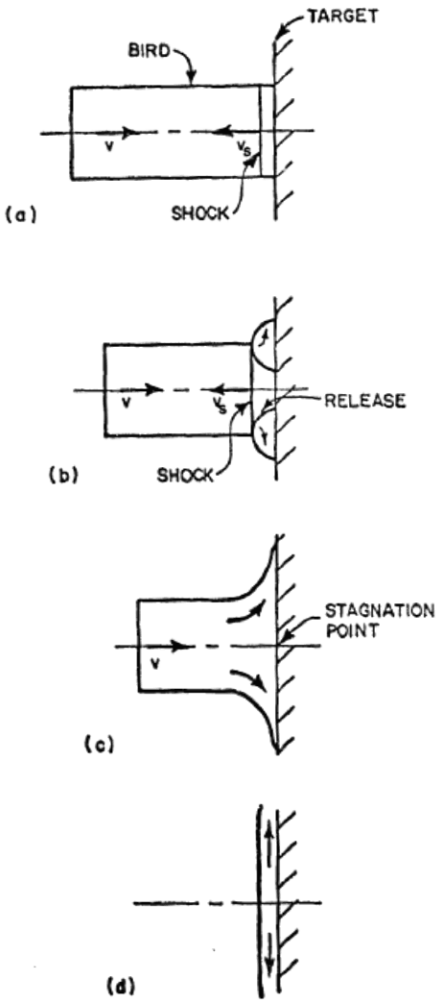

Figure 2.1: Bird impact phases [23]

I. Initial Impact

A shock wave is created at the front face of the impactor. At this moment, the Hugoniot pressure which refers to the pressure in the shocked region starts to appear defined as:

$$P_H = \rho_1 u_s u_p \quad (1)$$

Where ρ_1 is defined as the density of the material of the projectile; u_s is the velocity of the shock wave and u_p is the impact velocity of the particle.
For the oblique impact of a projectile, the component of the velocity normal to the plate is defined as $u_s \sin(\theta)$ where θ is the oblique angle of impact with respect to the plate.

The shock in the initial Impact, can take three different paths depending on its velocity. These different paths represent the same situation from three different points of views:

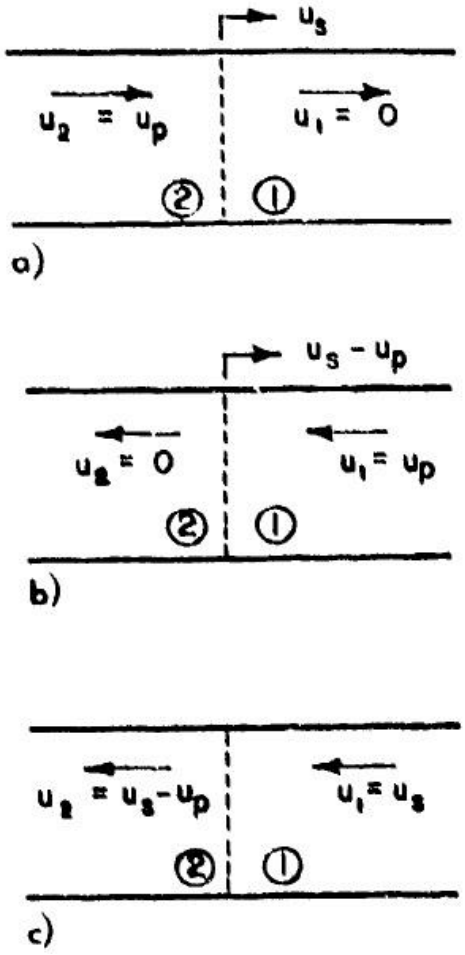

Figure 2.2: One Dimensional Shock Flow [30]

(a) Observer over the plate. Shock propagating into a fluid at rest.

(b) Observer over the projectile. Flow brought to a rest across the shock
(c) Observer over the release wave. Standing Shock

The only difference between case a) b) and c) is the reference system from where the velocity is seen.

The initial impact of a projectile against a rigid plat plate can be considered as a one-dimensional, adiabatic and irreversible. If an impact is considered hydrodynamic, it means that the impactor is composed of air and liquid; and variable z is considered as the porosity (air percentage in the projectile).

For the point of view c) where the observer stands over the release wave, few conditions and equations must be used:

- Mixture relation

$$(\frac{\rho_1}{\rho_2})_{porous} = (1-z)\left(\frac{\rho_1}{\rho_2}\right)_{water} + z(\frac{\rho_2}{\rho_1})_{air} \quad (2)$$

Not only the composition of the projectile is taken into account, but the two main equations of conservation considering the steady state shock equation.

- Conservation of mass

$$\rho_1 u_s = \rho_2 \ (u_s - u_p) \quad (3)$$

- Conservation of momentum

$$P_1 + \rho_1 u_s^2 = P_2 + \rho_2 \ (u_s - u_p)^2 \quad (4)$$

Using the linear Hugoniot relationship

$$u_s = c_o + k u_p \quad (5)$$

And the two state equations of the materials of the projectile based on James S. Wilbeck´s theory developed in his doctoral thesis the year 1978 [30].

- State equation of water

$$\frac{\rho_{1water}}{\rho_{2water}} = \left(\frac{P_2}{A} + 1\right)^{-\frac{1}{B}} \quad (6)$$

Being

$$A = \frac{\rho_1 {C_o}_{water}^2}{4k_{water} - 1} \quad (7)$$

$$B = 4k_{water} - 1 \quad (8)$$

$${c_0}_{water} = 1482.9 \ m/s \quad (9)$$

$$k_{water}=2 \quad (10)$$

- State equation of air

$$\frac{\rho_{1_{air}}}{\rho_{2_{air}}} = (1 - q) \quad (11)$$

Being

$$q = q_1 - q_2 \quad (12)$$

$$q_1 = \frac{2Pk_{air}+\rho_{1_{air}}{c_o}_{air}^{\,2}/P_1}{2Pk_{air}^{\,2}} \quad (13)$$

$$q_2 = \frac{\{[2Pk_{air}+\frac{\rho_{1_{air}}{c_o}_{air}^{\,2}}{P_1}]^2-4P^2k_{air}^{\,2}\}^{\frac{1}{2}}}{2Pk_{air}^{\,2}} \quad (14)$$

$$P = \frac{P_2}{P_1} \quad (15)$$

$$k_{air} = 1.03 \quad (16)$$

$${c_o}_{air} = 343 \text{ m/s} \quad (17)$$

The Hugoniot pressure defined in the initial impact phase as a combination of the Equations 5, 6, 8 and 13 can be explained in the following figure:

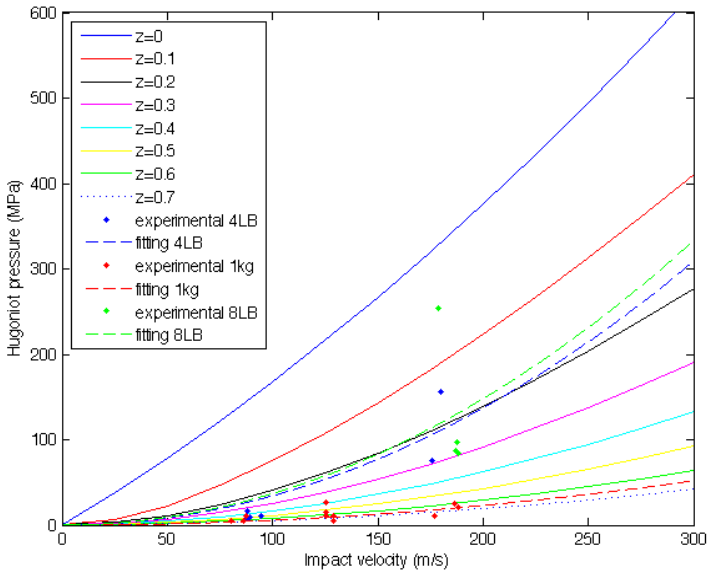

Figure 2.3: Effect of the porosity in the Hugoniot pressure

The dots represent the results of the tests done in Germany of the peak pressures for each of the three categories of birds: 1

kg, 4 LB and 8 LB. The dotted lines represent the fitting curves for the experimental results. The solid lines represent the theoretical evolution of the Hugoniot pressure with the impact velocity for different variations of the values of porosity.

The results of the graph show that for impactors of 1 kg, the porosity should be z=0.65; for 4 LB birds, z=0.2; and for 8 LB birds, z=0.19. These results can no longer be trustable because the real birds launched in Germany had expected values for porosity between 0 and 0.1.

Results and comparison evaluating the porosity show that the experimental peak pressures in the tests are wrongly measured. To make a correct study of the results obtained in the tests and correctly compare to a numerical simulation, the experimental pressures are discarded and only the experimental forces are taken into account.

II. Impact pressure Decay

The shock created at the initial impact starts to propagate in the normal direction to the plate along the bird; meanwhile the waves propagate in towards the centre from the free surface edges of the bird. When the release waves have converged at the centre of impact, the pressure on the target begins to decay. When the release waves have converged at the centre of the shock, a region of fully shocked material no longer exists. The projectile keeps moving with a velocity u_p [23].

III. Steady Flow

As the radial pressures decrease during the shock pressure decay, shear stresses develop in the impactor material. If the shear stresses in the projectile become much larger than the shear strength of the material, it will start to "flow". The shear strength of birds is so low that the pressures generated are usually sufficient to cause flow. After several reflections of the release waves, a condition of steady flow is stablished and steady pressure and velocity fields are stablished too [23].

The Hugoniot pressure transforms into stagnation pressure defined as:

$$P_s = k\rho u_p^2 \quad [30] \qquad \textbf{(18)}$$

Where k is a material constant and ρ is the projectile´s density.

IV. Flow termination

The impact velocity starts to decrease until it reaches zero value but at the same time the local pressure starts to increase until it reaches its maximum. At the end of this pressure field,

steady flow does no longer exist and the pressure starts to decrease till zero. At this point the impact time can be calculated as the length of the projectile divided by the impact velocity.

$$t = L/u_p \tag{19}$$

2.2. THEORETICAL VARIATIONS

2.2.1. Variation of kinetic energy

Kinetic energy of the impact varies with the impact velocity and mass as following:

$$E_K = \frac{1}{2} m {u_p}^2 \tag{20}$$

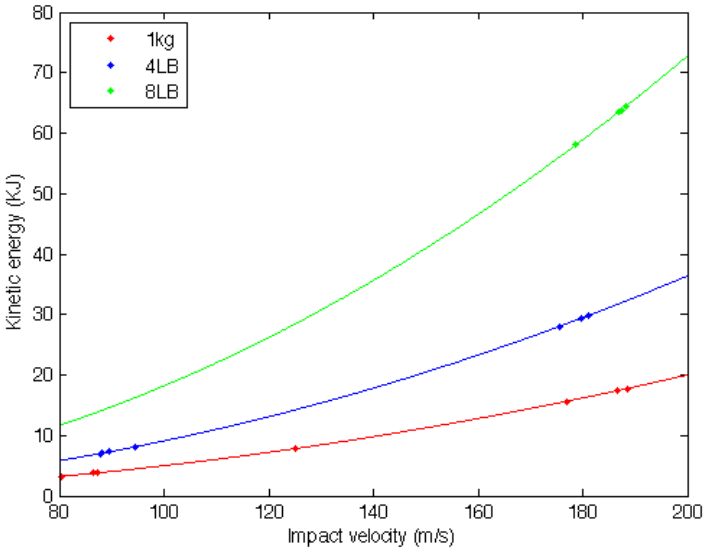

Figure 2.4: Variation of kinetic energy with impact velocity

The dots represent the experimental results of the test for the three weights. The lines represent the fitting for the experimental results for each of the weights. It can be appreciated that kinetic energy increases with mass and velocity. This kinetic energy will be transformed into internal energy representing the deformation of the projectile.

2.2.2. Variation of Hugoniot pressure

As the impact can occur at 90 and 45 degrees with respect to the plate, the peak pressure will vary as a function of its impact angle as well as the mass of the projectile and the impact velocity.

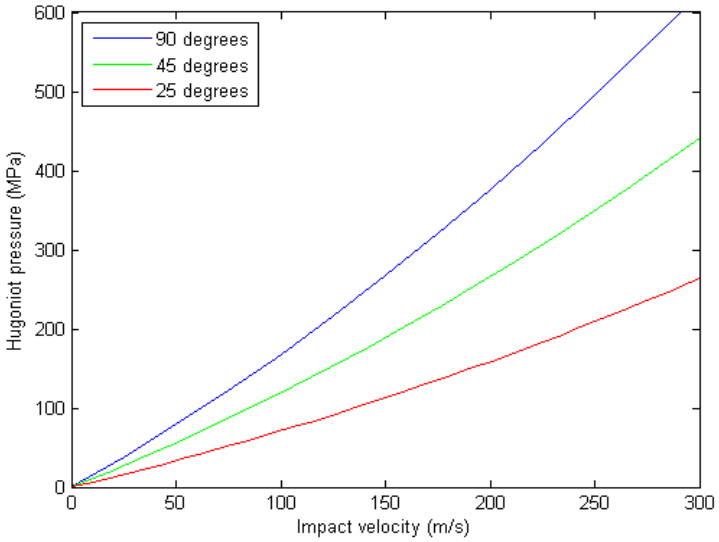

Figure 2.5: Variation of the Hugoniot pressure as a function of the impact velocity

For a normal impact, the peak pressure in the normal direction to the plate is maximal. As the impact angle turns smaller, the peak pressure in the normal direction to the plate becomes smaller too. This is due to the fact that the resistant pressure of the plate in its normal direction reduces if its normal velocity is minor.

CHAPTER 3

IMPACT TESTS AGAINST RIGID FLAT PLATE

3.1. AVAILABLE TEST RESULTS

For the correct analysis of the comparison between results of the numerical simulation and the real impact, available test results on rigid surface must be post processed and treated.

Firstly, the projectile is measured in a scale. As the projectiles need to weight approximately 1 kg, 4 LB or 8 LB, some ends need to be removed to adjust the weight of the birds.

Figure 3.1: Measurement of a 1 kg projectile [18]

As seen in ***Figure 3.1***, the projectile remains inside a capsule to keep the bird integrity and fit the gun dimensions.

Secondly, the necessary equipment for the launching is studied.

Figure 3.2: Bird strike test set-up [18]

The red tube consists on a compressed air gun of approximately 7 meters which allows the projectile to reach the necessary velocity at the correct orientation without breaking it-up. When the projectile reaches the edge of the gun, it is launched to the plate and the capsule remains inside the gun.

The projectile reaches the rigid plate instrumented by 17 pressure gauges which measure the pressure values at impact.

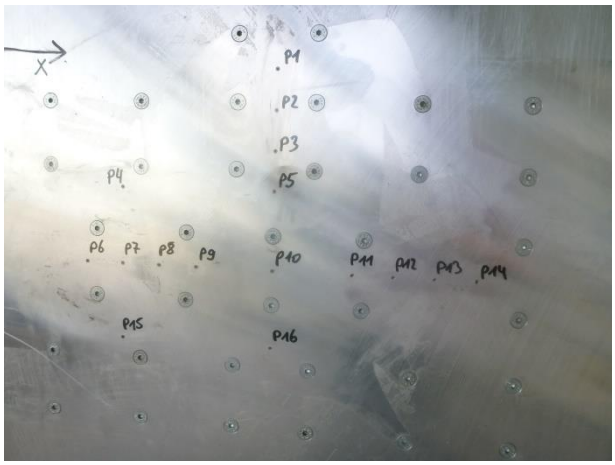

Figure 3.3: Pressure gauges located at the rigid flat plate [18]

At the moment of impact, pressures are measured at each of the pressure gauges and forces are measured at two load cells located behind the plate (see ***Figure 3.4***).

Figure 3.4: Load cells located behind the rigid flat plate [18]

The load cell shown in ***Figure 3.4*** is defined as the "left" load cell. Located at its right, a second cell is attached to the plate. It is located exactly at the centre of the rigid flat plate and it is called "centre" load cell. Cells are used to record information about loads at impact.

34 different tests have been fulfilled. Test results are subdivided into two main groups: impact angle of 45 degrees and impact angle of 90 degrees. As some of these tests may be of no use due to launching error or human miscalculations, the first task would be to discard the erroneous tests. To afford this task, comparison of a concrete force between the first 13 test and the remaining 20 test is plotted. Dissimilar graphs are removed and never used for comparison with numerical results.

Table 3.1: Runs at 45 degrees [18]

Test #	Setup	Impact angle	Bird mass [g]	Group mass	Target Vel. [m/s]	Velocity [m/s]
PT01*	Rigid Plate	45°	1735	4 LB	125	126.6
1	Rigid Plate	45°	1000	1 kg	85	84.6
2	Rigid Plate	45°	1000	1 kg	85	87.5
3	Rigid Plate	45°	1002	1 kg	85	88.4
4	Rigid Plate	45°	1013	1 kg	125	130.6
5	Rigid Plate	45°	1007	1 kg	125	129.6
6	Rigid Plate	45°	1006	1 kg	125	122.5
7	Rigid Plate	45°	1013	1 kg	180	190.5
8*	Rigid Plate	45°	1819	4 LB	125	131.5
9	Rigid Plate	45°	1003	1 kg	180	188.5
10	Rigid Plate	45°	1007	1 kg	180	179.7
11	Rigid Plate	45°	1821	4 LB	125	126.6
12	Rigid Plate	45°	1815	4 LB	125	125.5
13	Rigid Plate	45°	1815	4 LB	125	124.7
*tests with a paper bird						

Table 3.2: Runs at 90 degrees [18]

Test #	Setup	Impact angle	Bird mass [g]	Group mass	Target Vel. [m/s]	Velocity [m/s]
14	Rigid Plate	90°	1005	1 kg	85	86.5
15	Rigid Plate	90°	1824	1 kg	85	94.5
16	Rigid Plate	90°	1004	1 kg	85	87.4
17	Rigid Plate	90°	1000	1 kg	85	80.3
19	Rigid Plate	90°	1002	1 kg	125	128.9
20	Rigid Plate	90°	1000	1 kg	125	128.9
21	Rigid Plate	90°	989	1 kg	125	125.2
22	Rigid Plate	90°	1817	4 LB	85	88.0
23	Rigid Plate	90°	1818	4 LB	85	87.8
24	Rigid Plate	90°	1815	4 LB	85	89.5
25	Rigid Plate	90°	1001	1 kg	180	186.5
26	Rigid Plate	90°	1000	1 kg	180	176.9
27	Rigid Plate	90°	1000	1 kg	180	188.5
28	Rigid Plate	90°	1820	4 LB	180	181.0
29	Rigid Plate	90°	1819	4 LB	180	179.7
30	Rigid Plate	90°	1816	4 LB	180	175.6
31	Rigid Plate	90°	3643	8 LB	180	178.7
32	Rigid Plate	90°	3632	8 LB	180	187.5
33	Rigid Plate	90°	3630	8 LB	180	188.4
34	Rigid Plate	90°	3635	8 LB	180	186.8
additional tests						

The tables are divided by groups. Each group includes between 3 or 4 runs with birds weighting approximately the same and shot at very similar velocities. Different colours in the tables represent different groups.

For impacts at 45 degrees, only projectiles of 1 kg and 4 LB are launched. Instead, for the impacts at 90 degrees, projectiles of 1 kg, 4 LB and 8 LB are launched.

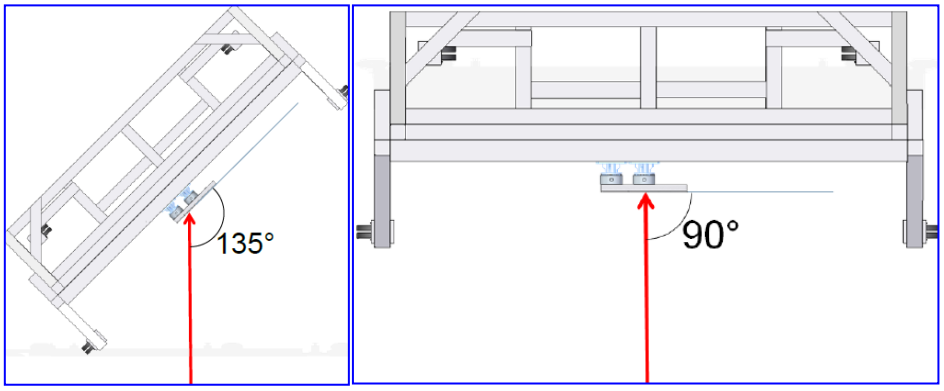

Figure 3.5: Representation impact angle against rigid flat plate [18]

For an impact at 45 degrees, the projectile crashes in the middle of the two load cells (left and centre) (see ***Figure 3.5 (left)***). Forces must be analysed in the two load cells located behind the plate to

estimate the total force at the impact point. For an impact at 90 degrees, the projectile impacts at the centre of the centre load cell (see ***Figure 3.5 (right)***). Forces on the centre load cell must be analysed.

In the following graphs, a real scenario of the points of impact is shown. For an impact at 45 degrees (see **Figure 3.6**), the projectile crashes in the pressure gauge number 10 (see **Figure 3.3** for better understanding) of the rigid flat plate, located at the middle of the two load cells. For an impact at 90 degrees (see **Figure 3.7**), the projectile crashes in the pressure gauge number 7 (see **Figure 3.3**), located at the centre of the centre load cell.

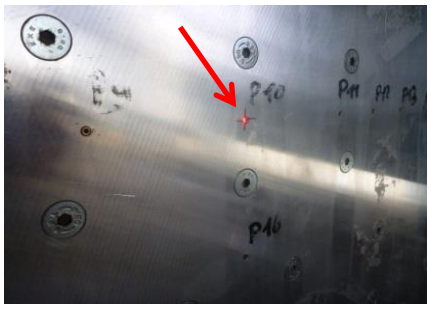

Figure 3.6: Impact at 45 degrees [18]

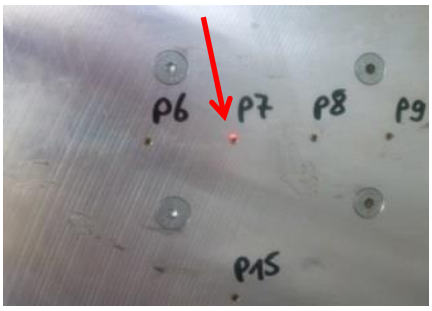

Figure 3.7: Impact at 90 degrees [18]

Each of the runs remains inside a launching group. To be able to compare the test results with the simulations, an average between all the time histories of the runs in the same group must be calculated.

For example, for the first launching group of 1 kg birds at 85 m/s and 90 degrees against the rigid plate, the time history of each run is plotted below:

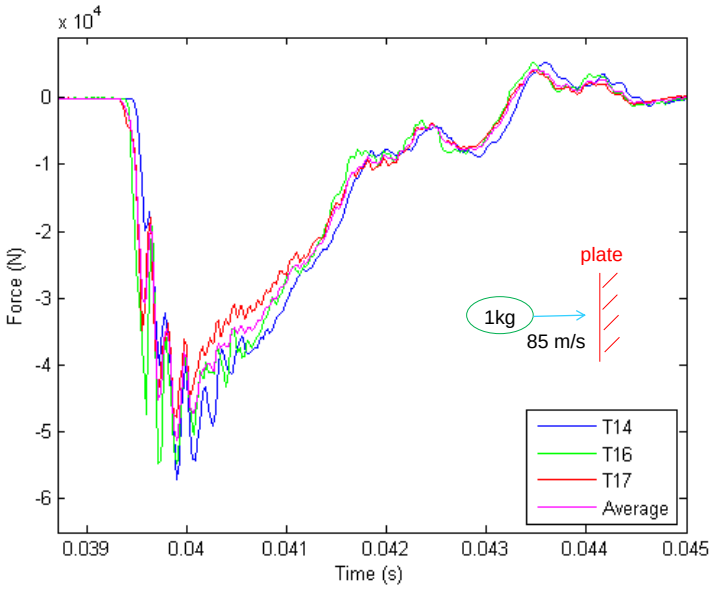

Figure 3.8: Runs for 1 kg projectile at 85 m/s and 90° impact

Test run number 14 has higher values for peak force compared to test 16 or 17. But as these tests are included in the same group, the average will be used for comparisons.

The rest of the groups for normal and oblique impact are also plotted:

Normal Impact

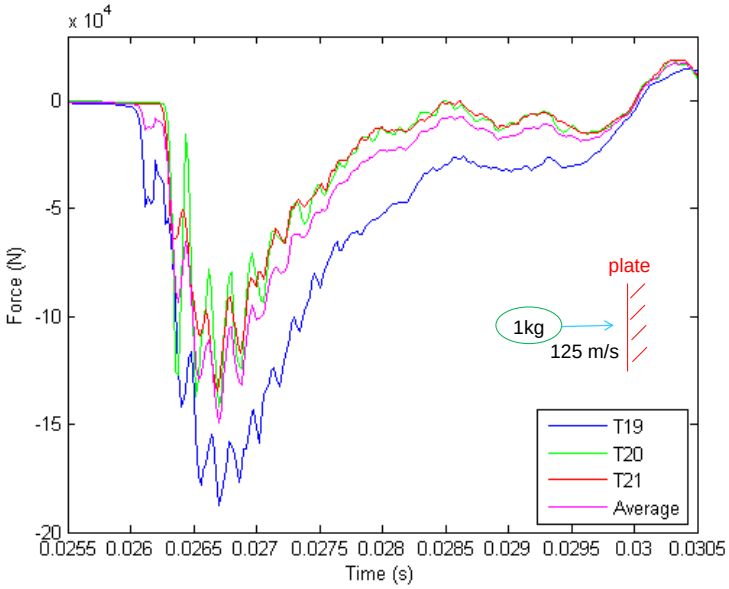

Figure 3.9: Runs for 1 kg projectile at 125 m/s and 90° impact

For the groups of 1 kg projectile at 125 m/s, test number 19 results tend to receive higher values for normal force, but as the particular

profile match with tests number 20 and 21, an average between the three of them is calculated and used for comparison.

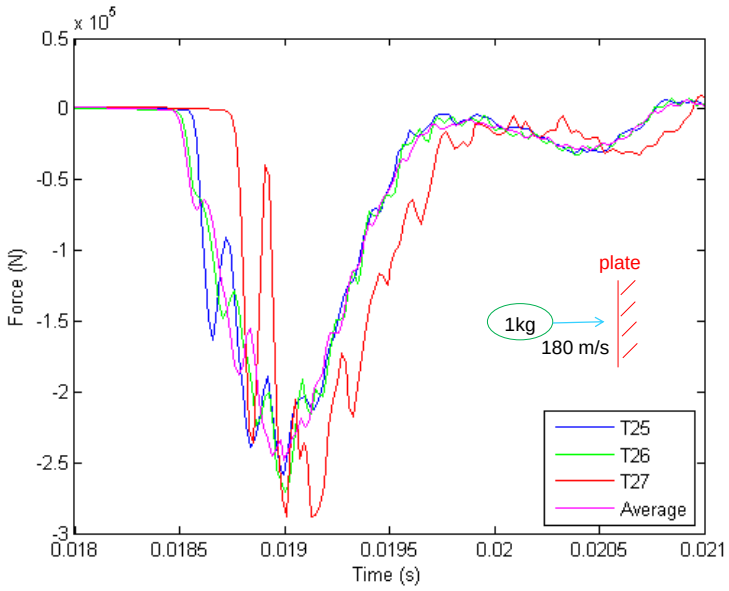

Figure 3.10: Runs for 1 kg projectile at 180 m/s and 90° impact

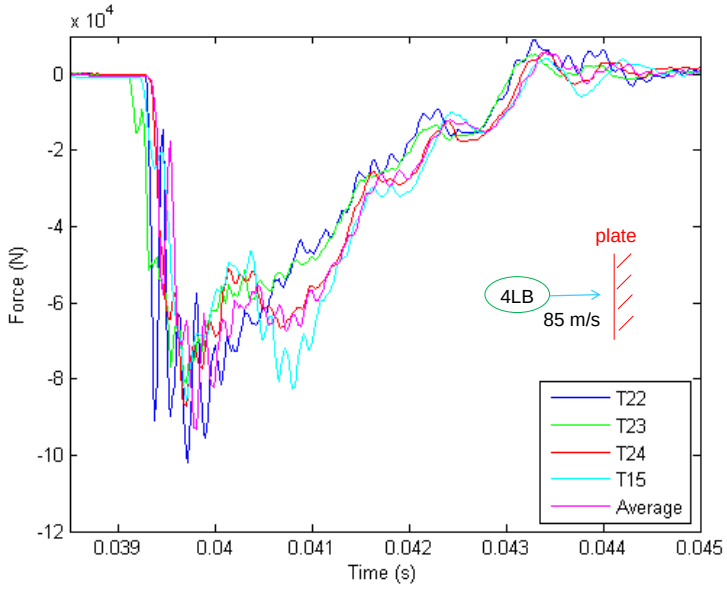

Figure 3.11: Runs for 4 LB (1.8 kg) projectile at 85 m/s and 90° impact

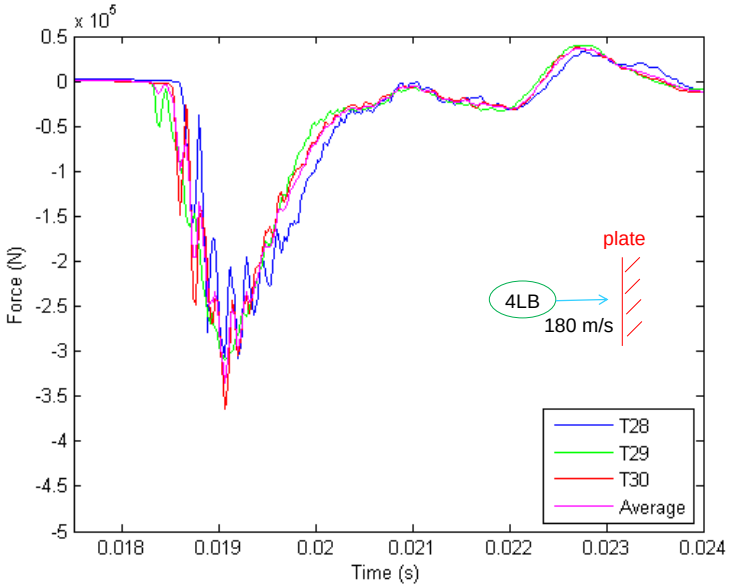

Figure 3.12: Runs for 4 LB (1.8 kg) projectile at 180 m/s and 90° impact

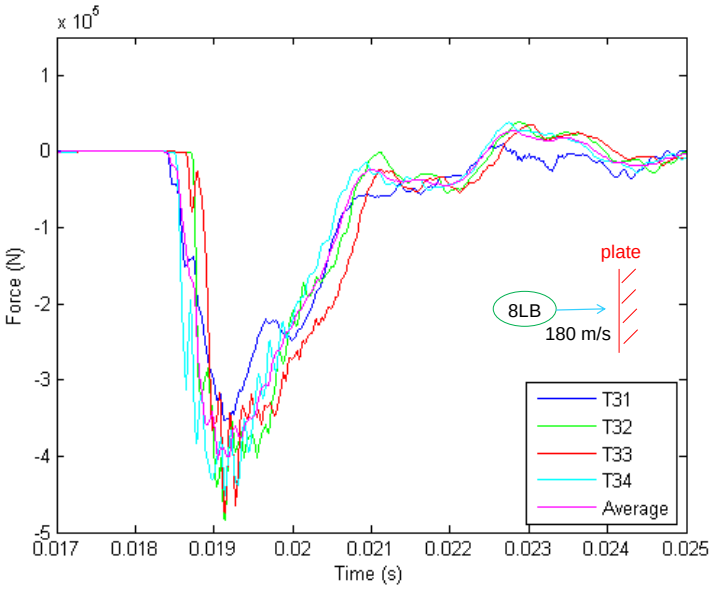

Figure 3.13: Runs for 8 LB (3.6 kg) projectile at 180 m/s and 90° impact

For the 8 LB projectiles at 180 m/s, four runs are analysed with same conditions instead of three. The four of them receive approximately same values for normal force.

Oblique Impact

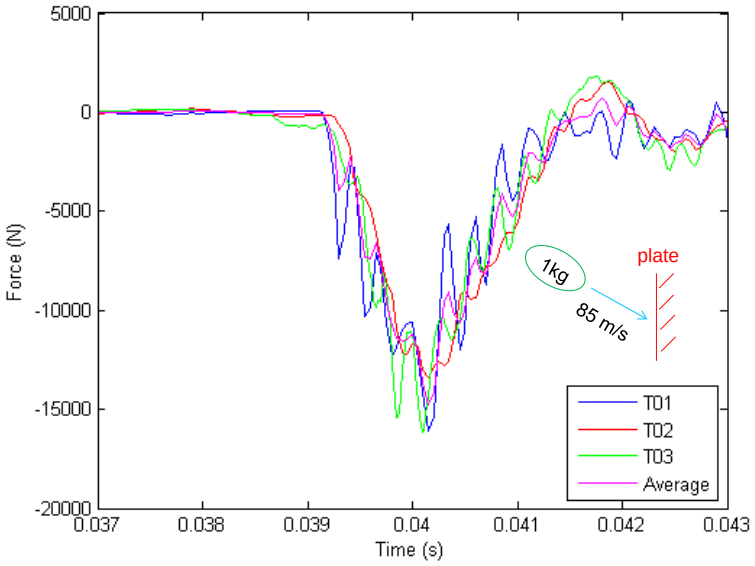

Figure 3.14: Runs for 1 kg projectile at 85 m/s and 45° impact

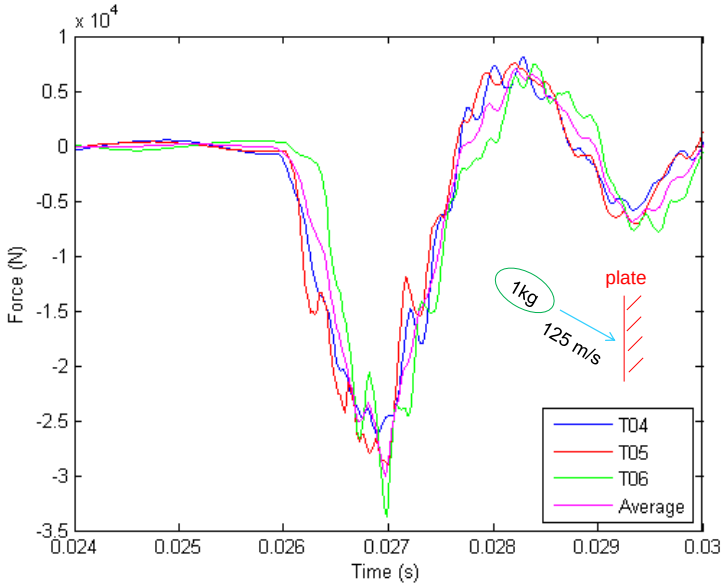

Figure 3.15: Runs for 1 kg projectile at 125 m/s and 45° impact

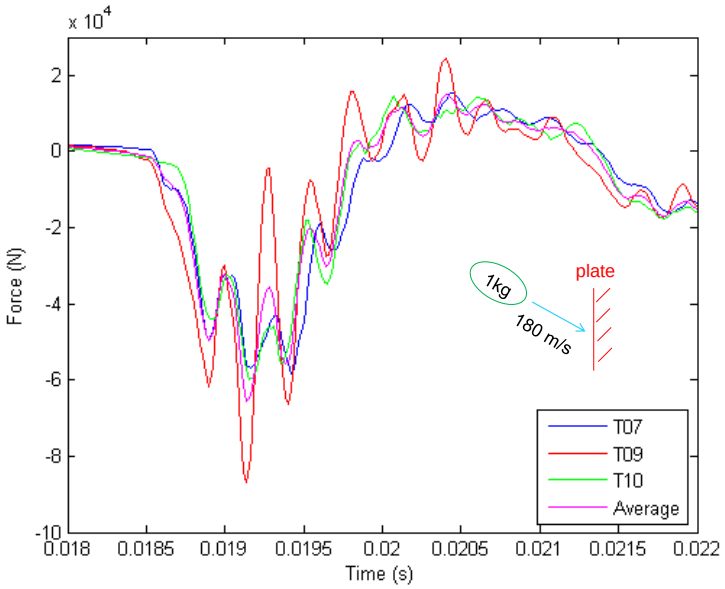

Figure 3.16: Runs for 1 kg projectile at 180 m/s and 45° impact

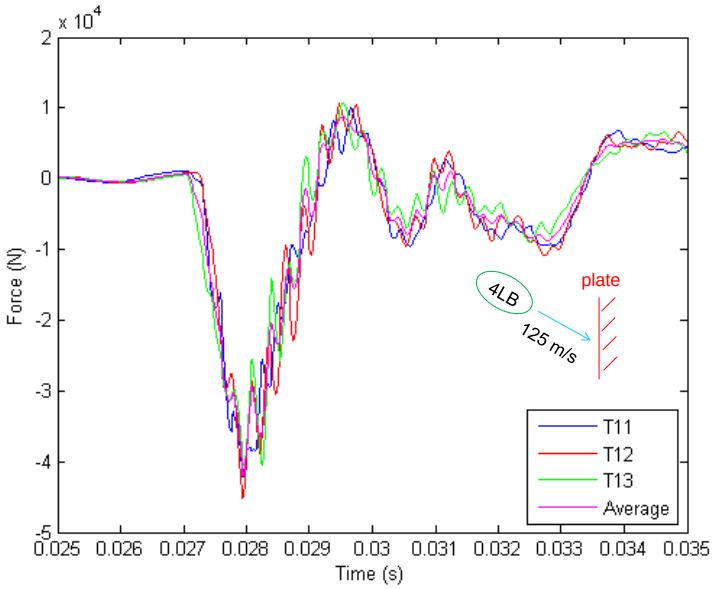

Figure 3.17: Runs for 4 LB (1.8 kg) projectile at 125 m/s and 45° impact

The graphs represented above can show how accurate were the results for the test launched in Germany. Although the tests complexity (different bird weights through an air compressed gun), all of the runs at each group represent very similar values for the force and the average calculated follows real and according information to the results. Likewise, the repeatability of the results is positive and satisfactory.

CHAPTER 4

NUMERICAL MODEL OF IMPACTORS USING SPH TECHNIQUE

4.1. GEOMETRY

For the correct simulation of the impacts, a projectile composed of SPH particles was developed. Taking into account the force results measured in the impacts against rigid flat plate, three projectiles (1 kg, 4 LB and 8 LB) were created.

The modelled projectile is formed by one cylinder attached to two semi spheres at it ends (see ***Figure 4.1***). It's the simplest and most efficient geometry for the measurements at impact, as was explained by Tamara Casillas in her thesis [8].

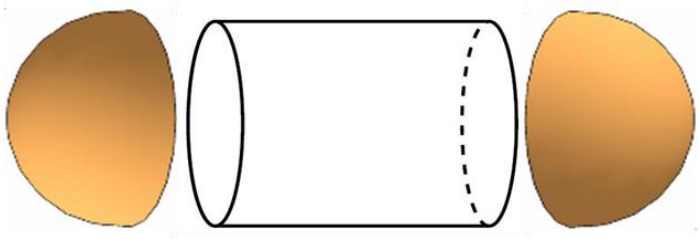

Figure 4.1: Geometry of the modelled projectile

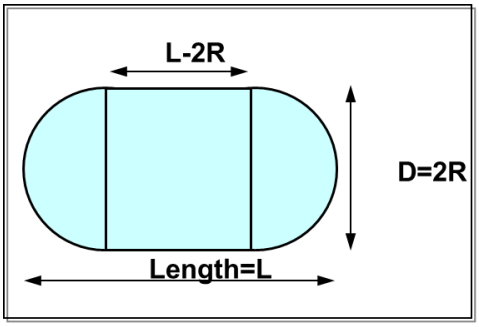

Figure 4.2: Dimensions of modelled projectile [8]

Two variables characterize the model of impactor: its length (L) and its radius (R).

For computing these values, experimental results for impact at 90 degrees and 45 degrees are handled.

4.2. POSTPROCESS OF EXPERIMENTAL DATA FOR NORMAL IMPACTS: BIRD DIMENSIONS ESTIMATION

The radius of the modelled projectile is calculated as a function of the experimental area of impact. The area of impact is defined as

$$A = \pi R^2 \qquad (21)$$

Being R the radius of the projectile. The area of impact can be understood as its section cut, in this case the area of a circle.

The peak force varies as following:

$$F_{peak}=\rho A u_o^{\,2} \quad [30] \qquad (22)$$

Being A the impact area and u_o the impact velocity.

The final density of the projectile is assumed as

$$\rho=962\ \frac{kg}{m^3} \quad [30] \qquad (23)$$

Being the density of the bird modelled as water and air and porosity z ≈ 0.1 [30].

Three weights of projectiles of 1 kg, 4 LB and 8 LB are studied:

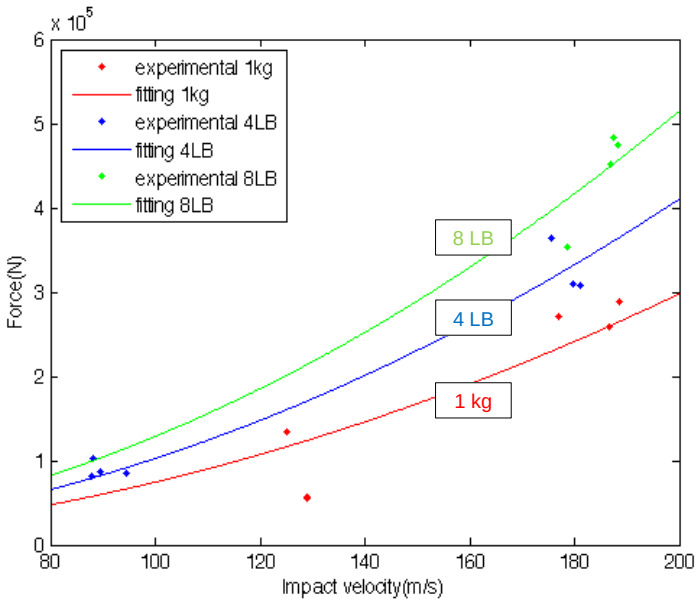

Figure 4.3: Peak Force as a function of impact velocity and bird weight

Lines represent the fitting curves for each weight to approximate the test results represented in dots. For three birds (1 kg, 4 LB, 8 LB) launched at the same velocity, the impact force is slightly higher for the 8 LB bird than the 1 kg bird. Force increases for higher kinetic energy impacts.

Knowing the fitting curves, the impact area can be computed and the radius for each of the three projectiles is found out.

Table 4.1: Dimensions for the modelled projectiles

Weight	Area	Radius
1 kg	7742 mm^2	$49.64mm$
4 LB	10660 mm^2	$58.25mm$
8 LB	13370 mm^2	$65.2mm$

The length of the projectile can be computed in two different ways:

a) As a function of experimental characteristic time of the impact

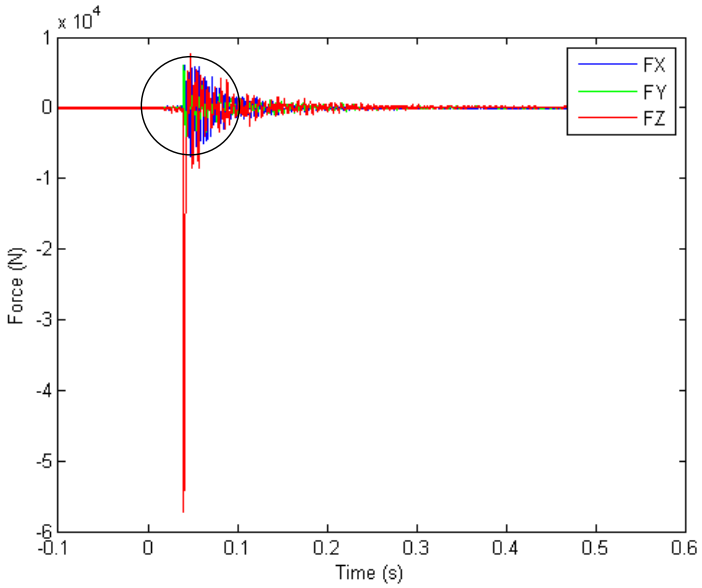

Figure 4.4: Force Time history Test 14

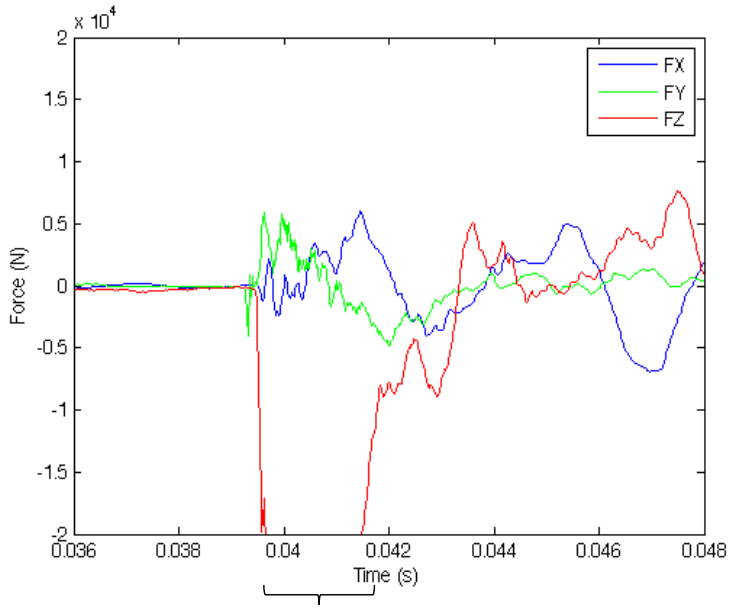

Figure 4.5: Force Time history Test 14 amplified

When plotting the time histories for each of the runs, the impact time can be computed. The impact time fulfils the range since the force increases from zero value till the force starts a periodic motion (see ***Figure 4.5***). The oscillatory motion is due to the response vibration of the target.

Table 4.2: Impact time for runs Test 14-Test 34

Test number	Group mass	Velocity(m/s)	Impact time (m/s)
T14	1 kg	86.5	1.98
T15	1 kg	94.5	2.14
T16	1 kg	87.4	1.92
T17	1 kg	80.3	1.98
T19	1 kg	128.9	1.9
T20	1 kg	128.9	1.7
T21	1 kg	125.2	1.7
T22	4 LB	88.0	1.9
T23	4 LB	87.8	2.16
T24	4 LB	89.5	1.96
T25	1 kg	186.5	0.9
T26	1 kg	176.9	1.14
T27	1 kg	188.5	0.9
T28	4 LB	181.0	1.3
T29	4 LB	179.7	1.4
T30	4 LB	175.6	1.4
T31	8 LB	178.7	1.58
T32	8 LB	187.5	1.54
T33	8 LB	188.4	1.6
T34	8 LB	186.8	1.5

The length of the projectile is computed as:

$$L = t_{impact} u_o \quad (24)$$

Three lengths are obtained by computing an average between every run of the same weight.

Table 4.3: Length dimensions for the modelled projectiles

Weight	Length
1 kg	190.5mm
4 LB	209.6mm
8 LB	288.2mm

b) As a function of experimental peak force

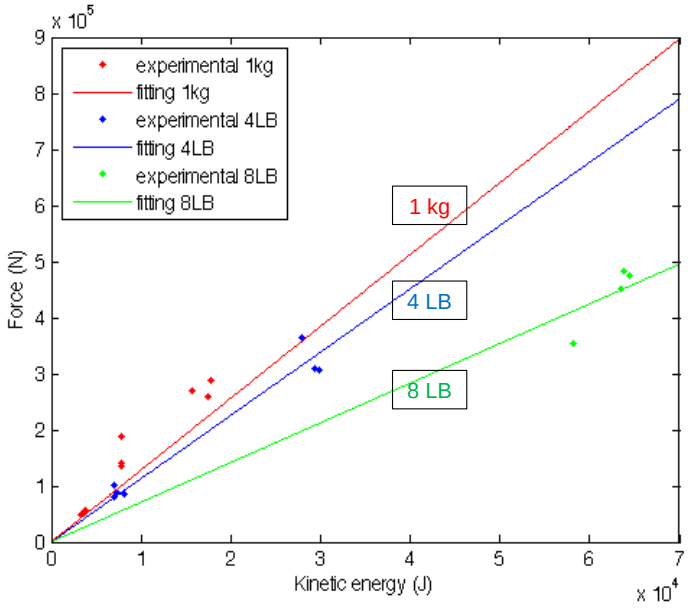

Figure 4.6: Peak Force as a function of kinetic energy

The relation between the kinetic energy and the peak force is:

$$F_{peak} = 2 \frac{A}{Vol} \left(\frac{1}{2} m u_o^2 \right) \quad (25)$$

$$\text{Where } Vol = \frac{m}{\rho} \quad (26)$$

$$\frac{A}{Vol} = \frac{1}{L - 2R + \frac{4}{3}R} \quad (27)$$

$$L = \frac{Vol}{A} + \frac{2}{3}R \quad (28)$$

M represents the three different weights and ρ the density of the projectile.

Table 4.4: Dimension values for the modelled projectiles

Weight	A/Vol	Radius	$L_{PeakForce}$
1 kg	6.403	49.64mm	198.3mm
4 LB	5.639	58.25mm	216.2mm
8 LB	3.538	65.2mm	326.1mm

Finally, an average between the lengths is computed and represented below.

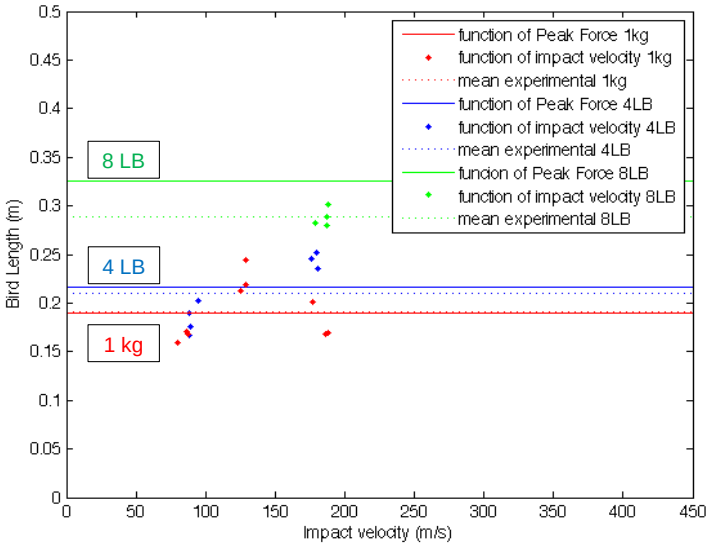

Figure 4.7: Comparison between lengths computed in different ways and average

The final results show that the average values cannot represent the real lengths of the projectile. When comparing results obtained from characteristic time of the impacts and the ones obtained from the peak force for the bird lengths, these last ones seem to be more coherent and approximated with real bird dimensions. For this reason, length computed from impact characteristic time has been discarded.

4.3. POSTPROCESS OF EXPERIMENTAL DATA FOR OBLIQUE IMPACTS: BIRD DIMENSIONS ESTIMATION

Following, the radius of the two modelled birds of 1 kg and 4 LB is computed:

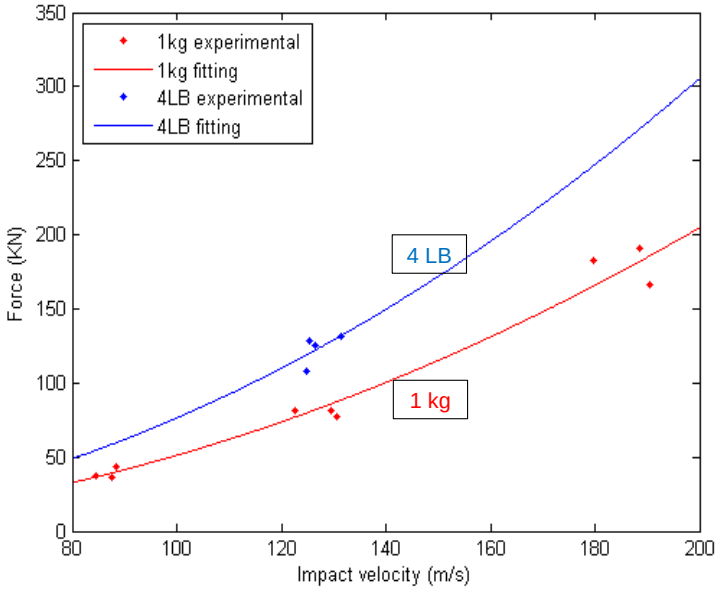

Figure 4.8: Peak Force as a function of impact velocity

Peak Force values are smaller than for 90 degrees impact.

$$F_{peak}=\rho A u_o^{\,2} \sin\left(\frac{\pi}{4}\right) \qquad (29)$$

Table 4.5: Dimensions for the modelled projectiles for impacts at 45 degrees

Weight	Area	Radius
1 kg	7522 mm^2	48.9mm
4 LB	11220 mm^2	59.8mm

Lately, the length taking into account the experimental peak force is calculated:

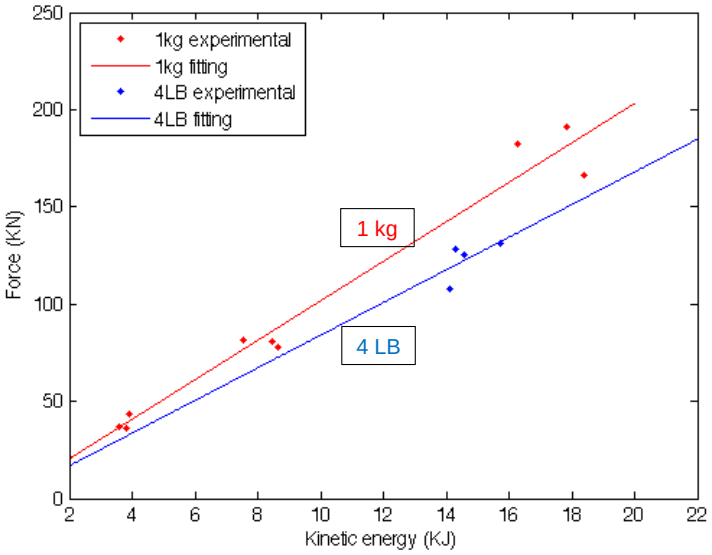

Figure 4.9: Peak Force as a function of kinetic energy

$$F_{peak}=2\,\frac{A}{Vol}\,\left(\frac{1}{2}mv^2\right)\,\sin\left(\frac{\pi}{4}\right)\,[30] \qquad \textbf{(30)}$$

The impact length of the projectile is called the efficient length. This value represents the sum of the actual and real length of the bird (L) and an extra component derived due to the oblique impact angle. The efficient length of the impact exemplifies the exact dimensions of the bird impacting against the flat plate.

$$(L_{eff})_{peakForce} = L + 2Rtan(\frac{\pi}{4})\ [30] \qquad \textbf{(31)}$$

Table 4.6: Dimensions for the modelled projectiles for impacts at 90 degrees

Weight	A/Vol	Radius	Length
1 kg	$7.178m^{-1}$	48.9mm	171.9mm
4 LB	$5.937\ m^{-1}$	59.8mm	208.3mm

4.4. FINAL BIRD FE MODEL DIMENSIONS

Conclusively, the final lengths and radius for the projectiles are formalized by computing the average between the results of impact at 90 and 45 degrees for the 1 kg and 4 LB projectiles. For the 8 LB projectile only results from normal impacts are used:

Table 4.7: Final Dimensions for the modelled projectiles

Weight	Radius	Length
1 kg	49.27 mm	185.1 mm
4 LB	59.03 mm	212.25 mm
8 LB	65.2 mm	326.1 mm

The results represented below are the final values for the dimensions of the modelled bird.

4.5. SPH DISTRIBUTION AND INTERNAL PROPERTIES OF THE BIRD MODEL

The modelled projectile is considered as a soft, isotropic, symmetric and homogeneous body because its yield point is one order of magnitude lower than the rigid target. Several references ([8], [23], [18] and [30]) suggest modelling the bird as a cylinder together with two semi spheres at its ends because it is closer in results as real birds. It is designed with Smoothed-particle hydrodynamics (SPH) method. One of its main advantages is that, due to the absence of a mesh, problems with irregular geometries can be easier to be solved. The modelled bird is considered as a set of particles or elements where all the characteristic properties such as density, are known. The particles are separated a distance called "smoothing length" where the computation of the properties of the particle can be obtained by summing the individual properties of each element inside this "smoothing length". The "smoothing length" is allowed to vary with time to adapt the properties according to its local conditions. This is the main difference with FEM method because particles in SPH can be distorted and modified to focalise in regions with higher density.

The most suitable program to develop the meshing of the bird is called Hyper Mesh, related to Hyper Works interface. Considering the geometry composed of one cylinder and two semi spheres and the values for radius and length, three projectiles of 1 kg, 4 LB and 8 LB are designed.

After defining the geometry, a 3-dimension mesh all over the model is plotted composed by hexahedral elements of 10 mm size. It is crucial that all the elements have the same dimensions. Once the elements are created, Pam Crash program transforms each element in SPH. The volume of each SPH corresponds to the volume of each hexahedral element.

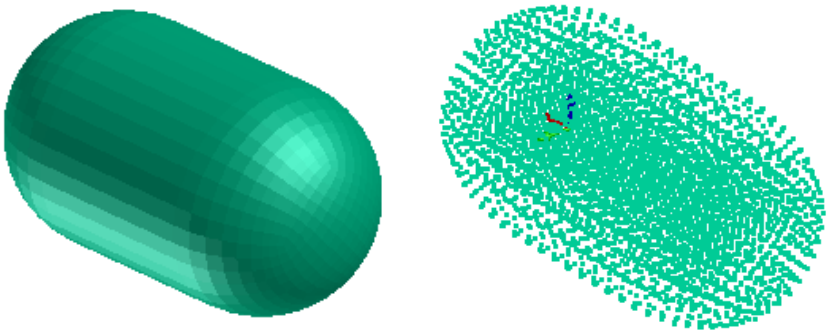

Figure 4.10: Projectile geometry as solid elements and SPH particles

Lately, the properties of the material for the three projectiles are derived. These properties are defined with Murnaghan equation of state:

$$p(Vol) = p_o + B[\left(\frac{\rho}{\rho_o}\right)^{\gamma} - 1] \quad [10] \qquad \textbf{(32)}$$

Equation 32 relates the volume of the projectile and the pressure it handles. Derived by Francis D. Murnaghan in 1944 he focused on high pressure conditions. "The more a solid is compressed, the more difficult is to compress it further" [21].

Descendent from continuum mechanics, the Murnaghan equation depends on two parameters: Bulk modulus or modulus of incompressibility (B), and specific heat ratio (γ) defined as the first derivative of the Bulk modulus with respect to the pressure

$$\text{Bulk Modulus (B=128000000 Pa)} \qquad \textbf{(33)}$$

$$\gamma = 7.98 \qquad \textbf{(34)}$$

Some more parameters are taken into account: viscosity parameters. As the projectile is deformed at the impact, its resistance to gradual deformation has to be adjusted. The deformation occurs by shear stresses or tensile stress existent because of the impact against a rigid surface at high velocities. Projectile´s material can no longer be considered as an inviscid fluid because it is resistant to shear stresses.

Dynamics and kinematic viscosity are the two constants that define the viscosity of the projectile:

$$\alpha = 1.5 \text{ mPa·s} \quad [8] \qquad \textbf{(35)}$$

$$\beta = 1.5 \text{ mPa·s} \quad [8] \qquad \textbf{(36)}$$

4.6. COMPARISON WITH AVAILABLE MODELS

Before developing a projectile model to simulate the test results against rigid flat plate and rigid edge surfaces, two different projectile models were studied:

4.6.1. Initial Model

The initial model consists on a "structured model" composed of Lagrangian elements. "Structured model" means that the distance between SPH is equal (between all of the SPH in the structure) and the volume of each of the SPH is the same. It was the first model used for simulations and gave approximated but not accurate results.

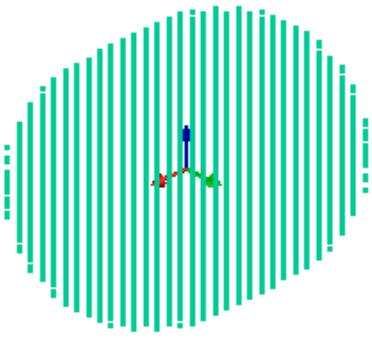

Figure 4.11: Initial Model of projectile

4.6.2. Improved Model

Modelled and mentioned by Tamara Casillas in her thesis [8], the CRAVHI SPH projectile consists on an "unstructured distribution" of SPH particles. "Unstructured distribution" means that the distance between SPH and the volume of each SPH is different between all of them. It was developed from the Lagrangian Model to improve simulation results due to the SPH distribution. SPH particles showed better affordance to large deformations because each SPH acts like independent.

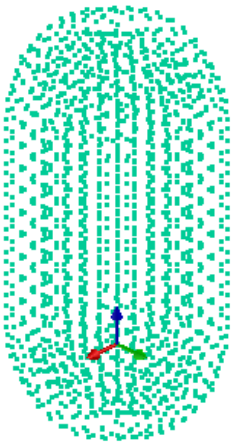

Figure 4.12: Improved Model of projectile

4.6.3. Optimized Model

The last model created follows the same distribution SPH as CRAVHI and the properties and geometry explained above.

This last model was developed to succeed the results obtained at simulations compared to test results. Improved from CRAVHI model because of its geometry and agreeing to the values measured for real projectiles, the only variable modified from CRAVHI is the dimensions, the rest of the properties remain constant due to its exceptional results.

CHAPTER 5

NUMERICAL SIMULATION OF IMPACTOR AGAINST FLAT PLATE

5.1. NUMERICAL METHOD USED IN THE SIMULATIONS

To develop and analyse the simulation for the impact of birds at a rigid plate, Finite Element Method (FEM) is applied. Finite Element Method is a numerical technique used for the approximation of partial differential equation numerical results. It is usually applied for relatively sophisticated and convoluted geometries. The body, structure or continuum is divided in an elevated number of non-intersecting sub-domains defined as "finite elements". In between each of the finite elements, some characterized points are distinguished. They are called nodes. The combination of the nodes together forms a mesh.

This method is being used due to its various advantages: incorporation of disparate materials for the same part, better definition and easier representation and embodiment, generalization to accomplish convoluted domains in two or three dimensions, etc.

The development of the mesh is usually done at specified computer programs called mesh generators at a pre-processing stage. At each of the nodes, the number of degrees of freedom is defined according to its relations of affinity and accordance. The set of relations at a node can be written as a linearized system of equations called stiffness matrix. The number of equations will be proportional to the number of nodes of the mesh. At pre-processing stage, geometry and boundary conditions are defined as well as definition of the materials for each of the parts. The next stage is the calculation, which evaluates the non-dependant time results of the pre-processing. It creates a set of N equations and N variables which can be solved dependently or independently. Last stage is the post-processing where the results at calculation are analysed. Discretization is characterized by the values of a certain set of functions at each node of the mesh. Additionally, determination of errors and interpolation can be carried out.

A relevant characteristic about FEM is its convergence. When narrower elements are being considered, the numerical results will converge much closer to the explicit solution of the system of equations.

FEM was firstly established by Richard Courant in 1943 [20]. He used Ritz method for vibrational operations, where a system of equations was developed after applying equations of equilibrium at each node in the mesh:

$$f=K\ u \quad [20] \qquad (37)$$

Where f represents the forces at the nodes, K is the stiffness matrix and u belongs to the displacement at the nodes. With this information, stresses can be subsequently identified in the elements.

For the bird splitting simulation, explicit FE method will be used. This type of methods doesn't require the exact resolution of the non-trivial system of equations at each time-step of the process. Very small time-step is required rather than the time-step for implicit methods. Although they are not unconditionally convergent methods, the time-step should be computed in advance, based on the time needed by the stress wave to propagate through the smallest element.

5.2. SOFTWARE CODE SELECTED: VPS (FORMERLY PAM-CRASH)

The analysis is performed using Virtual Performance Solution 2010 explicit solver (formerly PAM-CRASH).

PAM CRASH in particular remains as the ESI package specialized in crash and impacts simulations. It was firstly used at nuclear and aerospace applications such as a simulation of a military plane crashing into a nuclear power plant in 1978.

5.3. SPECIMEN STRUCTURE MODEL

The rigid plate finite element model consists on a linear elastic isotropic thick squared shell composed of 16913 elements and 17074 nodes. It is composed of three parts:

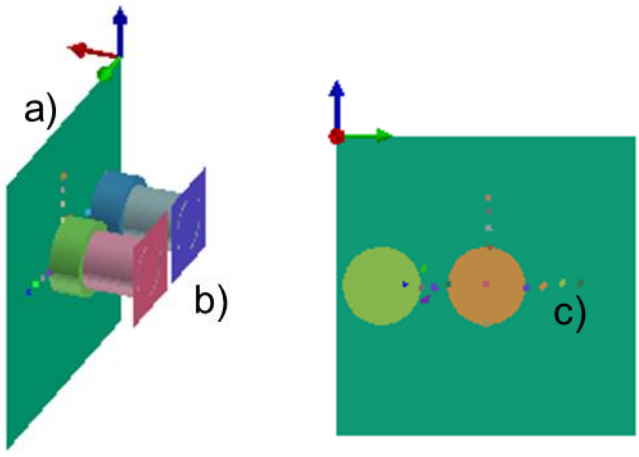

Figure 5.1: Parts of the numerical simulation for rigid plat plate

a) Flat plate
b) Rigid load cells
c) Pressure sensors

For the flat plate (a), the material used is Aluminium 5083 with density of 2660 kg/m^3 and Young Modulus of 72GPa. The matrix related to this material is defined in PAM CRASH as MAT ELASTIC 4-NODED THICKSHELL LAGRANGIAN.

Table 5.1: Main properties of the modelled target

Target Property	Units
Length	1499.558 mm
Height	1020 mm
Thickness	10 mm
Tapered angle	0 degrees

For appropriate comparison with test results, loads at Load Cells (b) will be figured in the main output.

Behind the plate, two load cells (b) (right and left) are installed to record the forces in the three directions x, y and z. At an impact of 90 degrees with respect to the plate the projectile is actually impacting on the centre cell, indeed the real results are recorded for this cell. The left cell records additional data for the better understanding of the impact test results. At an impact of 45 degrees with respect to the plate, the projectile impacts in between the two cells. Data at the centre and left load is recorded. The two cells can be clearly appreciated in ***Figure 3.29***. Load cells have been modelled as very rigid and with very similar geometry that the ones used in the tests. They are used for loads recovery from the numerical simulation at some positions as it was measured during the tests.

Located along the rigid plate, 17 pressure sensors (c) are settled to record how is the force varying from one sensor to another. It is easy to predict that the local forces at the pressure sensors adjoining the right cell are going to be larger than those located a distant apart. Some of this pressure sensors are going to record a magnitude force tending to zero due to its location.

- Transducers modelling

The pressure transducers have been modelled as SPH pressure gauge particles. They are SPH particles "not visible" to regular particles but that can prove the properties of the nearby particles within a spherical region with radius equal to twice the smoothing length. For such gauges, the pressure is evaluated as the weighted average of all its neighbour particles.

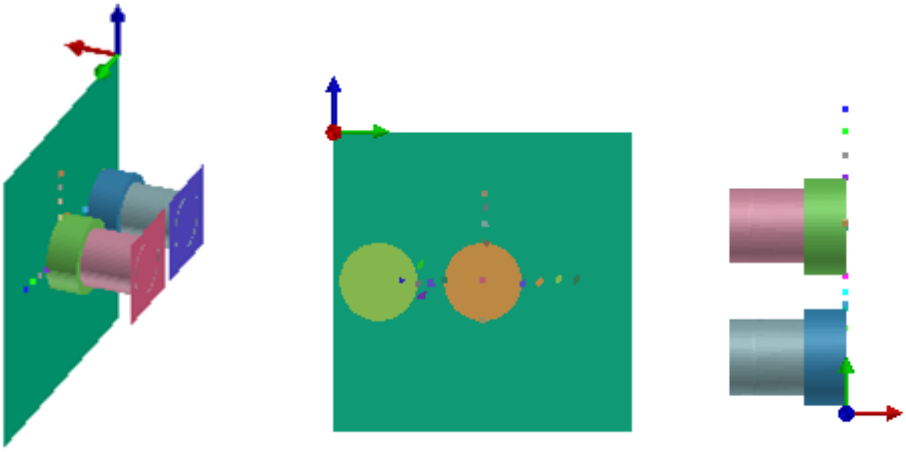

Figure 5.2: Views of numerical model of rigid plate at PAM CRASH

The three projectiles modelled before are introduced into de numerical model of the plate for each run.

- Contacts

But for the model to perform the bird impact simulation properly, a contact must be specified. The most relevant contact is the one relating the projectile with the plate, a type NON-SYMETRIC NODE-TO-SEGMENT WITH EDGE TREATMENT that has been defined in PAM CRASH.

- Initial and boundary conditions

These are the initial impact velocity of the modelled projectile with the flat surface, which will remain in between a range of 85 and 180 m/s; and the boundary conditions based on fixing the plates at the bottom of the load cells.

- Outputs

Lastly, it’s absolutely important to define which points, elements, nodes, parts or sections are going to display the output. These will be the right and left cells behind the rigid plate, and their supports, which leads to four outputs. All these outputs are necessary to compare the results obtained with the experimental simulation.

5.4. NUMERICAL SIMULATION RESULTS

The simulations that have been performed for the normal bird impact against the rigid flat plate are:

- Impact at 90 degrees measured at centre cell
  - ❖ 1 kg at 180 m/s
  - ❖ 4 LB at 180 m/s
  - ❖ 8 LB at 180 m/s

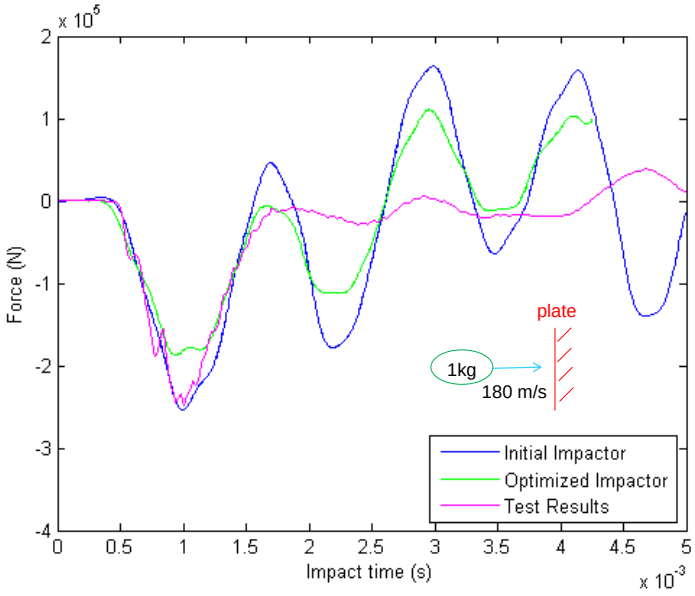

Figure 5.3: Initial approach 1 kg projectile at 180 m/s and 90 degrees impact angle

The optimized impactor (in green colour and the one defined above in this thesis) is assumed to approach the best results to test results. As seen in the graph, results for initial impactor (blue colour in the graph) seem to be closer to the peak force obtained in the test. However, the overall response of the structure is not close to the response obtained in the tests (there is a huge vibration). This means that a re-examination of the structural model has to be performed to improve the numerical simulation results.

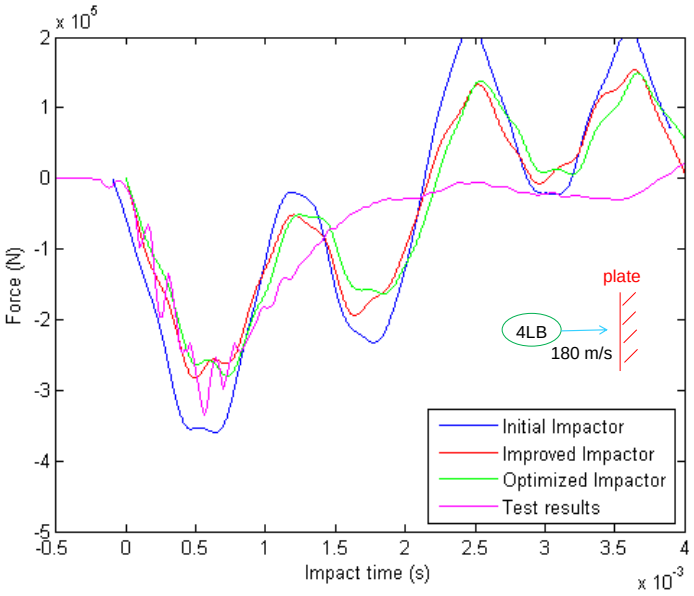

Figure 5.4: Initial approach 4 LB projectile at180 m/s and 90 degrees impact angle

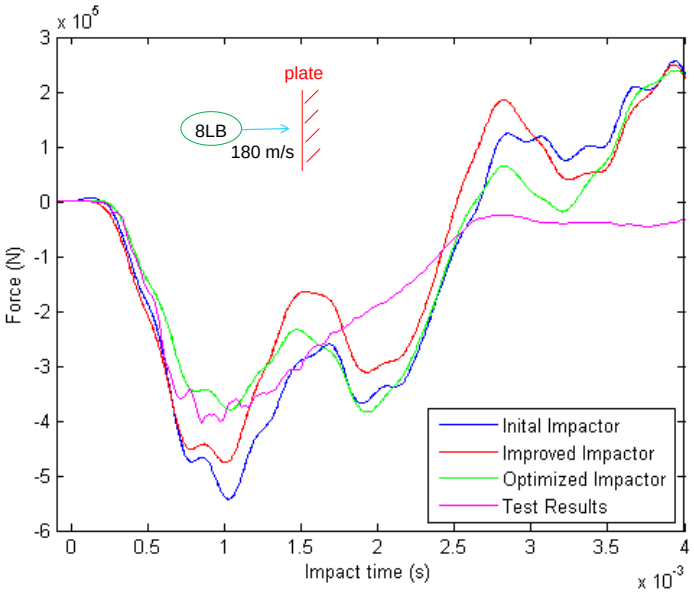

Figure 5.5: Initial approach 8 LB projectile at 180 m/s and 90 degrees impact angle

As the kinetic energy starts to increase to considerable values, results for the optimized impactor (in green colour) approximate quite better to test results rather than the initial impactor(in blue colour). The values for the peak forces at impact are obtained with accurate precision for high kinetic energy impacts, but yet the simulation response oscillation needs to be improved.

5.5. REVISION OF THE FE MODEL AND SENSITIVITY ANALYSIS

As seen in the figures for the initial approach of the model for 1 kg, 4 LB and 8 LB projectiles, the optimized impactor is not always the best approximation to test results. This phenomenon is due to the vibrations in the response after the moment of impact. The modelled load cells in the simulation seem to be creating an unrealistic vibration in the model of the structure.

As it seems that the load cells in the test are more rigid that as have been modelled before, to reduce the vibrations in the global response the load cells are removed from the model. To adjust a better model to test results and optimize the simplified model, three improvements will be better studied:

1. Variation of the friction coefficient in right and left cells to improve oblique impacts.
2. Variation of the thickness of the flat plate from 7 cm to 1 cm to improve oblique impacts.
3. Changing model boundary conditions to optimize global response.

Variation of the friction coefficient in right and left cells

For the impact against rigid plate at 45 degrees, there are two section forces to be measured. As the projectile impacts in between the centers of the two cells (center and left) in the positive direction of Y and negative direction of X, the variation of the parameters will vary from one cell to another.

When changing the friction coefficient from $\mu=0$ to $\mu=0.2$ and assuming the normal force is constant for both cases because the mass and the gravity is not changing, the value of the friction force will be slightly higher for the second friction coefficient.

For the right cell the particles being measured are moving in the positive direction parallel to the plate and the friction force will be opposing the movement in its negative direction. Friction force will increase in the negative direction parallel to the plate. On the opposite hand, for the left cell the particles are moving in the negative direction parallel to the plate, and so, the friction force will be increasing in its positive direction.

As the normal force (force in the Z direction) is depending on the friction force, for the right cell the total force in the normal direction will decrease when increasing the friction coefficient and the opposite will happen with the left cell.

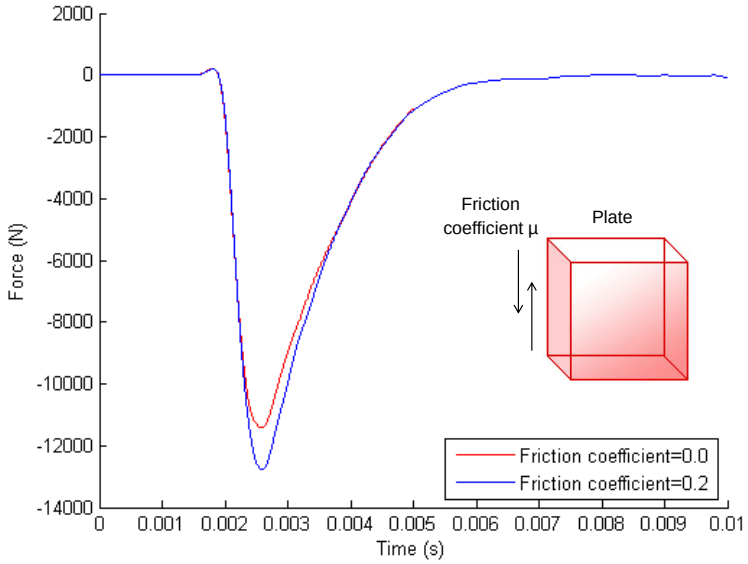

Figure 5.6: Variation of the friction coefficient for a 1 kg bird at 85 m/s and 45 degrees of impact angle

Variation of the width of the plate

When decreasing the thickness of the target, the friction force will decrease and the total force will increase due to the flexibility of the plate. Changing the width of the target from H=0.07 m to H=0.01 m, turns the friction force of the right cell to be smaller in the negative direction parallel to the plate. The friction force of the left cell turns to be smaller in its positive direction due to the movement of the particles.

To sum up, let`s conclude that for absolute values of the force when increasing the friction coefficient, the right cell will decrease its total force and the left will increase it.

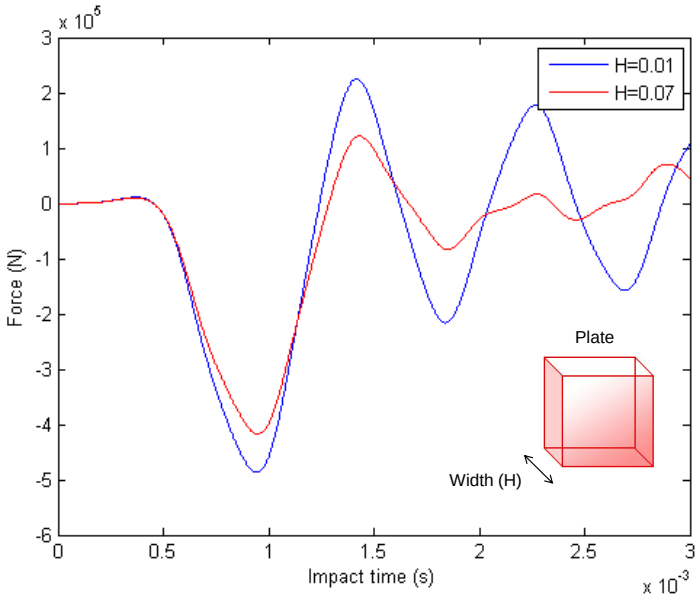

Figure 5.7: Variation of the width of the plate for the same impact at 90 degrees of impact angle with friction coefficient of μ=0.2

Changing model boundary conditions

For the initial approach of the model, the plates at the bottom of the load cells are completely clamped which means they are not able to rotate either translate in any of its three axes.

After removing the load cells, boundary conditions have been applied on the plate (plate is clamped in the sections where the load cells were).

In ***Figure 5.8*** a schematic representation can be seen. The boundary conditions are defined by 6 coordinates; 3 for translation in x, y and z axis and 3 for rotation in the three directions. Number 1 for the coordinates represent fixed boundary conditions (no translation/rotation) and number zero represent free conditions (able to translate/rotate).

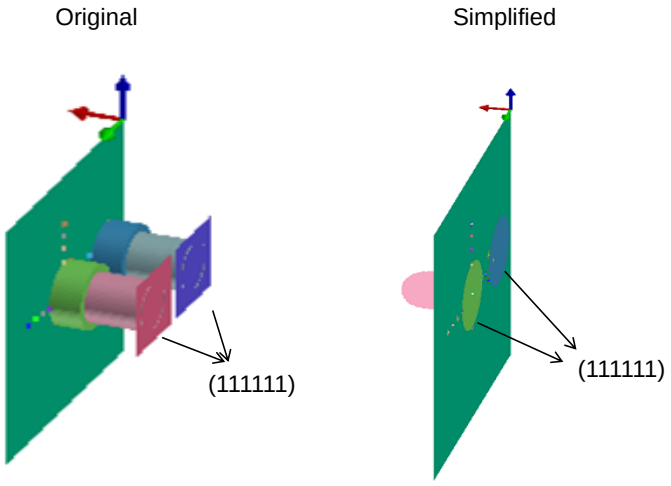

Figure 5.8: Comparison of the boundary conditions between original model and simplified model. Condition (111111) represents no translation either rotation.

5.6. NUMERICAL SIMULATION RESULTS WITH IMPROVED "SIMPLIFIED" FE MODEL

The runs for the simulations are the same cases for the runs in the test:

- Impact at 90 degrees analysed at centre cell
  - 1 kg at 85 m/s
  - 1 kg at 125 m/s
  - 1 kg at 180 m/s
  - 4 LB at 125 m/s
  - 4 LB at 180 m/s
  - 8 LB at 180 m/s
- Impact a 45 degrees analysed at both cells (left and centre)
  - 1 kg at 85 m/s
  - 1 kg at 125 m/s
  - 1 kg at 180 m/s
  - 4 LB at 125 m/s

Normal Impact

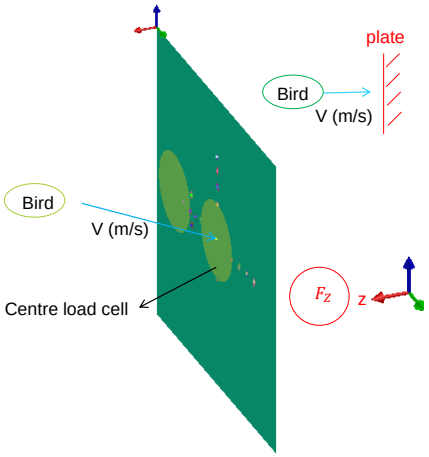

Figure 5.9: Brief summary about the normal impact, forces measured and location of these measurements

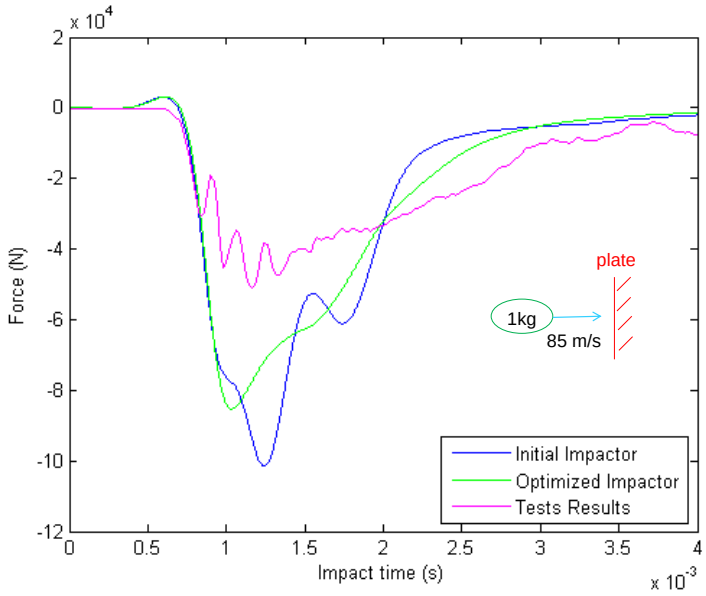

Figure 5.10: Simplified model 1 kg projectile at 85 m/s and 90 degrees impact angle

The optimized impactor (green colour in ***Figure 5.10***) represents a better approximation than the initial impactor (blue colour) for the simplified model simulation. As seen in the graph, the response oscillations from the simulation have disappeared after the impact and trend to represent much better the results of the tests.

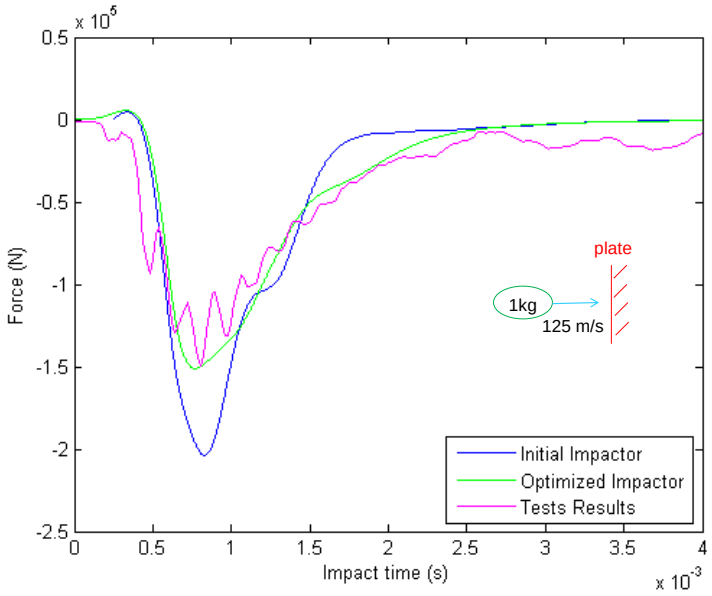

Figure 5.11: Simplified model 1 kg projectile at 125 m/s and 90 degrees impact angle

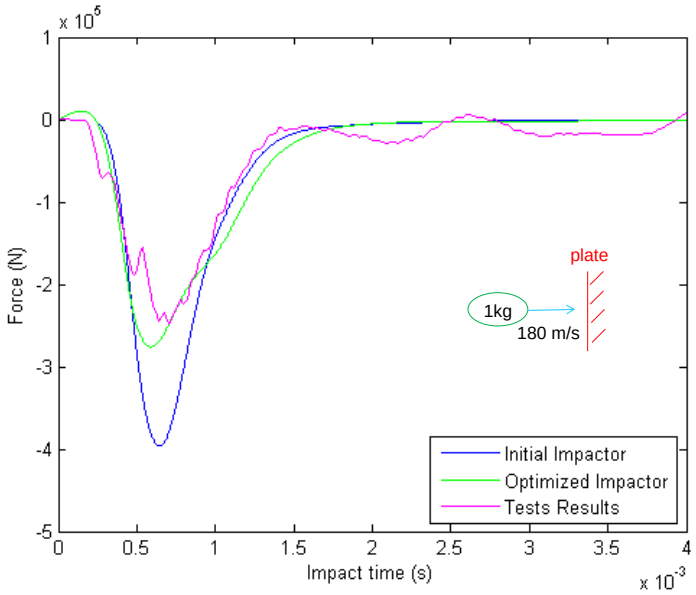

Figure 5.12: Simplified model 1 kg projectile at 180 m/s and 90 degrees impact angle

For higher velocities launching with the same weight projectile, this means higher kinetic energies, the optimized impactor follows the finest outcome.

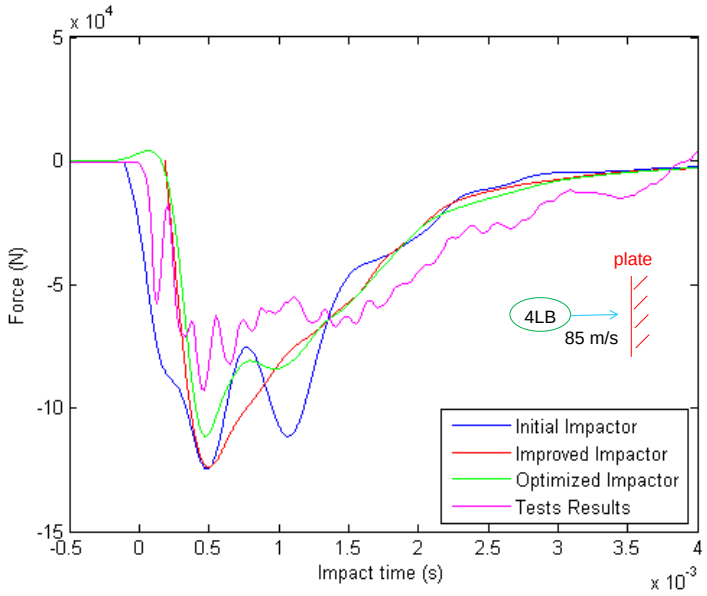

Figure 5.13: Simplified model 4 LB projectile at 85 m/s and 90 degrees impact angle

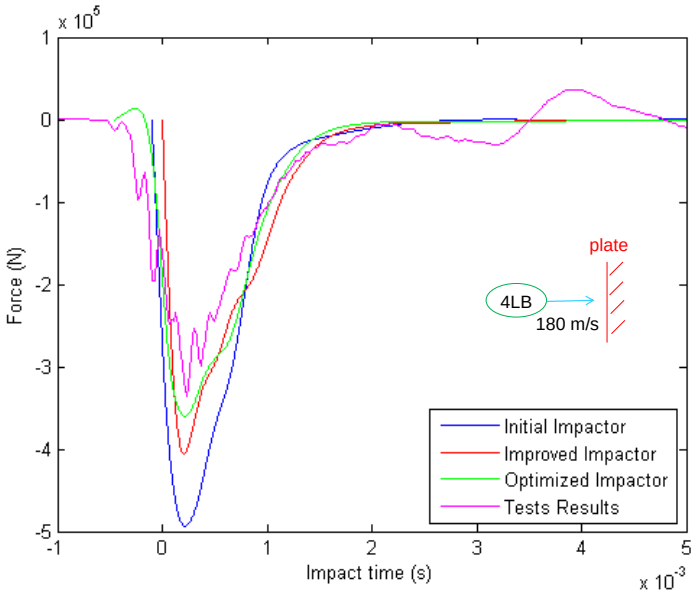

Figure 5.14: Simplified model 4 LB projectile at 180 m/s and 90 degrees impact angle

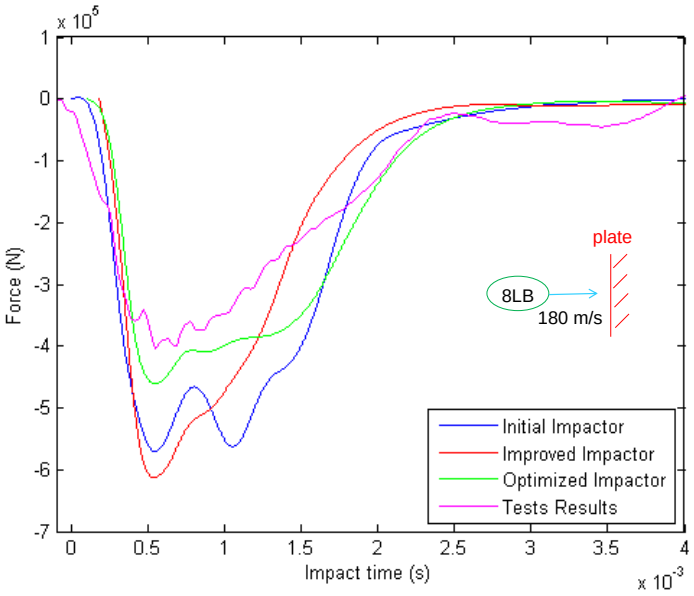

Figure 5.15: Simplified model 8 LB projectile at 180 m/s and 90 degrees impact angle

There is a very good adjustment of numerical simulation results with tests in terms of peak force and duration of the impact. The correlation is even better as the kinetic energy increases.

Oblique Impact

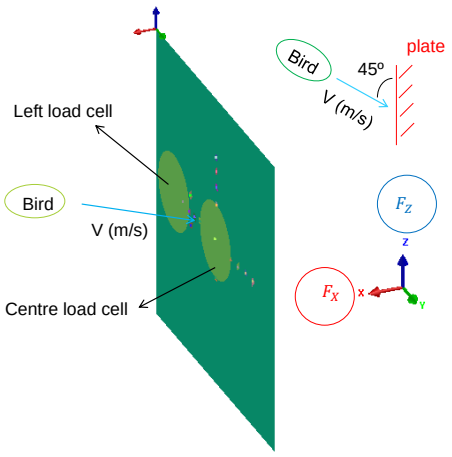

Figure 5.16: Brief summary about the oblique impact, forces measured and location of these measurements

For an oblique impact at 45 degrees against the rigid flat plate, two results of forces are analysed in two different directions: F_X represents the parallel direction to the plate and F_Z represents the normal direction to the plate.

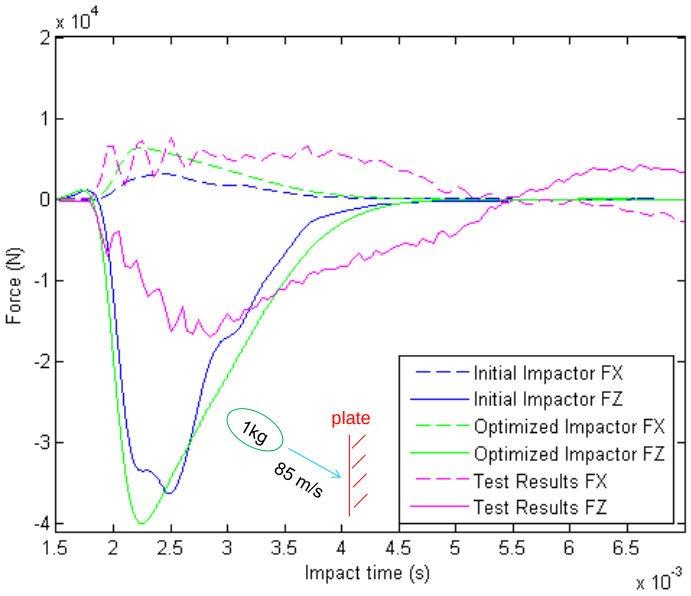

Figure 5.17: Simplified Model 1 kg projectile at 85 m/s and 45 degrees impact angle at Left load cell

The values for F_X are relatively lower than F_Z due to the boundary conditions and properties of the plate. As z axis is the normal direction to the plate, x and y axis represent the length and height of the plate. For an oblique impact in the x and z directions against a plate of such characteristics, the force in the x direction is always smaller than the force measured in the normal direction to the plate.

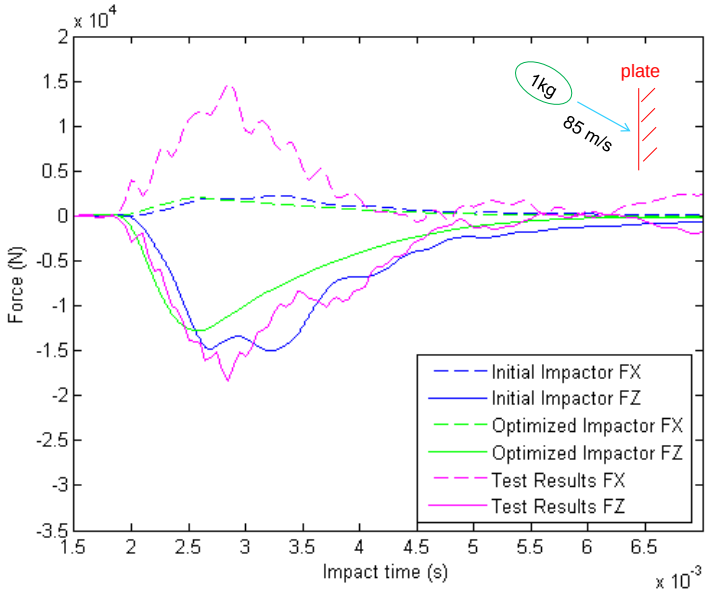

Figure 5.18: Simplified Model 1 kg projectile at 85 m/s and 45 degrees impact angle at Centre load cell

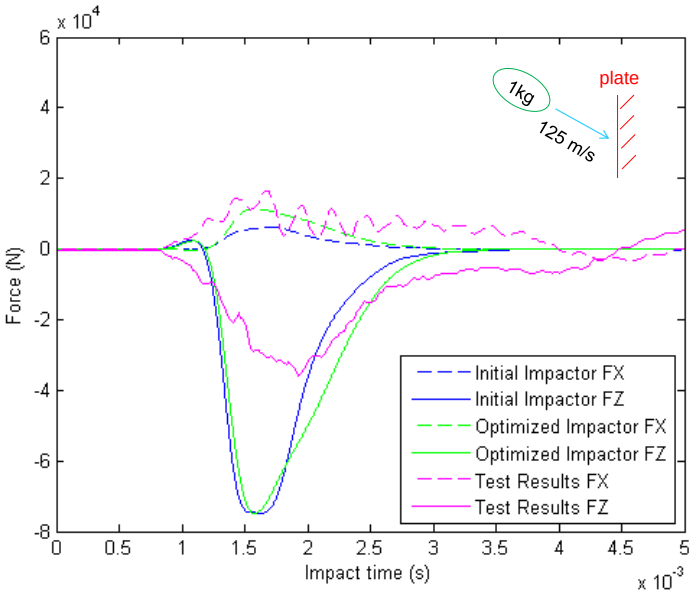

Figure 5.19: Simplified Model 1 kg projectile at 125 m/s and 45 degrees impact angle at Left load cell

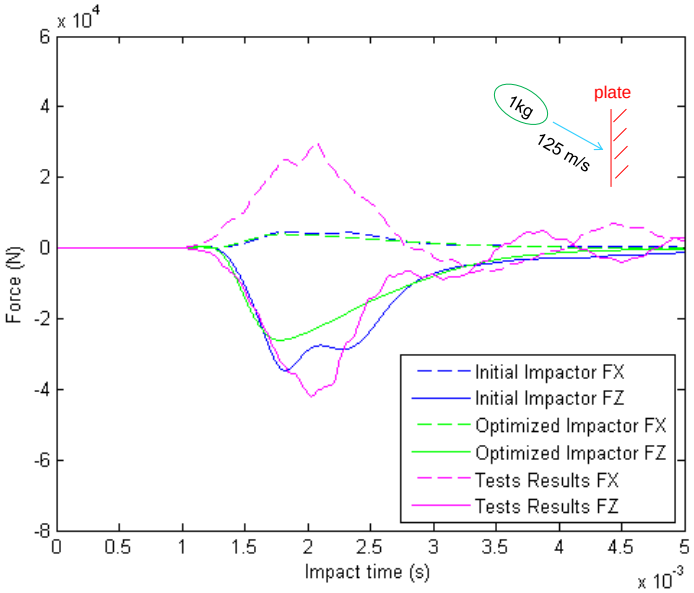

Figure 5.20: Simplified Model 1 kg projectile at 125 m/s and 45 degrees impact angle at Centre load cell

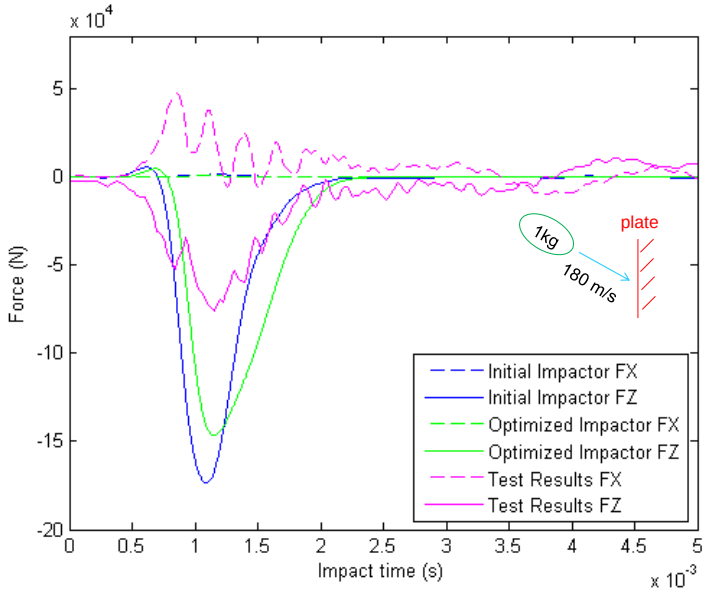

Figure 5.21: Simplified Model 1 kg projectile at 180 m/s and 45 degrees impact angle at Left load cell

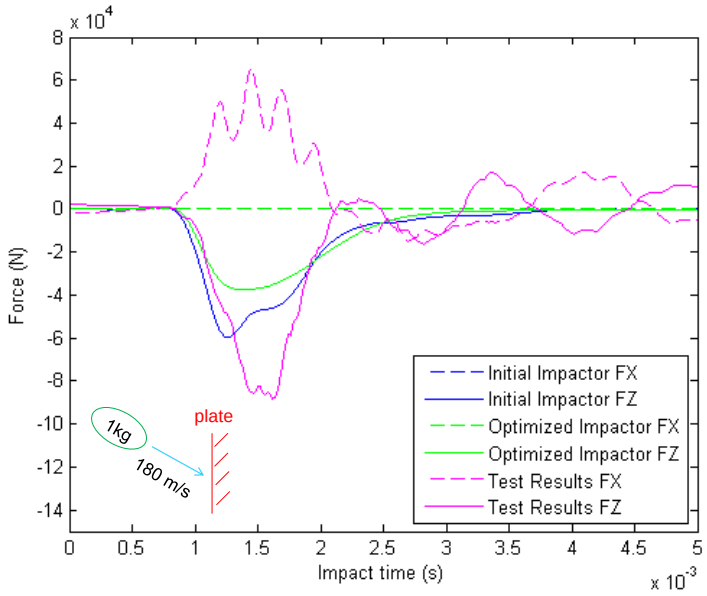

Figure 5.22: Simplified Model 1 kg projectile at 180 m/s and 45 degrees impact angle at Centre load cell

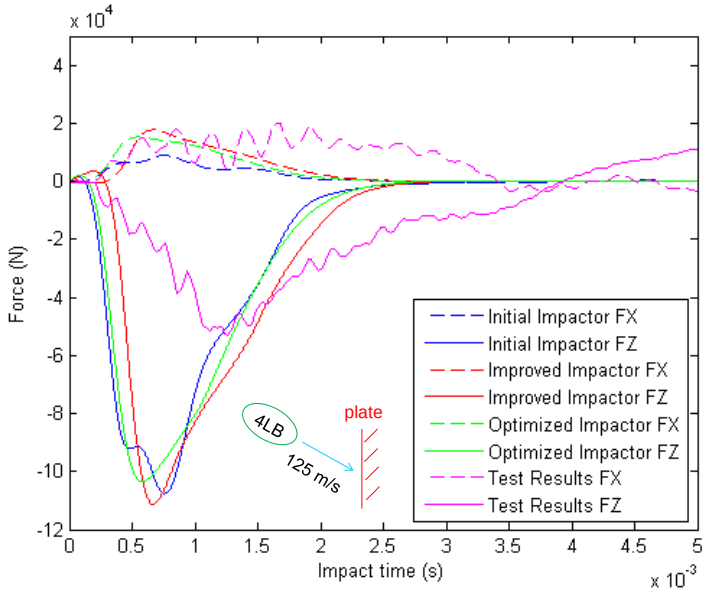

Figure 5.23: Simplified Model 4 LB projectile at 125 m/s and 45 degrees impact angle at Left load cell

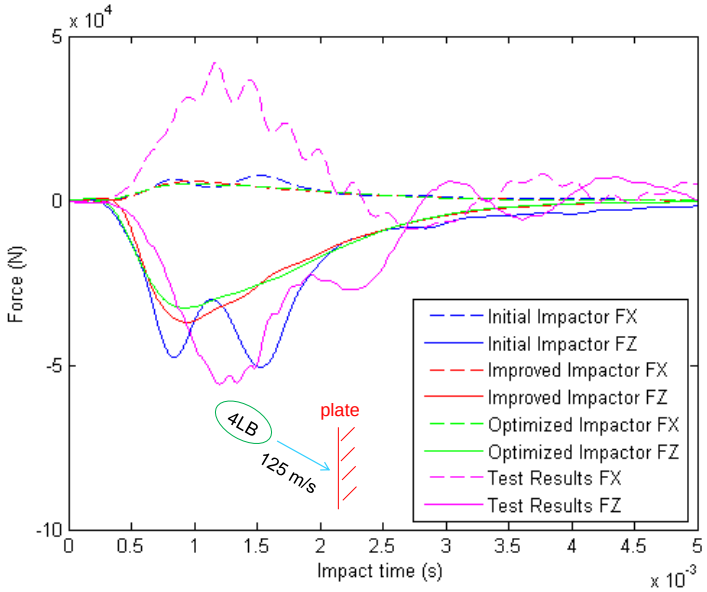

Figure 5.24: Simplified Model 4 LB projectile at 125 m/s and 45 degrees impact angle at Centre load cell

For the forceF_X, results at left load cell are more accurate than the ones obtained in the centre load cell. This can be due to the fact that the symmetry of the plate with respect to the impact is changing because for an impact at 45 degrees, the impact point is no longer in the centre of the plate.

As seen in some graphs, F_X and F_Z tend to have coincident values in some concrete groups of tests. This phenomenon could be because the

impact point in the plate represents a more sophisticated symmetry than in the simulation.

As well as for normal impact, the oscillation is no longer existing and the simulation results in more accurate outcomes for high kinetic energy impacts.

CHAPTER 6

NUMERICAL SIMULATION OF IMPACTOR AGAINST RIGID EDGE

6.1. AVAILABLE TEST RESULTS

The process of launchings of projectiles against rigid edge follows the same pattern as for the rigid flat plate.

Firstly, the projectile is weighted inside the capsule to identify the different group masses, and lately the projectile is thrown through the air compressed gun at the required velocity.

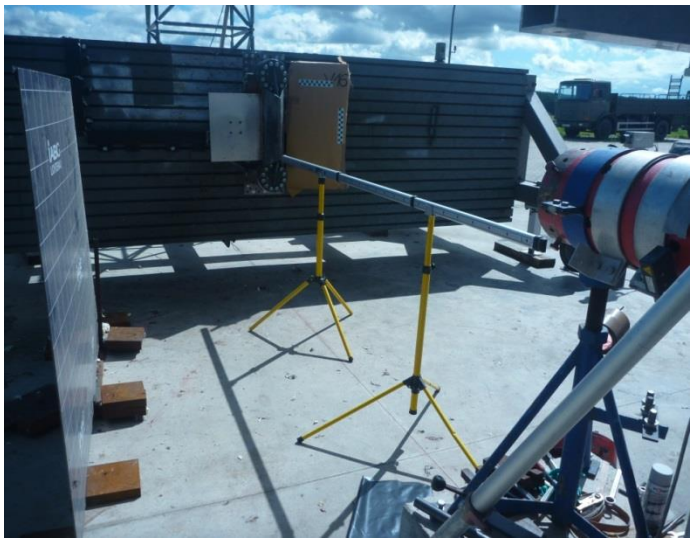

Figure 6.1: Scenario for impact against rigid edge [18]

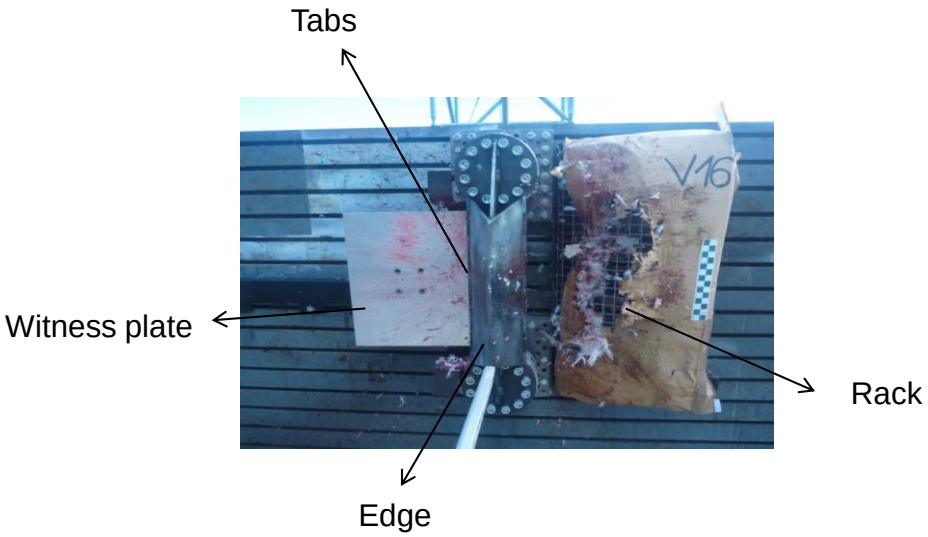

Figure 6.2: Scenario for rigid edge test [18]

The main parts of the rigid edge summarize:

- **Edge**

The rigid edge is the first part the bird impacts with at the launching. The bird splits at the contact moment with the edge in two different parts (not necessary have to be equal). The edge is the most important part of the launching because it represents the splitting of the bird.

- **Tabs**

One of the parts of the bird (left one) travels through the edge to impact against the tabs.

- **Witness Plate**

After the impact against the tabs, the bird ends at the witness plate. The main function of the witness plate is measure the force received by one of the parts of the bird to evaluate how much force is lost during travelling of the bird, and to know how much mass has each of the parts of the birds.

- **Rack**

The other part of the bird (right one after splitting against the edge) travels through the edge till the rack. The rack has no measurement of the forces but keep the bird safe.

Table 6.1: Runs at 22.5 degrees [18]

Test #	Set up	Impact angle	Bird mass [g]	Group mass	Target Vel. [m/s]	Velocity [m/s]
01	Rigid Edge	22.5°	1010	1 kg	85	86.9
02	Rigid Edge	22.5°	1017	1 Kg	85	83.3
03	Rigid Edge	22.5°	1001	1 kg	85	85.1
04	Rigid Edge	22.5°	1828	4 LB	180	188.9
05	Rigid Edge	22.5°	1813	4 LB	180	187.7
06	Rigid Edge	22.5°	1810	4 LB	180	185.0

Table 6.2: Runs at 90 degrees [18]

Test #	Setup	Impact angle	Bird mass [g]	Group mass	Target Vel. [m/s]	Velocity [m/s]
07	Rigid Edge	90°	998	1 kg	85	83.4
08	Rigid Edge	90°	1018	1 kg	85	85.3
09	Rigid Edge	90°	1006	1 kg	85	87.9
10	Rigid Edge	90°	1819	4 LB	125	130.4
11	Rigid Edge	90°	1820	4 LB	125	132.7
12	Rigid Edge	90°	1822	4 LB	125	130.8
13	Rigid Edge	90°	1819	4 LB	180	182.6
14	Rigid Edge	90°	1822	4 LB	180	177.0
15	Rigid Edge	90°	1839	4 LB	180	178.0
16	Rigid Edge	90°	3449	8 LB	125	152.0
17	Rigid Edge	90°	3454	8 LB	125	147.0
18	Rigid Edge	90°	3498	8 LB	125	148.1
19	Rigid Edge	90°	3624	8 LB	180	184.0
20	Rigid Edge	90°	3644	8 LB	125	131.0
21	Rigid Edge	90°	3606	8 LB	125	127.0
22	Rigid Edge	90°	3650	8 LB	125	128.0
23	Rigid Edge	90°	3652	8 LB	180	175.1
24	Rigid Edge	90°	3609	8 LB	180	179.9
additional tests						

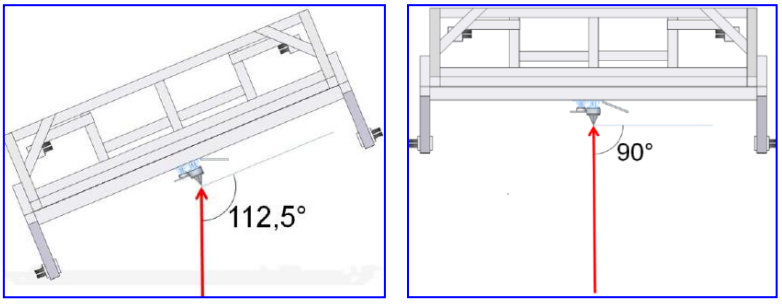

Figure 6.3: Representation impacts at 22.5 and 90 degrees [18]

Impact of projectiles against a rigid edge surface consists in three important phases:

1. Splitting in two parts
2. Impact against Tabs
3. Impact against Witness Plate

Figure 6.4: Phases a rigid edge impact [18]

Firstly, the bird impacts against the tip of the rigid edge with the required velocity at each run. It is important to notice that the rigid edge forms 22.5 degrees with the vertical axis. At this moment, the projectile splits in two parts. These two parts do not necessary have to be equal in mass or in size, it depends on the conditions of the launching. Let's analyse the left half of the projectile. After the splitting, it will travel through the edge until it reaches the tabs. The tabs are located below the edge and consist on a small border of the plate connecting the end part of the ends of the edge. At phase 2, the half of the projectile will impact against the left tab and this impact will be seen in the time history of the peak force.

Lastly, the half projectile will continue its trajectory by impacting against the witness plate. This plate is instrumented with one load cell at its bottom. The load cell will measure the time history data for the forces.

As for the impact runs for rigid plate, the test for rigid edge are analysed as terms of average between runs of the same group to take into account all possible scenarios. The variables measured are the forces at each phase. The forces are measured on the normal direction to the witness plate and the rigid edge (top and bottom load cells). Not only the forces will be analysed and compared, but the impulses. The impulses will be calculated using a relation between the time histories and the forces at each phase. The time histories are analysed at three different moment or phases:

1. Impact against the edge (bird splitting)
2. Impact against tab support
3. Impact against witness plate

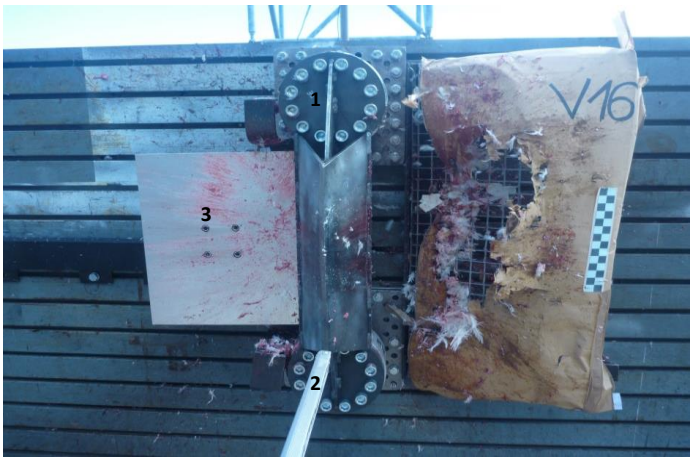

Figure 6.5: Load Cells at rigid edge model [18]

Load cells number 1 and number 2 represent the top and bottom cells. These cells record the time history at the splitting moment (phase 1) and at the tab impact (phase 2) because they are still located at the rigid edge. On the other hand, load cell number 3 located at the witness plate records the time history of the forces at the impact moment of the half projectile against the witness plate (phase 3). This load cell is not located anymore at the rigid edge structure, but below and separated.

6.1.1. Splitting analysis: post process of the test results

- Hypothesis: the objective of this section is to stablish which is the percentage of energy absorb by the splitting of the bird. As the weight of the birds and the speed tested with the rigid edge are the same than tested with the rigid plate, the following hypothesis can be done:

The impulse received by the rigid edge represents the sum of the three contributions during impact on the rigid edge:

TOTAL IMPULSE=Impulse Split + Impulse Tab + Impulse Rest ***(38)***

Assuming (based on test measurements evidence), a similar duration and slope of impulses time histories, this expression may lead to a simplified approximation like:

$$F_{Z_{Rigid\ Edge}} = F_{Z_{Split}} + F_{Z_{Tab}} + 2\frac{F_{Z_{Rest}}}{\cos 22.5} \quad \textbf{(39)}$$

The total force of the rigid edge remains as the sum of the splitting force of the projectile, the impact tab force and twice the witness plate force divided by the cosine of 22.5°.

Being the impulse the integral of the force F_Z over the time interval of the impact such as:

$$I = \int_{t_o}^{t_f} F_Z(t)\, dt \quad \textbf{(40)}$$

The impulses are analysed for the test comparing the rigid edge and the rigid plate results as following:

- Normal Impact
  - ❖ 1 kg at 85 m/s
  - ❖ 4 LB at 180 m/s
  - ❖ 8 LB at 180 m/s

The graphs for the force time history of all the groups of runs in the test are going to be represented to show the explicit moment when the splitting, impact against tabs and impact against witness plate occurs. Lately, impulse time history is plotted to determine the values at the three moments calculated before. Finally, a statistical representation of the splitting, impact against tabs and impact against witness plate is represented against the value for an impact against a rigid flat plate. This is done for both forces and impulses.

Normal Impact 1kg projectile at 85 m/s

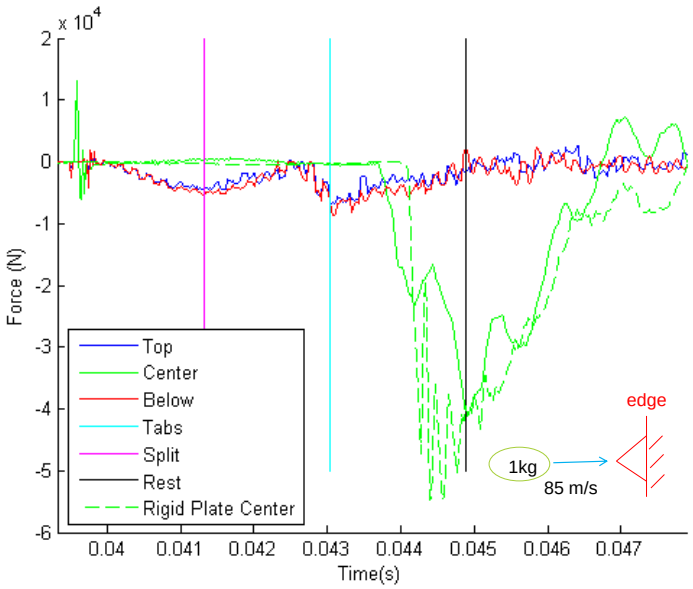

Figure 6.6: Force time history for a normal impact of 1 kg projectile at 85 m/s

The impact of the projectile against the rigid edge represents the splitting moment (pink colour in ***Figure 6.6***). When the half of the projectile impact against tabs (light blue) the force in the normal direction to the witness plate increases to its maximum value for the top and bottom cells. The rest of the projectile finally impacts against the witness plate (black colour) and the centre cell receives its maximum value. Rigid plate results for $F_Z$compare the peak values with respect to the witness plate.

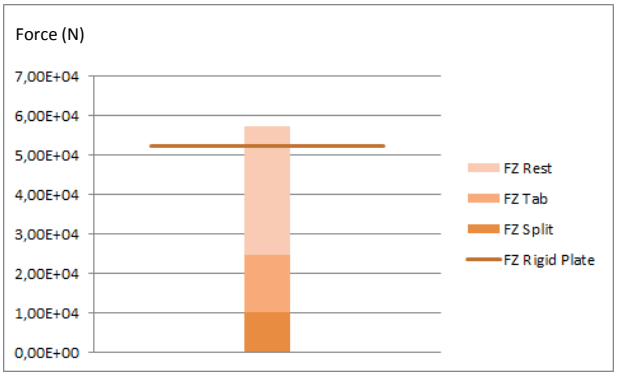

Figure 6.7: Statistical values for impact force for a normal impact of 1 kg projectile at 85 m/s

The splitting force represents 19.23 % of the rigid flat plate force.

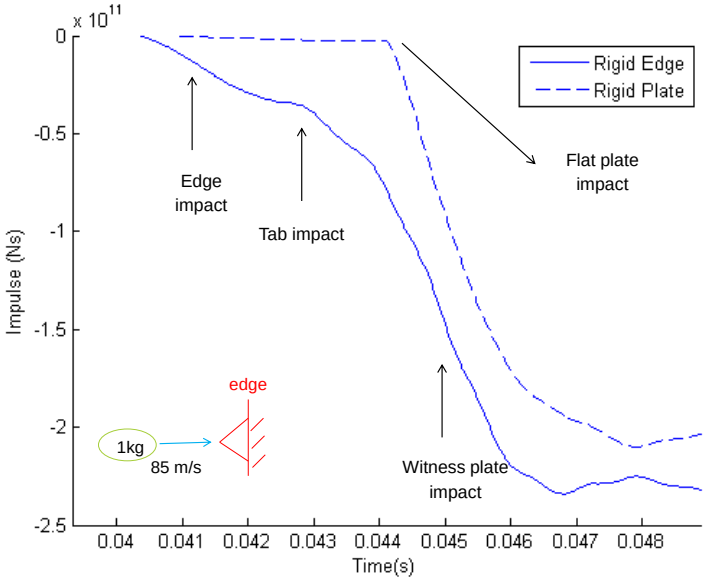

Figure 6.8: Impulse time history for a normal impact of 1 kg projectile at 85 m/s

Locating the specific times for the impact against rigid edge, against tabs and against the witness plate, impulses can be estimated in the previous graph. The rigid flat plate impulse follows a quite noticeable step after zero value, which represents the start impact of the projectile against the plate.

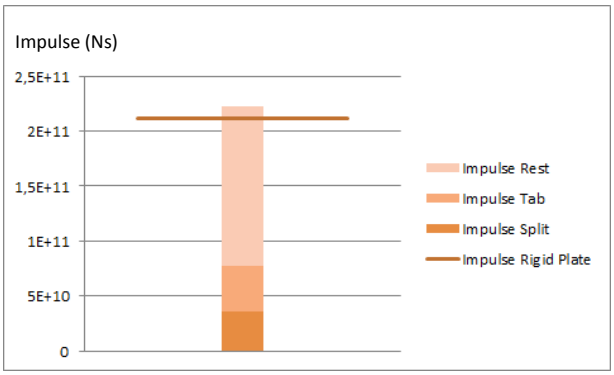

Figure 6.9: Statistical values for impulses for a normal impact of 1 kg projectile at 85 m/s

The splitting impulse represents 18.18 % of the rigid flat plate impulse.

Normal Impact 4 LB projectile at 180 m/s

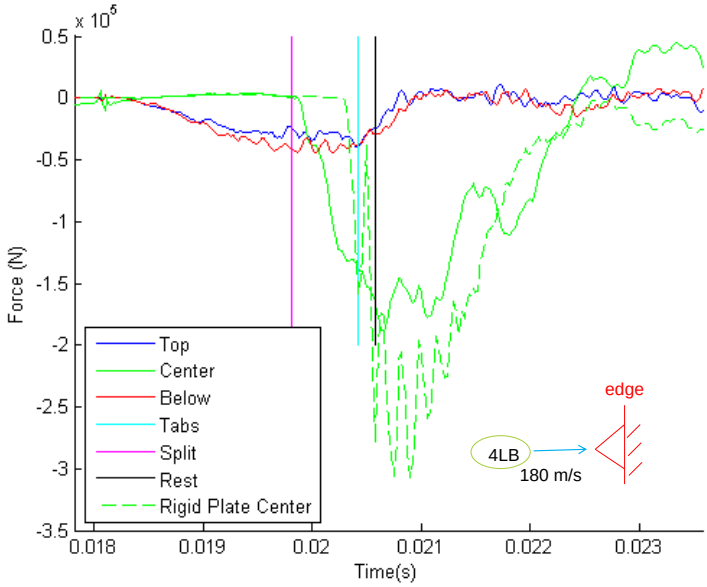

Figure 6.10: Force time history for a normal impact of 4 LB projectile at 180 m/s

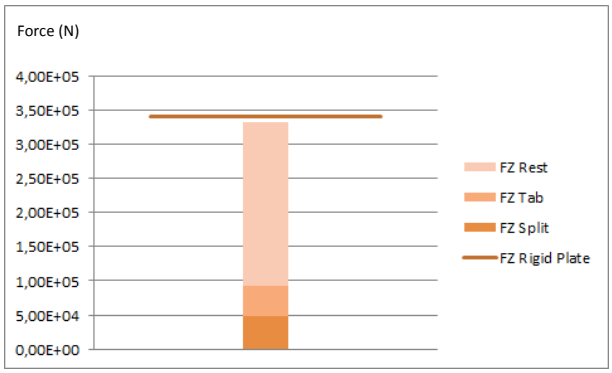

Figure 6.11: Statistical values for impact force for a normal impact of 4 LB projectile at 180 m/s

The splitting force represents 14.45 % of the rigid flat plate force. The total flat plate force represents approximately the same amount as the sum of the three contributions for the rigid edge impact. This information requires that the concrete simulation is surpassing than expected developed.

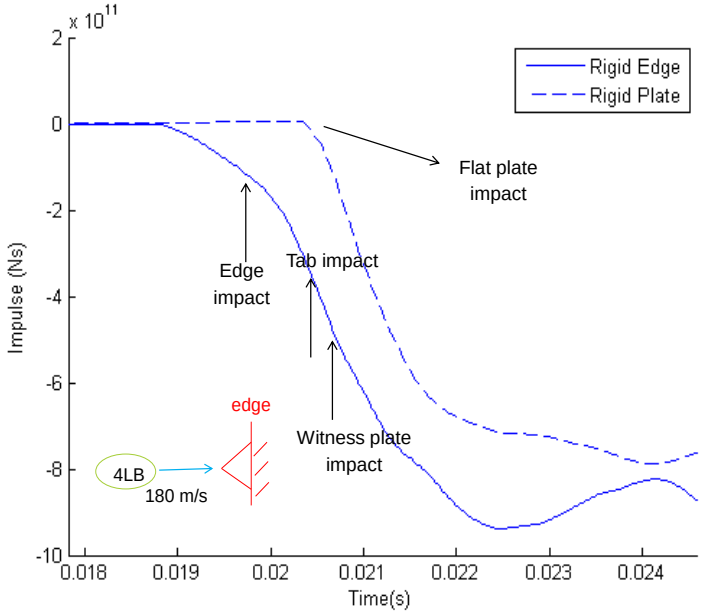

Figure 6.12: Impulse time history for a normal impact of 4 LB projectile at 180 m/s

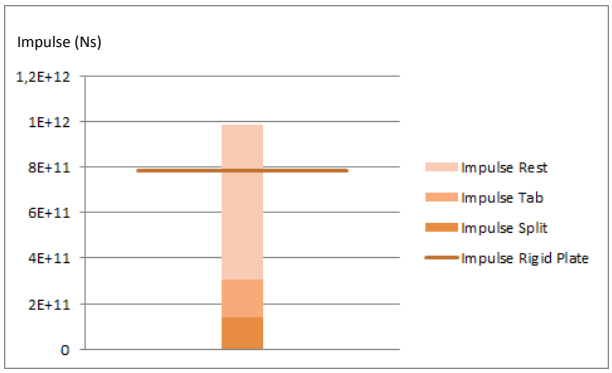

Figure 6.13: Statistical values for impulses for a normal impact of 4 LB projectile at 180 m/s

The splitting impulse represents 17 % of the rigid flat plate Impulse.

Normal Impact 8 LB projectile at 180 m/s

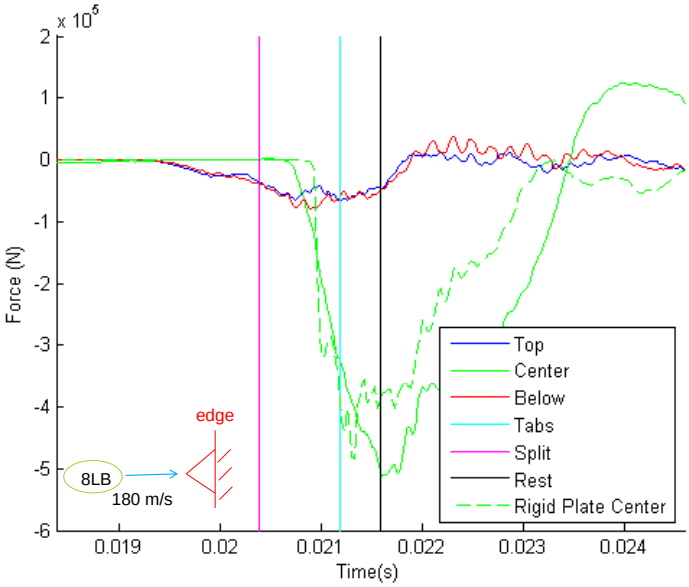

Figure 6.14: Force time history for a normal impact of 8 LB projectile at 180 m/s

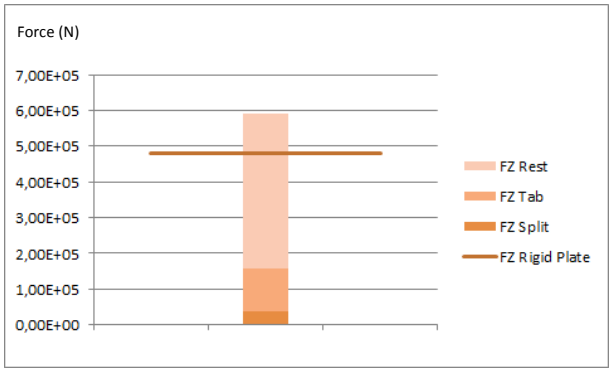

Figure 6.15: Statistical values for impact force for a normal impact of 8 LB projectile at 180 m/s

The splitting force represents 7.44 % of the rigid flat plate force.

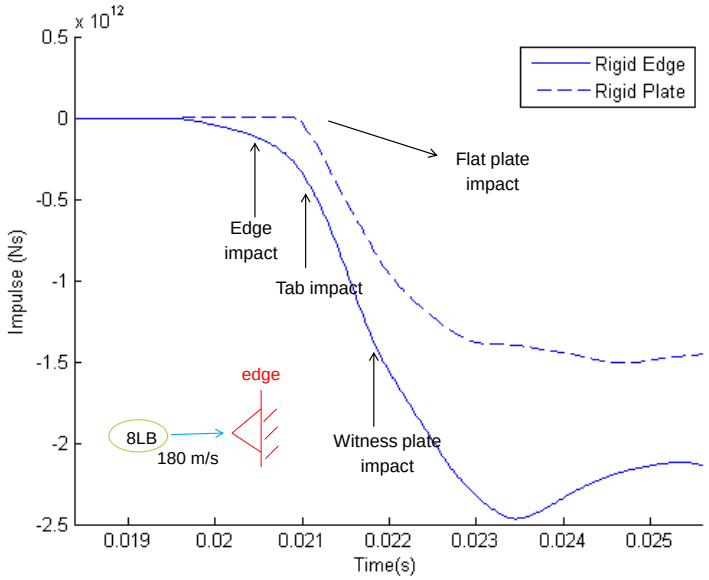

Figure 6.16: Impulse time history for a normal impact of 8 LB projectile at 180 m/s

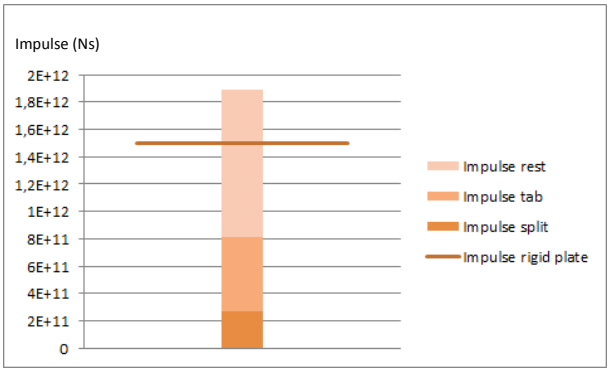

Figure 6.17: Statistical values for impulses for a normal impact of 8 LB projectile at 180 m/s

The splitting impulse represents 7.54 % of the rigid flat plate impulse.

The energy, force and impulse destined for the splitting decreases as the total kinetic energy increases (see ***Figure 6.18***).

$$(\frac{1}{2}m_{bird}{v_{bird}}^2) \qquad \textbf{(41)}$$

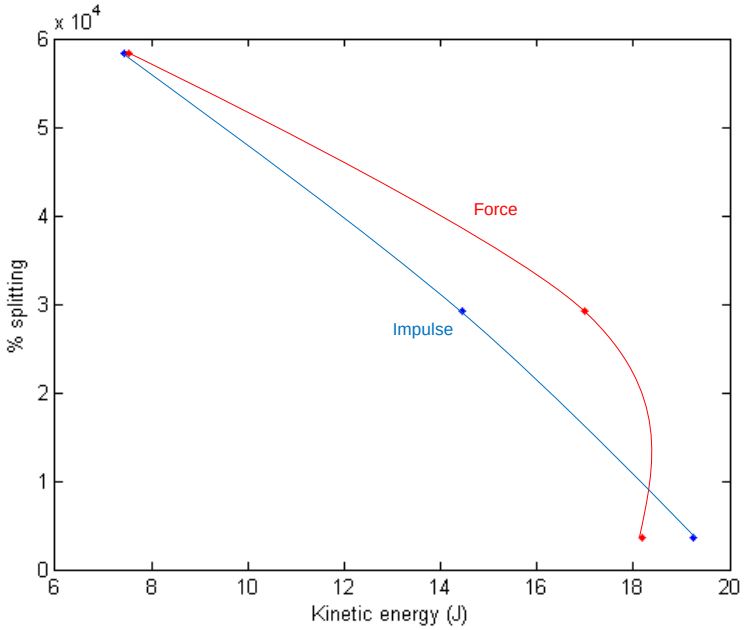

Figure 6.18: Laboured plot relating splitting percentage with kinetic energy

This is due to the fact that the energy, force and impulse applied at the splitting begin to maintain constant although the kinetic energy changes between impacts (the splitting effort is mostly the same for different runs remaining constant and does not depend on the mass or the impact velocity). Instead, the rest of the energies, forces and impulses continue to increase when the kinetic energy increases.

6.2. RIGID EDGE NUMERICAL SIMULATION

To perform the simulations of bird against rigid edge, FEM method will be used, as the simulation against rigid flat surface.

6.2.1. Rigid Edge FE Model description

- Structure:

The rigid edge is a sharp structure designed to withstand the bird to impact at the edge and split into two more or less equally pieces. It is equipped with two load cells which measure the forces at impact. Although all the impact force of the bird crashes against a single structure, less surface is being subjected to the first impact at highest velocity, making forces and pressures lower than in the flat plate impacts.

Another relevant part of the structure is the witness plate. This plate is located at the right side and below the rigid edge and receives the buffer of the right piece of bird after the first impact at the edge. Below this witness plate, one load cell is located to measure the forces at the witness plate.

One last part is going to be relevant for the impact results. They are called the tabs. The tabs are located right below the edge (see ***Figure***

6.19). The effect of the tabs is absolutely influential because it will affect the forces on the structure.

The material used for this structure is Aluminium 5083 with density of 2660 kg/m^3, Poisson´s ratio of 0.33 and Young Modulus of 72 Giga Pascal (GPa). The matrix related to the material of the structure is defined in PAM CRASH as MAT_ELASTIC_4NODED_THICKSHELL_LAGRANGIAN, with the same properties as for the flat plate.

- Impactor:

The SPH bird model is exactly the same as the one explained for the flat rigid plate.

- Contacts:

One of the aspects changing compared to the flat rigid plate is the contacts:

1. Contact between bird and rigid edge
   The first contact is the one connecting the bird with the rest of the structure excluding witness plate and tabs. It is defined in PAM CRASH as NON-SYMETRIC-NODE-TO-SEGMENT WITH EDGE TREATMENT The contact thickness remains constant (H=0.001m) but friction coefficient changes to zero.
2. Contact between bird and tabs
   Of the same type as the first contact, the second one related the bird with the so-called tabs. The contact thickness varies to 0.0023 m and the friction coefficient relies at zero.
3. Contact between bird and witness plate
   The contact adjoining the bird with the witness plate is defined in PAM CRASH as NON-SYMETRIC-NODE-TO-SEGMENT WITH EDGE TREATMENT with a contact thickness of 0.001 m and a constant friction coefficient of 0.3.

- Initial conditions and boundary conditions
  As for the rigid flat plate, the initial conditions cover the velocity of the bird. Depending on the run simulation, the velocity can vary from 85 m/s, 125 m/s to 180 m/s.
  The boundary conditions are quite similar to the rigid flat plate. The three load cells are clamped in the three directions (x, y and z). The rest of the structure remain attached and to the load cells without any boundary condition. Vibrations and deformations are produced at impact due to the elasticity of the material, but the load cells do not suffer from deformations.
- Outputs
  The three load cells are the ones recording the results of the forces at impact, as for the tests.

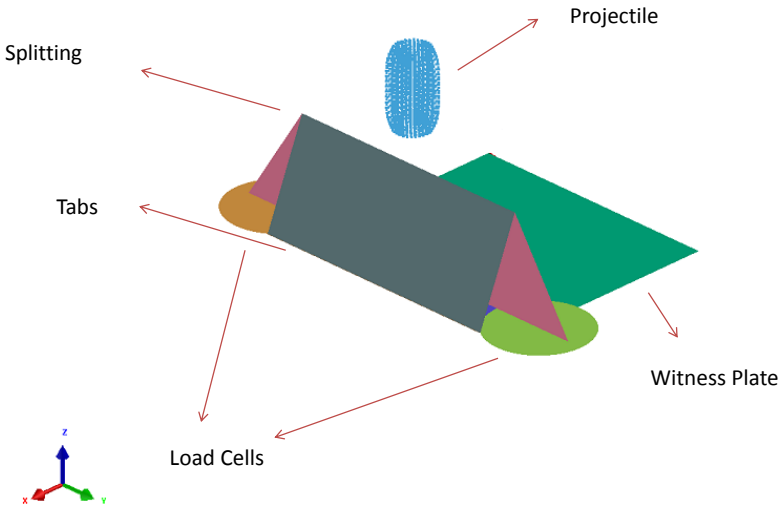

Figure 6.19: Numerical model of rigid edge at PAM CRASH

6.2.2. Numerical Simulation results of rigid edge

The variables are analysed in the simulation of the impact against rigid edge are forces (F_Z) and impulses (I) and they are going to be compared with test results.

The simulation assumes that the projectile was being fissured in two equal parts at the rigid edge, but there is no certainty that this hypothesis is accomplished in the tests.

The simulations launched in Pam Crash are the same runs as in the tests:

- Impact at 90°/normal impact

    1. 1 kg at 85 m/s
    2. 4 LB at 125 m/s
    3. 4 LB at 180 m/s
    4. 8 LB at 125 m/s
    5. 8 LB at 180 m/s

- Impact at 22.5°/oblique impact

    1. 1 kg at 85 m/s
    2. 4 LB at 180 m/s

Normal Impact

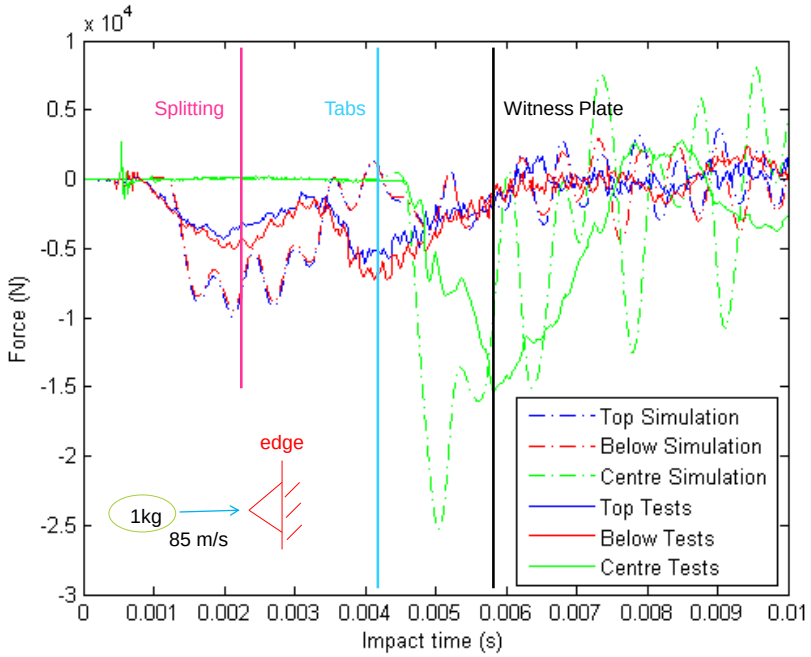

Figure 6.20: Simplified Model 1 kg projectile at 85 m/s

The dotted lines represent the simulation and the straight lines represent the test results. As seen in ***Figure 6.20*** and explained before, low kinetic energy impacts do not represent the best approximation of simulation to test results.

The fitting for the forces F_Z of the numerical simulation with respect to the test results as following:

- Peak force at the edge impact:
  The moment of impact against the rigid edge results to be the same for both simulation and results, but the magnitude is higher for the simulation.
- Peak force at the tabs impact:
  The time is quite similar; instead the magnitude results to be much smaller for the simulation. Tabs effect is not as good as the edge representation in the simulation.
- Peak force at the witness plate impact:
  Both simulation and tests represent a very similar time history for the impact of the bird against the witness plate for the exact moment and the magnitude of the force. The best representation for the simulation in comparison to the tests results to be the witness plate.

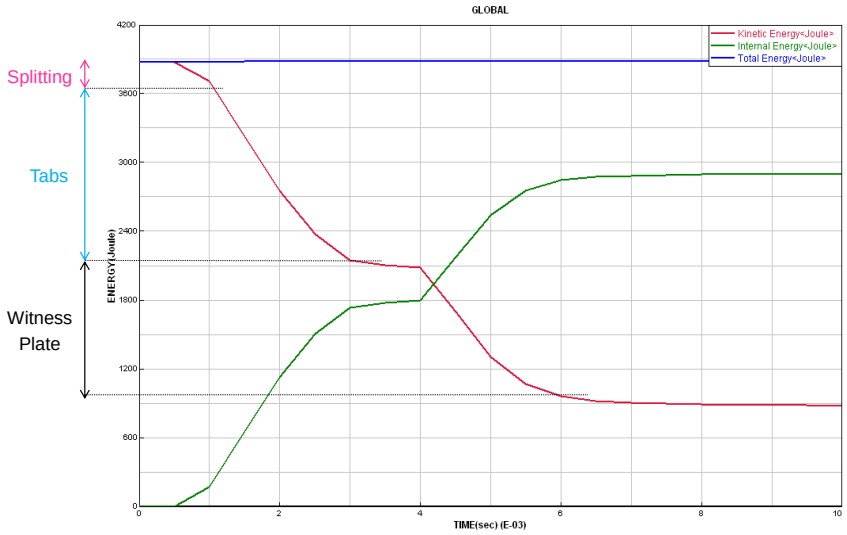

Figure 6.21: Energy 1 kg projectile at 85 m/s

The kinetic energy lost in the splitting phase represents 9.76 % of the total energy.

The small steps shown in ***Figure 6.21*** are due to the change in phase of the projectile (the different phases are splitting, impact against tabs and witness plate).At the moment the splitting is completed, the kinetic energy changes to follow a different path till the impact against tabs is completed and so on for the impact against the witness plate. The total kinetic energy tends to decrease at whole impact because its velocity is decreasing. The internal energy tends to increase while the kinetic energy decreases due to the projectile´s internal deformation due to impact against edge, tabs or plate. The total energy of the system remains constant along the whole impact as it is the sum of the kinetic energy and the internal energy.

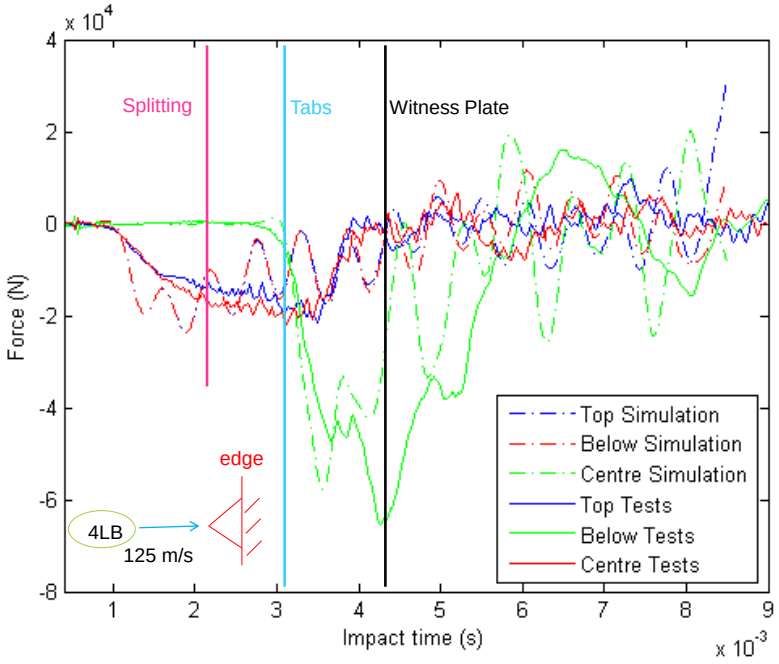

Figure 6.22: Simplified Model 4 LB projectile at 125 m/s

- Peak force at the edge impact:
  Simulation and tests forces appear to be quite similar for the 4 LB bird at 125 m/s.
- Peak force at the tabs impact:
  Simulation reproduces exactly the moment of impact of the bird against the tabs, as well as the magnitude.
- Peak force at the witness plate impact:
  The magnitude of the force is well represented in the simulation compared to the tests but the impact moment does not coincide.

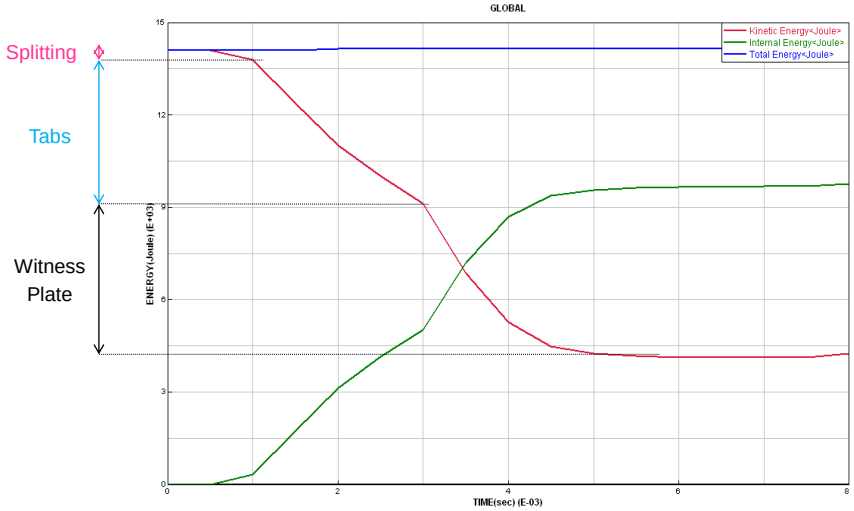

Figure 6.23: Energy 4 LB projectile at 125 m/s

The kinetic energy lost in the splitting phase represents 3.44 % of the total energy.

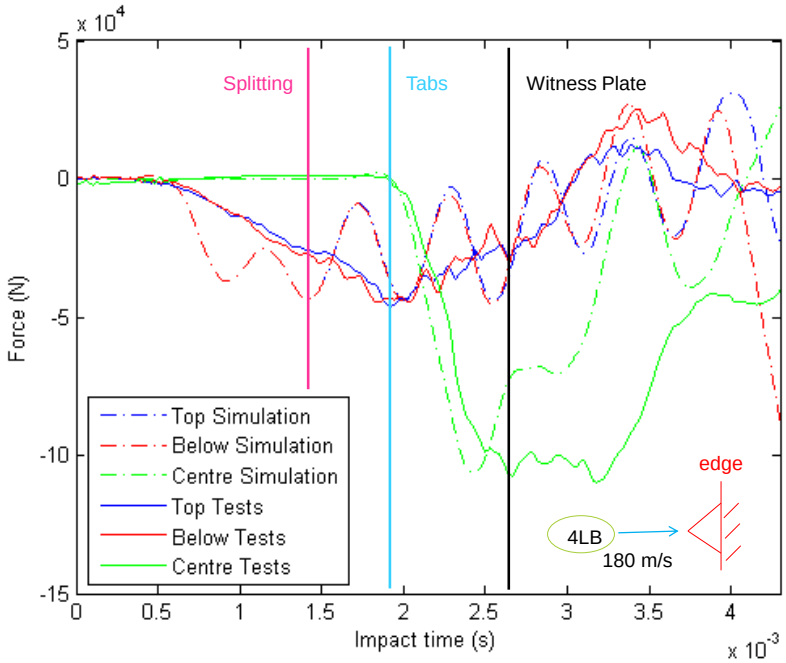

Figure 6.24: Simplified Model 4 LB projectile at 180 m/s

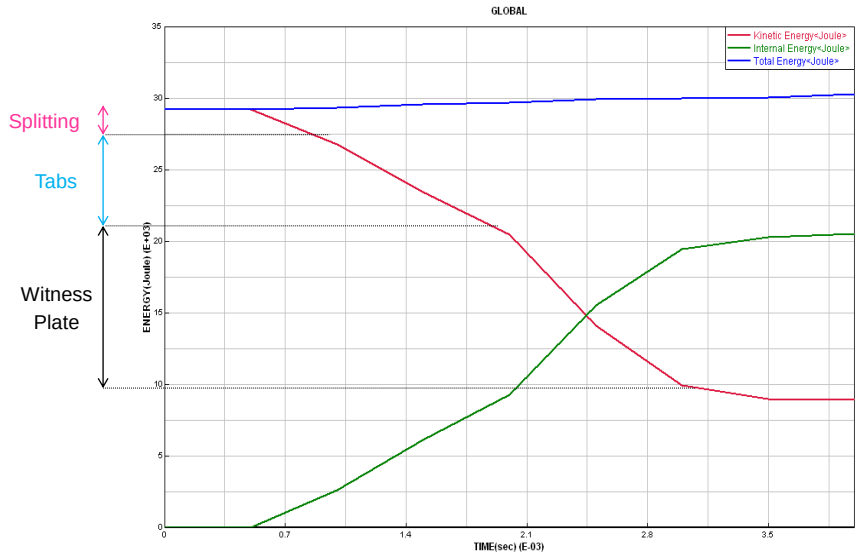

Figure 6.25: Energy 4 LB projectile at 180 m/s

The kinetic energy lost in the splitting phase represents 8.62 % of the total energy.

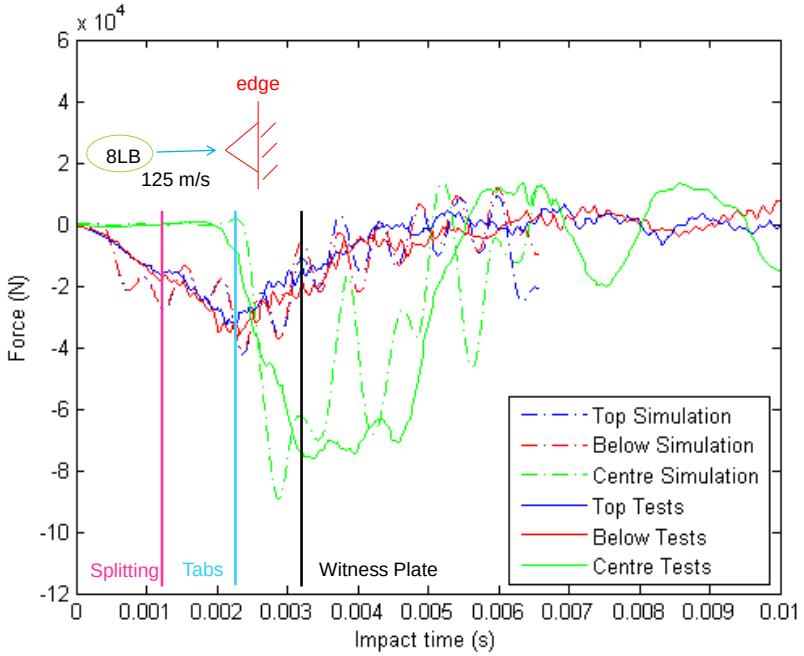

Figure 6.26: Simplified Model 8 LB projectile at 125 m/s

- Peak force at the edge impact:
  Very approximate representation for the impact moment as well as for the magnitude of the force recorded.
- Peak force at the tabs impact:

Exactly representation for both cases (simulation and tests).

- Peak force at the witness plate impact:
  Both simulation and tests provide similar time history for the impact against witness plate including impact time and magnitude.

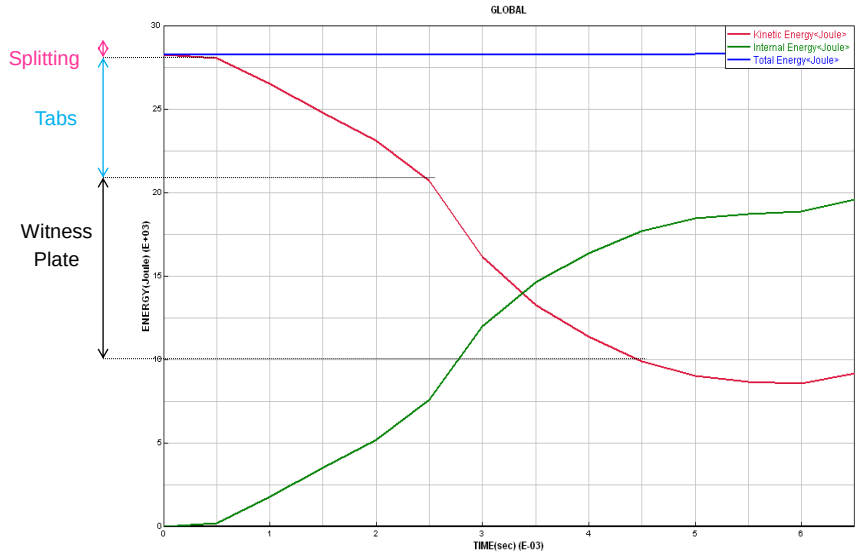

Figure 6.27: Energy 8 LB projectile at 125 m/s

The kinetic energy lost in the splitting phase represents 1.1 % of the total energy.

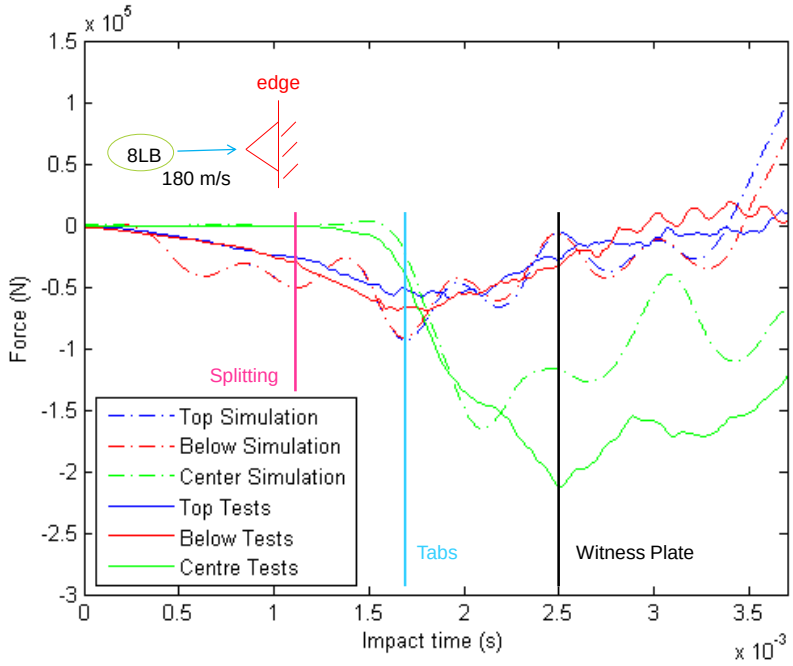

Figure 6.28: Simplified Model 8 LB projectile at 180 m/s

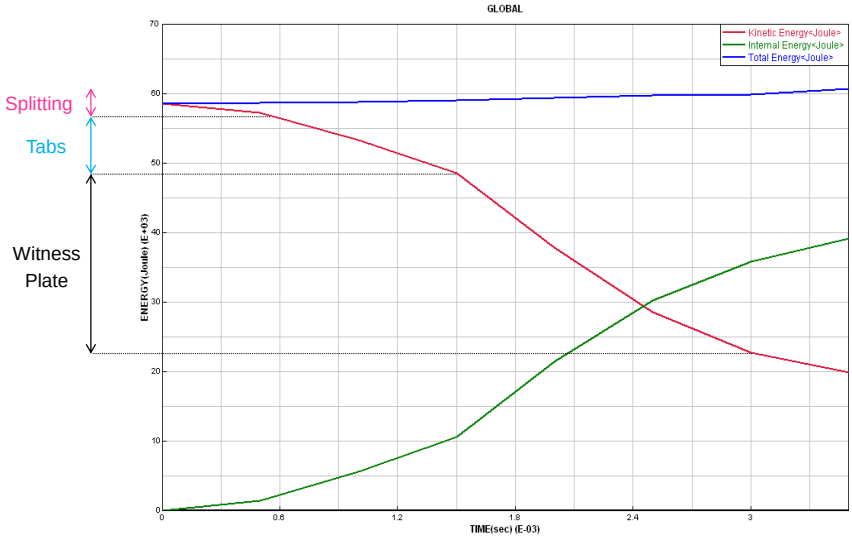

Figure 6.29: Energy 8 LB projectile at 180 m/s

The kinetic energy lost in the splitting phase represents 3.4 % of the total energy.

Oblique Impact

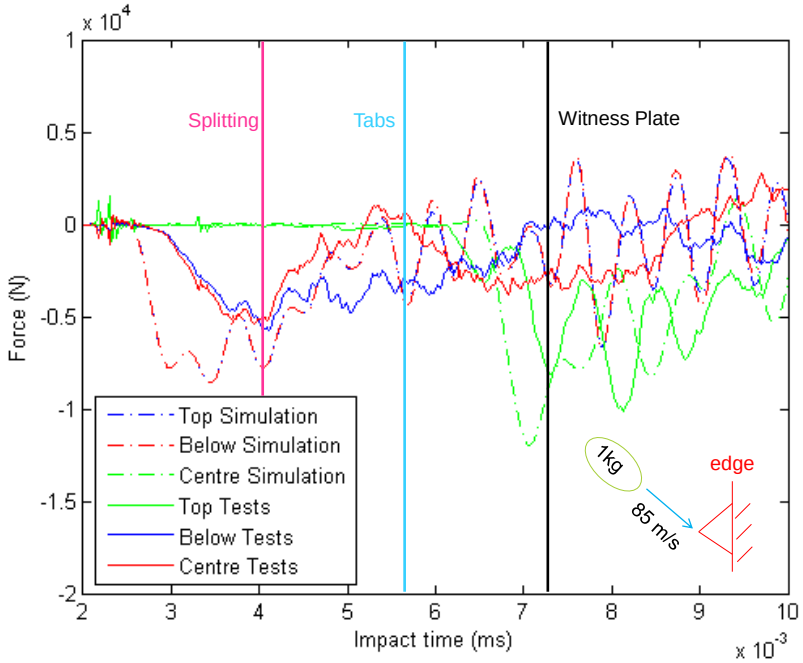

Figure 6.30: Simplified Model 1 kg projectile at 85 m/s

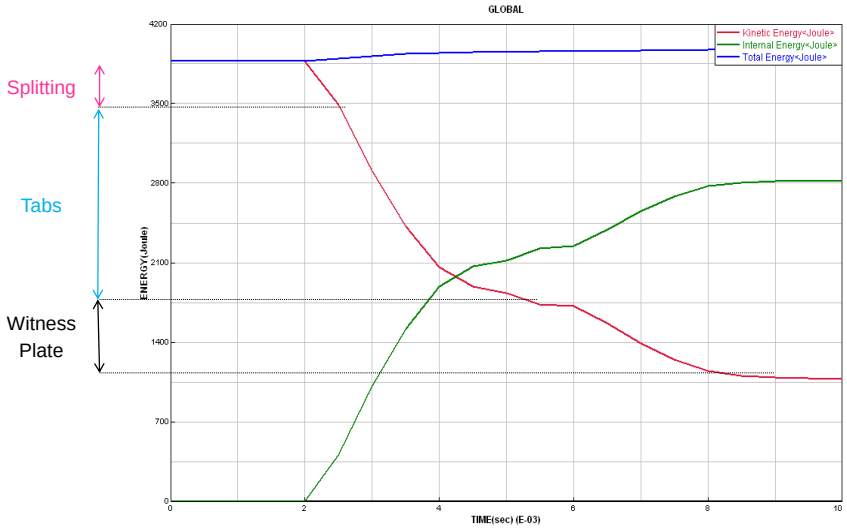

Figure 6.31: Energy 1 kg projectile at 85 m/s

The kinetic energy lost in the splitting phase represents 10.25 % of the total energy.

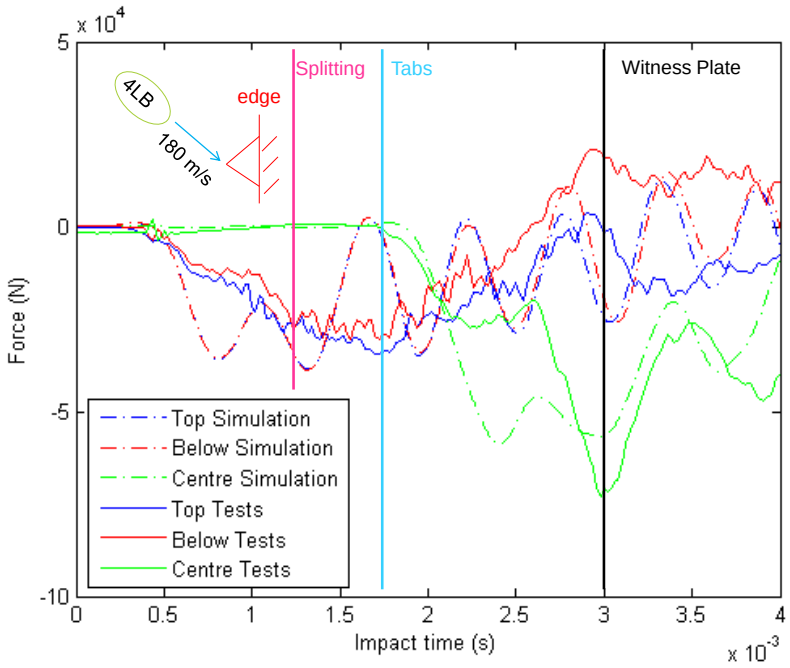

Figure 6.32: Simplified Model 4 LB projectile at 180 m/s

The three moments of impact (rigid edge, tabs and witness plate) represent quite accurate the results of the simulation compared to the results for the tests. This is due to the high values for kinetic energy of the impact (4 LB at 180 m/s). The best results are measured in the witness plate, which follows to be the finest modelled part of the simulation followed by the rigid edge. The geometry of the tabs, in the other hand, is not as approximate.

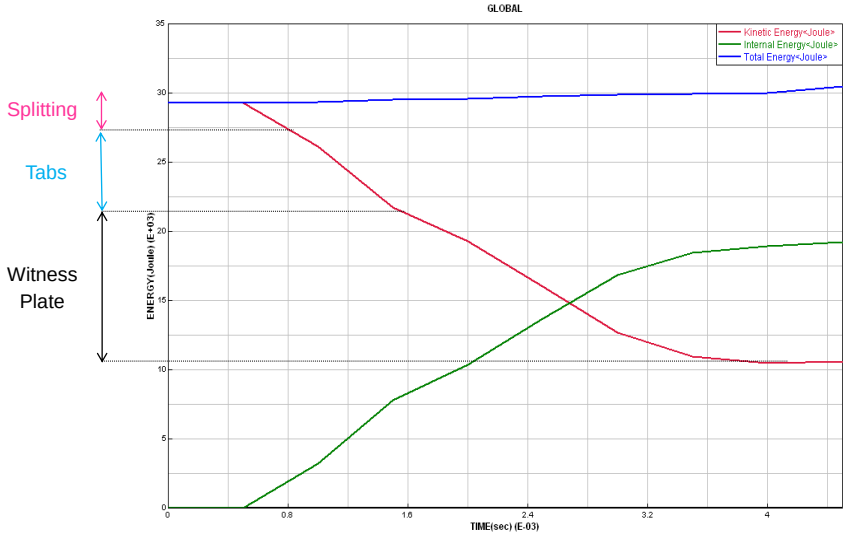

Figure 6.33: Energy 4 LB projectile at 180 m/s

The kinetic energy lost in the splitting phase represents 8.33 % of the total energy.

The simulations for the impact against rigid edge work highly better for normal impacts at high values for kinetic energy rather than for oblique impacts. This can be due to the stiffness of the model of the rigid edge, which resists much better the impacts in its normal direction rather than its parallel/oblique direction. It is important to note that the correlation of numerical and test results is much better.

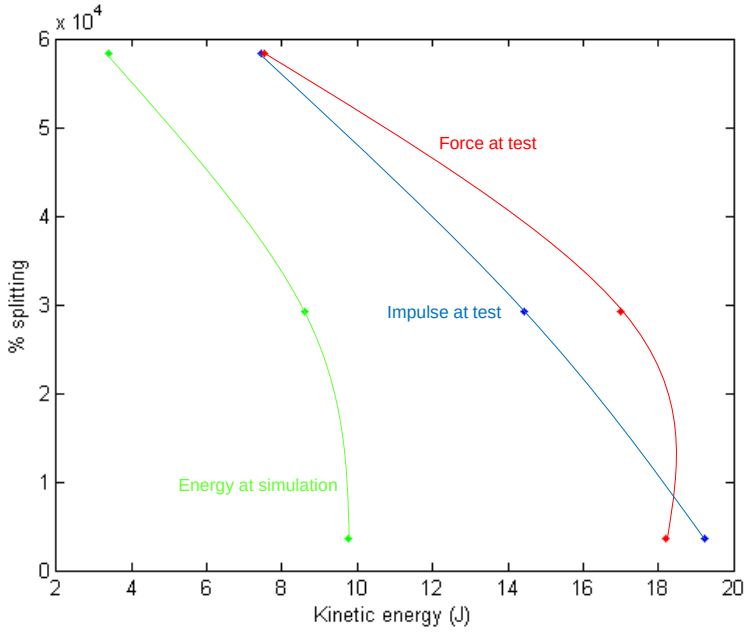

Figure 6.34: Comparison of the percentage of the splitting of the bird between the tests and the simulation for force, impulse and energy

Thanks to the simulations, it is possible to reproduce the tendency of the bird splitting observed in the tests. As seen in ***Figure 6.34***, the three curves represent the same path although the values are slightly different. This is due to the fact that the green curve represents the splitting percentage of the energy at simulation, and the blue and red curves represent the impulse and force at the tests. The important conclusion is that the three of them follow a very similar curve which means the simulations recreate in a quite accurate manner the results of the tests.

CHAPTER 7

CONCLUSIONS

According to the three main topics explained in this Bachelor´s Thesis, conclusions from each of the topics will be complied here:

7.1. GEOMETRY OF THE IMPACTOR

- To calculate the length of the modelled impactors (1 kg, 4 LB and 8 LB) for the numerical simulations, only the impact forces should be used neglecting the characteristic impact time at test results.

- The properties of the modelled impactor can allow changing conditions at impact. The constants for the Murnaghan equation and the density should be carefully checked in order not to change impact conditions.

- For the modelling of the projectile as a bird for numerical simulation, Smoothed-Particle Hydrodynamics (SPH) model is the best option. And for the specimen (plate, load cells, edge and pressure gauges) the best approximation is the Lagrangian approach made of solid elements forming a mesh.

- The optimization of the model of the impactor has led to the improvement of numerical results from the models used previously (remember the geometry of the optimized impactor was obtained from the test results) for simulations against rigid flat plate and rigid edge. The best results with the optimized bird were for the rigid flat plate impact.

7.2. RIGID FLAT PLATE

- For the test results, it exist an exceptional repetitiveness for each run (same bird weight and velocity).

- Pressure measurements from the tests had to be discarded due to the wrong measurement of the pressure gauges located at the flat plate at impacts.

- After testing the first approximation model with load cells and the simplified model without cells, the one that correlates the tests results better is the second. This is due to the fact that the load cells in the simulation are creating a vibrational response which is not related to the response in the test results, which has lower amplitude.

- Simplified model gives most accurate results for impacts with higher values of kinetic energy.

- For a better correlation of simplified model to test results, one option can be to include a spring together with a damper representing the stiffness of the load cells. This system will allow the simulated specimen to vibrate in such lower amplitude as for the test specimen. Spring and damper can allow defining the exact constants for the system and matching the simulation to the test results.

7.3. RIGID 22.5° EDGE

- The effect of the tabs has completely contaminated the test. The best results for the test and simulations would have been for a system which didn´t allow tabs on it.

- Impulses have been analysed for the test runs to obtain the relevance of the splitting of the bird in the overall impact process.

- For low kinetic energies impact such as an 1 kg projectile at 85 m/s, the percentage of splitting with respect to normal impact on flat plate is quite high. The splitting plays a fundamental roll in the impact.

  Instead, for high kinetic energies such as an 8 LB projectile at 180 m/s, the percentage of splitting with respect to normal impact on flat plate is quite low.

- Total bird splitting at the moment of impact against the rigid edge represents between a 7 % and a 19 % of the rigid flat plate impact, both in forces and in impulses.

- The most accurate numerical simulation results are given by normal impacts with high values of kinetic energies.

CHAPTER 8

OBJECTIVES ACHIEVEMENT

The fundamental objective of this Bachelor´s Thesis was the comparison between numerical simulations implemented based on tests results, with the tests results for impact against flat rigid plates and rigid edges. This objective was well completed and concluded by plotting the graphs where the time histories for both launches can be compared.

The simulations could be done thanks to the implementation of the optimization of the impactor (bird) model which gave better results than the ones used previously.

Thanks to these preceding objectives achieved, the statistical treatment of the splitting analysis of the bird against rigid edge could be easily evaluated. Different graphs are shown to explain how does the splitting occur and the percentage it covers over the total impact.

CHAPTER 9

ECONOMIC FRAMEWORK

The approximated budget for this Bachelor´s Thesis follows to be:

Table 9.1: Economic Budget

CONCEPT			TOTAL COST (€)
Bird Splitting Tests			72.000
1.) Set up preparation	12.000		
2.) Cost/run (1.000) X 60 runs	60.000		
Engineering Works			16800
Total engineer hours (h)		535	
1.) Documentation	90		
2.) Learning skills	40		
3.) Tests results post process	125		
4.) Geometry of the bird	130		
5.) Numerical simulation	150		
Engineer cost/hour (€/h)		35	
Pam Crash Licence (6 months)	25.000/year		12.500
Mat Lab Licence (6 months)	8.000/year		4.000
Other			250
TOTAL (€)			105.550

To prepare an approximate calculation for the needed budget for this study, the costs of the tests, engineering works, licences and other have been taken into account.

In learning skills, knowledge of the computer programs is included as well as research and learning about impact field. For the engineer cost per hour, a junior engineer cost of 35 € have been used. The costs per license of Pam Crash and Mat Lab programs fully depend on the company or university last for 6 months. For the concept called "Other", required material to develop the thesis is included.

CHAPTER 10

FURTHER STUDIES

10.1. IMPROVEMENT ON TEST MEASUREMENTS

As stated in the first part of the thesis, the impact pressures were not measured properly. This was found out at the moment of analysing the results of the tests, when its values were outside the estimated values for pressures.

The main goal of this further study is to repeat the measurements at the pressure gauges to obtain valid results at the same tests studied in this thesis on the rigid plate.

10.2. IMPROVEMENT ON TEST RESULTS FROM 22.5 DEGREES RIGID EDGE

It was assumed at the rigid edge impact that the projectile splits in two equal halves. There was no prove that this assumption was appropriate because only one witness plate located at the right side of the edge was recording forces measurements. This witness plate was exclusively measuring the forces for the half right projectile. But if there were two different witness plates at the left and right side of the edge, forces will be measured in both parts of the projectile and an estimation of the mass of each part of the projectile could be reported such as:

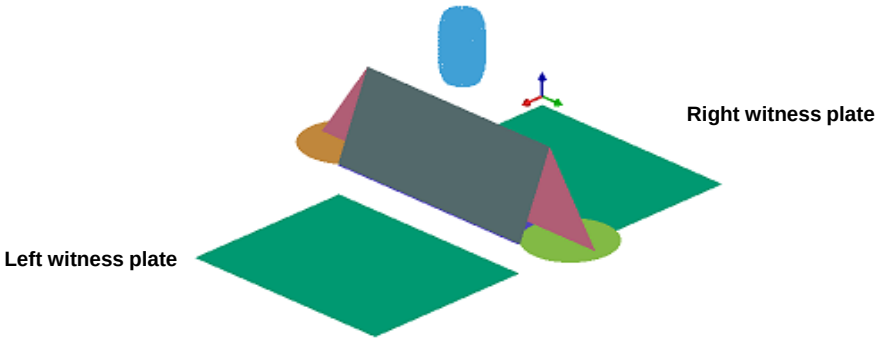

Figure 10.1: Approximate Model for further studies

10.3. IMPROVEMENT ON LOAD CELLS MODEL

After studying the simplified model for the rigid plate and recognizing that it is still not reproducing exactly the test results, a new model must be developed to approximate better to the test time histories. As the initial approach of the model presented several oscillations that never tend to zero which meant the cells were acting as a spring which never stopped, and the simplified model presented no oscillations which meant the system would stop at the final moment of impact, a system in between these two must be developed to approximate best results to tests.

Analysing the results of the tests, it can be found that the model is acting like a simple harmonic system. After the complete impact of the bird (approximately 4 milliseconds), the time history shows oscillations in time with values of peak forces smaller than the peak force decreasing with time till zero. This suggests a free vibration together with damping without external forces acting on it.

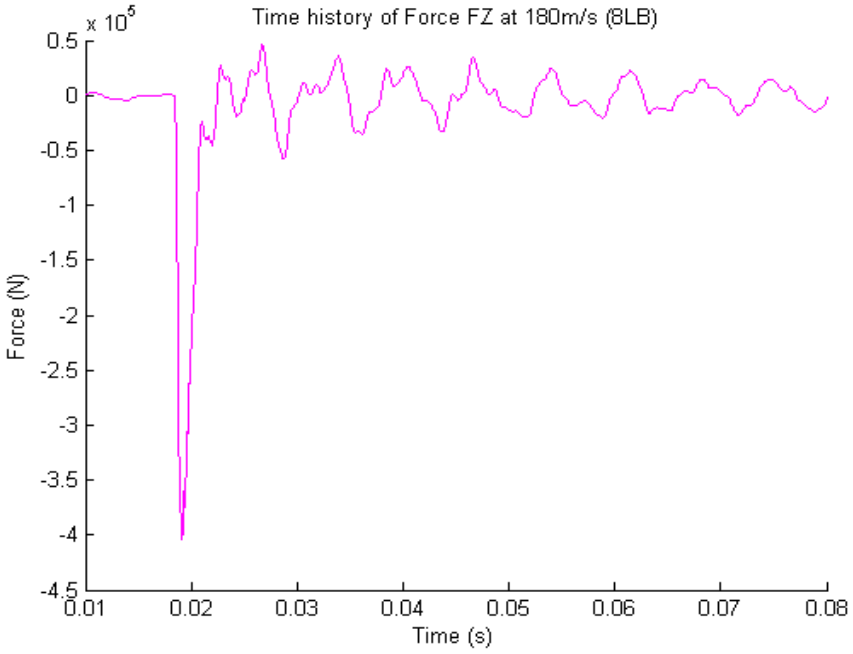

Figure 10.2: Response for an 8 LB projectile at 180 m/s impact obtained in the tests

The first peak after the impact of the projectile, this means after the highest peak value of approximate -4E5 Newton, represents the first point to measure the amplitude ($x_1 \, and \, t_1$). After a complete wave through the time history, the second point is measured ($x_2 \, and \, t_1 + T_d$). Between these points, the amplitude and the period (T_d) is found out.

While a spring tends to save the potential energy of impact by creating periodic motion along its time history, the damper represents a model created to dissipate energy and damp the response of a dynamic system. The force exerted by the damper is defined as

$$f_c = -c\dot{x}(t) \quad (42)$$

Where c is the damping constant measured in $\frac{Ns}{m}$.

The differential equation of state is defined as a simple harmonic system:

$$m\ddot{x} + c\dot{x} + kx = F(t) \quad (43)$$

Being F (t) are external forces.

$$F(t)=0 \quad (44)$$

As the external forces are zero, the system will be defined as free harmonic.

To find out which type of damping is being created by the cells, the logarithm decrement will be used,

$$\gamma = ln\frac{x_1}{x_2} \quad (45)$$

Being x_1 is the peak force after the impact at time t_1 and x_2 in the next peak force at time $t_1 + T_d$

The damping frequency of the system is defined as

$$\omega_d = \frac{2\pi}{T_d} \quad (46)$$

Being T_d is the damping period of the oscillations measured in the graphs.

The natural frequency of the system is related to the movement without friction such as:

$$\omega = \frac{\omega_d}{\sqrt{1-\xi^2}} \quad (47)$$

The symbol ξ is the damping ratio and can be calculated from the response in time of the system:

$$\xi = \frac{\gamma}{\sqrt{4\pi^2+\gamma^2}} \quad (48)$$

And is the value defined to analyze the system:

- If $0<\xi<1$ the system is sub damped and the solutions of the system are complex conjugated.
- If $\xi > 1$ the system is overdamped and the solutions of the system are real. The response is clearly not oscillatory, tending to its equilibrium position.
- If $\xi = 1$ the system if critical damped and the two solutions of this system are equal and = ω

After calculating the value for ξ, we can determine that the damped system is considered as subdamped because $0<\xi<1$. To calculate the damping constant c of the system, we will use conditions of the critical damping constantc_c.

$$\xi = \frac{c}{c_c} \tag{49}$$

$$c_c = 2m\omega \tag{50}$$

To find the constant of the spring acting as the load cells, the following equation will be used, where $\omega_d$is measured from the force time history obtained in the tests.

$$\omega_d = \sqrt{\frac{k}{m} - (\frac{c}{2m})^2} \tag{51}$$

The value for the constant of the spring in the three directions is obtained by analyzing the graphs at 90 and 45 degrees for the three different weights (1 kg, 4 LB, 8 LB). The value of k_z in the direction normal to the plate is obtained by the impact at 90 degrees and $k_x = k_y$ because of the symmetry of the cells, obtained by the impact at 45 degrees.

Finally, the three spring constants (k_x, k_y, k_z) and the three damper constants (c_x, c_y, c_z) are introduced into the simplified simulation model in Pam Crash such as:

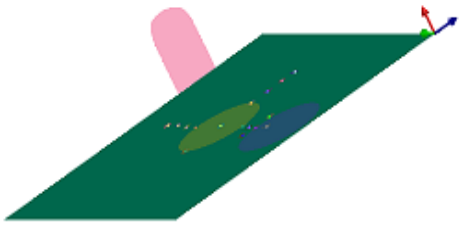

Figure 10.3: Actual Model

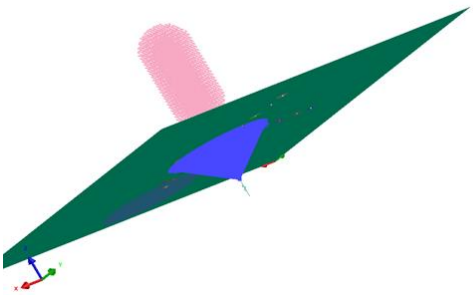

Figure 10.4: Future Model

The nodes located at the load cell are connected to a unique node representing a nodal constraint (see ***Figure 10.4*** in blue color). This last node connects one end of the spring with damper to the fixed end node in the three directions.

REFERENCES

[1] Agency, E. A. (December 2009). *Bird Strike Damage and Windshield Bird Strike.* Cologne, Germany.

[2] Airbus. (2004). *Birdstrike Threat Awareness.* Blacnac Cedex France.

[3] Aircraft extreme security tests. (n.d.). *BBC.*

[4] Airports, A. A. (September 2013). *Wildlife Strikes to Civil Aircrafts in the United States 1990-2012.* Washington, US.

[5] *AirSafe-Bird Strike Hazards to Aircraft.* (1996). Retrieved from http://www.airsafe.com/birds.htm

[6] *Bird Strike.* (2015, September 2). Retrieved from http://en.wikipedia.org/wiki/Bird_strike#Species

[7] *Calbraith Perry Rodgers.* (2015, June 18). Retrieved from https://en.wikipedia.org/wiki/Calbraith_Perry_Rodgers

[8] Casillas, T. (2015, June). Final year project. Bird Strikes on Trasparencies. Madrid, Madrid, Spain.

[9] *Celda de carga.* (2015, April). Retrieved from https://es.wikipedia.org/wiki/Celda_de_carga

[10] D.Murnaghan, F. (2015, August). *The compressibility of Media under Extreme Pressures.* National Academy of Science of the United States of America.

[11] Delgado, C. A. (2008). Tesis. Diseño de un acelerómetro utilizando tecnología de navegación óptica a partir de un mose para computador para la Universidad Austral de Chile. Chile.

[12] Dolbeer, E. C. (2005). Manejo del riesgo por fauna silvestre en aeropuertos. *Digital Commons University of Nebraska*, 389.

[13] *Edilatex. Oscilaciones libres.* (2011, August). Retrieved from http://www.edilatex.com/index_archivos/mecanica.pdf

[14] Fernández, J. M. (2008, November). Proyecto fin de carrera. Diseño y desarrollo para un banco de ensayo de un balancín de soldadura para la Escuela Técnica Superior de Ingenieros Industriales de Vigo. Vigo, Galicia, Spain.

[15] Fowler, A. B. (2008). Capítulo 10. Vibraciones. In *Dinámica: Mecánica para Ingeniería* (p. 548). Pearson Educación.

[16] Kulak, C. B. (2003). Comparison of Lagrangian, SPH and MM-ALE approaches for Modeling large deformations in soil. *11th International LS-Dyna Users Conference*, (p. 45). IL, US.

[17] L. Benítez Montañés, J. L.-G. (2012). Bird Strike Numerical Simulation. *Madrid* (p. 62). Madrid: Airbus Military.

[18] M. Janewers, D. R. (2013). *Bird Strike Testing Campaign.* Lichtenau: EADS, IABG.

[19] Meruane, V. (n.d.). *Vibraciones Mecánicas para la Universidad de Chile.* Chile.

[20] *Método de los elementos finitos*. (2015, August). Retrieved from https://es.wikipedia.org/wiki/M%C3%A9todo_de_los_elementos_finitos

[21] Moskvitch, K. (2014, March 30). Pruebas extremas para garantizar la seguridad de los aviones. *BBC*.

[22] Ortecho, C. A. (November 2010). *Robust Bird Strike.Modelling using LS-Dyna.* VDM Verlag.

[23] Peterson, R. L. (1978, November 16). Bird Impact Forces and pressures on rigid and compliant targets. *1978*. Dayton, Ohio, US.

[24] Sevilla, U. d. (2010, Marzo). Movimiento Oscilatorio. Sevilla, Andalucía, Spain.

[25] Sevilla, U. d. (2010, October). Oscilaciones Mecánicas. Sevilla, Andalucía, Spain.

[26] *Skybrary-Bird Strike*. (n.d.). Retrieved from http://www.skybrary.aero/index.php/Bird_Strike

[27] *Smooth Particle Hydrodynamics*. (2015, July). Retrieved from https://en.wikipedia.org/wiki/Smoothed-particle_hydrodynamics

[28] Vijay K. Goyal, C. A. (2013). Arbitrary Lagrange Eulerian Approach for Bird-Strike Analysis using LS-Dyna. *American Transactions on engineer and applied Sciences*, 132.

[29] Vijay K. Goyal, C. A. (2013). *Smooth Particle Hydrodynamics for Bird-Strike Analysis using LS-Dyna.* Puerto Rico and Connecticut.

[30] Wilbeck, J. S. (1978, October 27). Impact Behavior of low stregth projectiles. Dayton, Ohio, US.